

AD-A256 311

②

# NAVAL POSTGRADUATE SCHOOL

## Monterey, California



**S** DTIC  
ELECTE  
OCT 23 1992 **D**  
**E**

### THESIS

FLOWFIELD STUDY OF A  
CLOSE-COUPLED CANARD CONFIGURATION

by

John F. O'Leary

June, 1992

Thesis Advisor:

Richard M. Howard

Approved for public release; distribution is unlimited

92 10 22 054

251450

92-27823  
96

UNCLASSIFIED

SECURITY CLASSIFICATION OF THIS PAGE

REPORT DOCUMENTATION PAGE												
1a. REPORT SECURITY CLASSIFICATION UNCLASSIFIED			1b. RESTRICTIVE MARKINGS									
2a. SECURITY CLASSIFICATION AUTHORITY			3. DISTRIBUTION/AVAILABILITY OF REPORT Approved for public release; distribution is unlimited.									
2b. DECLASSIFICATION/DOWNGRADING SCHEDULE												
4. PERFORMING ORGANIZATION REPORT NUMBER(S)			5. MONITORING ORGANIZATION REPORT NUMBER(S)									
6a. NAME OF PERFORMING ORGANIZATION Naval Postgraduate School		6b. OFFICE SYMBOL (If applicable) 31	7a. NAME OF MONITORING ORGANIZATION Naval Postgraduate School									
6c. ADDRESS (City, State, and ZIP Code)  Monterey, CA 93943-5000			7b. ADDRESS (City, State, and ZIP Code)  Monterey, CA 93943-5000									
8a. NAME OF FUNDING/SPONSORING ORGANIZATION		8b. OFFICE SYMBOL (If applicable)	9. PROCUREMENT INSTRUMENT IDENTIFICATION NUMBER									
8c. ADDRESS (City, State, and ZIP Code)			10. SOURCE OF FUNDING NUMBERS									
			<table border="1"> <tr> <td>Program Element No.</td> <td>Project No.</td> <td>Task No.</td> <td>Work Unit Accession Number</td> </tr> <tr> <td></td> <td></td> <td></td> <td></td> </tr> </table>		Program Element No.	Project No.	Task No.	Work Unit Accession Number				
Program Element No.	Project No.	Task No.	Work Unit Accession Number									
11. TITLE (Include Security Classification) FLOWFIELD STUDY OF A CLOSE-COUPLED CANARD CONFIGURATION												
12. PERSONAL AUTHOR(S) O'Leary, John F.												
13a. TYPE OF REPORT Master's Thesis		13b. TIME COVERED From To	14. DATE OF REPORT (year, month, day) June 1992	15. PAGE COUNT 96								
16. SUPPLEMENTARY NOTATION The views expressed in this thesis are those of the author and do not reflect the official policy or position of the Department of Defense or the U.S. Government.												
17. COSATI CODES			18. SUBJECT TERMS (continue on reverse if necessary and identify by block number)									
FIELD	GROUP	SUBGROUP										
			Close-Coupled Canard									
			Post-Stall									
			Agility									
			Vortex Interaction									
			High Angle of Attack									
19. ABSTRACT (continue on reverse if necessary and identify by block number) A nulling five-hole pressure probe was used to complete a flowfield survey behind a close-coupled canard and wing model set at 22 degrees angle of attack. The canard and wing were both low-aspect-ratio, highly-swept, delta planforms with rounded leading edges. The model was set at the condition of maximum lift enhancement of the canard/wing configuration over a corresponding wing-alone configuration, based on previous force measurements. For comparison, the pressure measurements were made with the canard on and with the canard off. From the pressure measurements, flowfield velocity-vector, velocity-streamline and total-pressure-coefficient contours were plotted. These plots showed the dramatic effect of the canard vortex on the wing flowfield. The location and interaction of the canard and wing leading-edge vortices were analyzed. Large-scale reattachment of previously reversed flow over the wing was noted, as well as the re-establishment and strengthening of the wing leading-edge vortex.												
20. DISTRIBUTION/AVAILABILITY OF ABSTRACT <input checked="" type="checkbox"/> UNCLASSIFIED/UNLIMITED <input type="checkbox"/> SAME AS REPORT <input type="checkbox"/> DTIC USERS			21. ABSTRACT SECURITY CLASSIFICATION Unclassified									
22a. NAME OF RESPONSIBLE INDIVIDUAL Richard M. Howard			22b. TELEPHONE (Include Area code) (408) 646-2870	22c. OFFICE SYMBOL AA/HO								

DD FORM 1473, 84 MAR

83 APR edition may be used until exhausted  
All other editions are obsoleteSECURITY CLASSIFICATION OF THIS PAGE  
Unclassified

Approved for public release; distribution is unlimited.

**FLOWFIELD STUDY OF A CLOSE-COUPLED  
CANARD CONFIGURATION**

by

**John F. O'Leary**  
Captain, United States Marine Corps  
B.S., United States Naval Academy, 1983

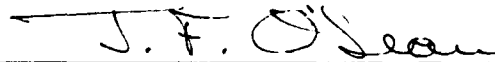
Submitted in partial fulfillment  
of the requirements for the degree of

**MASTER OF SCIENCE IN AERONAUTICAL ENGINEERING**

from the

**NAVAL POSTGRADUATE SCHOOL**  
June 1992

Author:

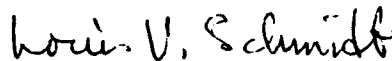


John F. O'Leary

Approved by:



Richard M. Howard, Thesis Advisor



Louis V. Schmidt, Second Reader



Daniel J. Collins, Chairman  
Department of Aeronautics and Astronautics

## ABSTRACT

A nulling five-hole pressure probe was used to complete a flowfield survey behind a close-coupled canard and wing model set at 22 degrees angle of attack. The canard and wing were both low-aspect-ratio, highly-swept, delta planforms with rounded leading edges. The model was set at the condition of maximum lift enhancement of the canard/wing configuration over a corresponding wing-alone configuration, based on previous force measurements. For comparison, the pressure measurements were made with the canard on and with the canard off. From the pressure measurements, flowfield velocity-vector, velocity-streamline and total-pressure-coefficient contours were plotted. These plots showed the dramatic effect of the canard vortex on the wing flowfield. The location and interaction of the canard and wing leading-edge vortices were analyzed. Large-scale reattachment of previously reversed flow over the wing was noted, as well as the re-establishment and strengthening of the wing leading-edge vortex.

Accession For	
NTIS CRA&I	<input checked="" type="checkbox"/>
DTIC TAB	<input type="checkbox"/>
Unannounced	<input type="checkbox"/>
Justification	
By	
Distribution/	
Availability Codes	
Dist	Avail and/or Special
<b>A-1</b>	

DTIC ORIGINATOR REQUESTED 1

## TABLE OF CONTENTS

I. INTRODUCTION.....	1
A. SUPERMANEUVERABILITY.....	1
B. CLOSE-COUPLED CANARD.....	1
C. THESIS OBJECTIVE.....	2
II. BACKGROUND.....	3
A. VORTEX GENERATION.....	3
B. CANARD CHARACTERISTICS.....	4
1. Canard Versus Tail.....	5
C. VORTEX INTERACTION.....	8
D. PREVIOUS TESTING.....	9
III. EXPERIMENT AND PROCEDURES.....	11
A. PURPOSE.....	11
B. APPARATUS.....	12
1. Wind Tunnel.....	12
2. Model Design.....	14
3. Velmex 8300 Three-Dimensional Traverser System.....	18
4. Rotary Pressure Transducer and Data Acquisition System.....	18
5. Five-Hole Pressure Probe.....	20
C. EXPERIMENT SOFTWARE.....	21
1. PPROBE.....	21
2. CALP.....	24
3. PVA (Pressure Velocity Angle).....	25
D. EXPERIMENTAL CONDITIONS AND PROCEDURES.....	28

IV. RESULTS.....	29
A. WING-ALONE.....	30
1. Mid-Point of the Main Wing (Grid 2).....	32
2. Trailing Edge of the Main Wing (Grid 3).....	32
B. WING/CANARD COMBINATION.....	39
1. Trailing Edge of the Canard.....	40
2. Mid-Point of the Main Wing (Grid 2).....	45
3. Trailing Edge of the Main Wing (Grid 3).....	51
C. CONCLUSION.....	55
LIST OF REFERENCES.....	57
APPENDIX A.....	58
APPENDIX B.....	74
APPENDIX C.....	81
INITIAL DISTRIBUTION.....	86

## LIST OF FIGURES

Figure 1. Flowfield Over the Top of a Delta Wing.....	3
Figure 2. Canard Catagories [Ref. 2].....	4
Figure 3. Characteristics of the F-4, F-106 and Viggen [Ref. 2].....	6
Figure 4(a). Lift Coefficient due to a Canard and Horizontal Tail [Ref. 2].....	7
Figure 4(b). Drag Polar for a Canard and Horizontal Tail [Ref.2].....	8
Figure 5. Lift Coefficient of Wing/body and Maximum Lift of Canard/Wing [Ref.6].....	10
Figure 6. Model Overview.....	11
Figure 7. Naval Postgraduate School Wind Tunnel [Ref. 8].....	12
Figure 8. Model Geometric Data.....	16
Figure 9(a). Side View of the Model Mounted in the Tunnel.....	17
Figure 9(b). Front View of the Model Mounted in the Tunnel.....	17
Figure 10(a). Velmex 8300 Traverser - Motor Controller.....	19
Figure 10(b). Velmex 8300 Traverser Assembly.....	19
Figure 11. Data Acquisition Hardware [Ref. 10].....	20
Figure 12. The Five-Hole Pressure Probe [Ref. 11].....	20
Figure 13. Data Flow Path.....	22
Figure 14. PPROBE Flow Chart.....	23
Figure 15. Calibration Manometer.....	24
Figure 16(a). PVA Program Flow Chart.....	26
Figure 16(b). PVA Program Flow Chart.....	27
Figure 17. Model Side View.....	29
Figure 18. Wing Alone Set at $22^\circ$ .....	31
Figure 19(a). Velocity Vectors, Mid-point of the Wing, No Canard.....	33

Figure 19(b). Streamlines, Mid-point of the Wing, No Canard.....	34
Figure 20. Total Pressure Coefficient Contours, Mid-point of the Wing, No Canard.....	35
Figure 21(a). Velocity Vectors, Trailing-Edge of the Wing, No Canard.....	36
Figure 21(b). Streamlines, Trailing-Edge of the Wing, No Canard.....	37
Figure 22. Total Pressure Coefficient Contours, Trailing-Edge of the Wing, No Canard.....	38
Figure 23. Model set at $22^\circ$ , Canard set at $7^\circ$ Incidence.....	40
Figure 24(a). Velocity Vectors, Trailing-Edge of the Canard.....	42
Figure 24(b). Streamlines, Trailing-Edge of the Canard.....	43
Figure 25. Total Pressure Coefficient Contours, Trailing-Edge of the Canard.....	44
Figure 26(a). Velocity Vectors Mid-point of the Wing, With Canard.....	47
Figure 26(b). Streamlines, Mid-point of the Wing, With Canard.....	48
Figure 27. Wing at $22^\circ$ with Canard Deflected $7^\circ$ .....	49
Figure 28. Total Pressure Coefficient Contours, Mid-point of Wing, With Canard.....	50
Figure 29(a). Velocity Vectors, Trailing-Edge of the Wing, With Canard.....	52
Figure 29(b). Streamlines, Trailing-Edge of the Wing, With Canard.....	53
Figure 30. Total Pressure Coefficient Contours, Trailing-Edge of the Wing, With Canard.....	54
Figure 31. Vortex Path .....	56



## **ACKNOWLEDGEMENTS**

I offer my sincere gratitude to Professor Richard M. Howard. His untiring dedication and hard work are the reason this thesis was completed. I wish all the best of luck to a man so deserving.

I also wish to thank Mr. Don Meeks and Mr. Ron Ramaker for their outstanding and timely technical support during this study.

Lastly, but most importantly, I would like to thank my neglected family, especially my wife Laurie, for their patience and understanding.

## **I. INTRODUCTION**

### **A. SUPERMANEUVERABILITY**

In modern aerial combat, the ability of an aircraft to maneuver into the post-stall regime for short periods of time is crucial to its survivability. Current fighter aircraft, such as the Israel Aircraft Industries Lavi, SAAB Gripen or European Fighter Aircraft (EFA), employ a close-coupled canard to allow for continued maneuvering where conventional aircraft may have departed from controlled flight. This increase in maneuverability results from the favorable interaction of vortices over a delta wing. Double-delta wings or leading-edge strakes, such as those on the F/A-18 or F-16, have been used to enhance the lift in the same way. However, until recently, only the SAAB Viggen had been successful at using a canard to maintain lift at high angles of attack.

### **B. CLOSE-COUPLED CANARD**

The advantages of a close-coupled canard have been known since the 1960's. It was found by Behrbohm [Ref. 1] that the combination of a close-coupled canard and delta-wing, of small aspect ratios, has significant advantages over a conventional delta-wing or wing/horizontal-tail configured aircraft. Both  $C_{Lmax}$  and the angle of attack for  $C_{Lmax}$  are increased by the addition of a delta-canard to a delta-wing. During the 1970's, an experiment was performed by Lacey [Ref. 2] to determine the correct canard geometry and location for maximum lift enhancement. As a result of Lacey's work, Behrbohm's conclusions concerning the use of a delta-canard with a delta-wing were confirmed. It was found that locating such a canard above, rather than coplanar with, the main wing produced the most favorable vortex interaction. In the 1980's canard research continued. Work by Er-El [Ref. 3], Stoll and Koenig [Ref. 4] and Calarese [Ref. 5] provided insight into

canard/wing vortex interaction. However, most of their work was done at low to moderate angles of attack with little or no canard deflection.

At the Naval Postgraduate School, a series of experiments has been conducted to compare a close-coupled canard model, designed in accordance with Lacey's work [Ref. 2], to a wing-alone configuration. The first tests, conducted by Kersh [Ref 6], were to determine the forces on the model up to  $50^\circ$  angle of attack. During these tests, the canard was deflected between plus and minus  $25^\circ$  to determine which canard incidence angle would produced the maximum lift at a given model angle of attack. It was determined that the maximum lift enhancement of the canard/wing configuration over the wing-alone configuration occurred at  $22^\circ$  model angle of attack with the canard set at a positive  $7^\circ$  incidence. At this angle of attack, the first stall (loss of lift) occurred on the wing for the wing-alone case; the canard vortex seemed to provide a reattaching mechanism. Reference 6 is a complete discussion of Kersh's work.

### **C. THESIS OBJECTIVE**

This thesis was the second in the series of tests conducted for canard/wing lift enhancement. The model was set for maximum lift enhancement conditions as described above. Wake surveys were then conducted using a nulling five-hole pressure probe. The objective was to gain quantitative data concerning the total pressure and velocity profiles at three crossplane locations, while the model was operating at  $22^\circ$  angle of attack, with and without the canard. By this approach the effect of the canard leading-edge vortex on the main wing leading-edge vortex would be further investigated. From the pressure data, velocity-vector plots and total-pressure contours were generated for a comparison between the wing-alone and canard/wing configurations. Such a comparison served to help reveal the enhancement mechanism at an angle of attack beyond those investigated previously.

## II. BACKGROUND

### A. VORTEX GENERATION

The dominant characteristic of flow over a highly-swept delta wing is the generation of a strong leading-edge vortex as shown in Figure 1. These vortices are the result of separated flow at medium to high angles of attack. As opposed to the chaotic, separated flow associated with stall, these vortices are stable, coherent sources of high energy and generate areas of low static pressure resulting in localized regions of enhanced lift at the leading edge.

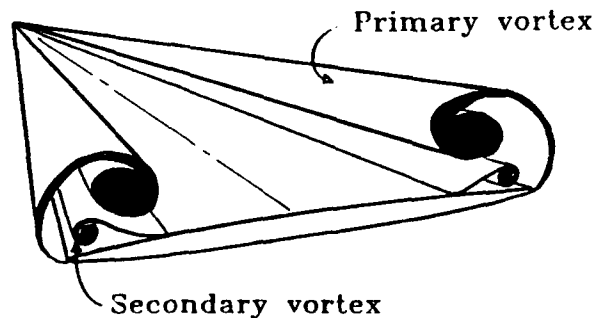


**Figure 1. Flowfield Over the Top of a Delta Wing**

The strongest vortices result from planforms with sharp, highly-swept ( $>50^\circ$ ) leading edges. The sharp leading edge promotes the leading-edge separation necessary for vortex generation. However, the combination of large sweep and a sharp leading-edge produces a large planform with a low  $(L/D)_{\max}$  and a shallow lift-curve slope. The net result is poor range and endurance, high approach speeds and large deck space requirements. These characteristics are extremely undesirable traits for a carrier-based aircraft. [Ref. 2]

The requirement for carrier suitability, therefore, dictates the design of an aircraft with rounded, moderately-swept leading edges. When such a planform maneuvers to high angles of attack the vortices produced are less coherent and of lower energy. Therefore, some mechanism is needed to energize or induce these vortices to remain coherent at high angles of attack, without the added penalty of poor cruise performance.

## B. CANARD CHARACTERISTICS

Canards are separated into two broad categories: long-coupled or close-coupled (see Figure 2).

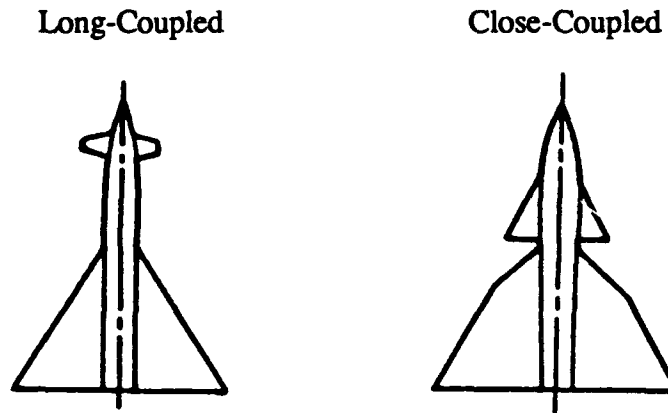


**Figure 2. Canard Categories [Ref. 2]**

Long-coupled canards are of the type used primarily as a control surface rather than as a lifting surface. Examples of this type are found on almost all missiles and on some aircraft, such as the XB-70, the Concorde and the X-31 experimental aircraft. A close-coupled canard may provide a significant portion of the aircraft total lift in addition to being a control surface. The aircraft listed at the beginning of the introduction are examples of close-coupled designs.

Extensive research has been performed related to the phenomenon of canard/wing interaction [Ref. 2,3,6,7]. These experimental results indicate two possible mechanisms by

which the flowfield from the canard affects the flowfield around a wing. One is the impingement of the canard downwash on the apex of the main wing; the other is the favorable interference between the canard and wing leading-edge vortices. For low angles of attack, the canard produces a downwash field within its span and an upwash field outside its span. The result is a nonuniform angle of attack on the main wing. The inner (inboard of the canard span) and forward portions of the wing have a lower effective angle of attack than the outer and rear portions. The flow over the wing behind the canard tends to remain attached while the flow outside the canard or at the rear of the wing tends to separate. The probable result is an overall loss of lift on the main wing which has to be compensated for by the increased lift of the canard. In fact, studies such as Reference 6 show that at low angles of attack ( $<10^\circ$ ) the lift-curve slope of a model with or without a canard is identical. The second mechanism occurs at higher angles of attack. As the angle of attack is increased, a strong leading-edge vortex is formed on the canard. As this vortex moves over the wing it acts to energize the wing leading-edge vortex, thereby delaying Vortex-Breakdown (VBD). [Ref. 3,7]

### **1. Canard Versus Tail**

The first advantage of the canard over the horizontal tail design arises from a difference in trim requirements. A conventional tail balances an aircraft in flight by producing a downward lift vector. This results in an initial decrease in lift for a trim to lower speed. A canard, on the other hand, produces a large nose-up pitching moment which must be balanced by a positive elevon deflection on the main wing. The result is increased lift for the canard aircraft due simply to the difference in the trim requirements. This effect is most dramatic when comparing a pure delta-wing aircraft with a canard/delta-wing combination. Figure 3 shows the wing loading, approach speed and lift coefficient for three high-performance aircraft. The Viggen has approximately the same wing loading

as the F-106, but the Viggen approach speed is 34 knots slower than that of the F-106 with a 70% higher lift coefficient.[Ref. 2]

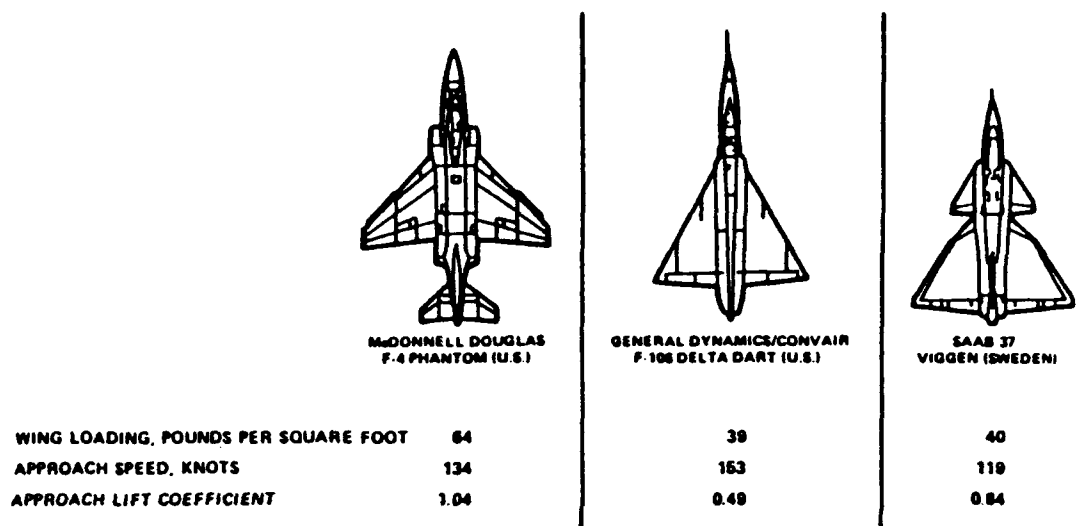


**Figure 3. Characteristics of the F-4,F-106 and Viggen [Ref. 2]**

Additionally, the increased lift of a canard-configured aircraft cannot be completely accounted for simply by the increased lifting area of the canard. Work done by Er-El [Ref. 3] showed an increase in normal-force coefficient of 18% at  $22^\circ$  angle of attack, over that of a corresponding wing-alone configuration. The canard itself added only 9% to the total lifting area. Likewise, extensive work done by Lacey [Ref. 2] showed similar results. Figure 4(a) shows that the stall of a wing alone and of a wing/conventional-tail combination occurs at about  $21^\circ$ , whereas there is no indication of stall for the canard-configured aircraft below  $32^\circ$ . Additionally, for low values of  $C_L$  drag of the all three configurations was the same, see Figure 4(b). Therefore, during cruise flight the canard/wing configuration would

configuration. Again, the increase in lift of the canard/wing configuration at high angles of attack could not be completely accounted for by the additional lifting area of the canard.

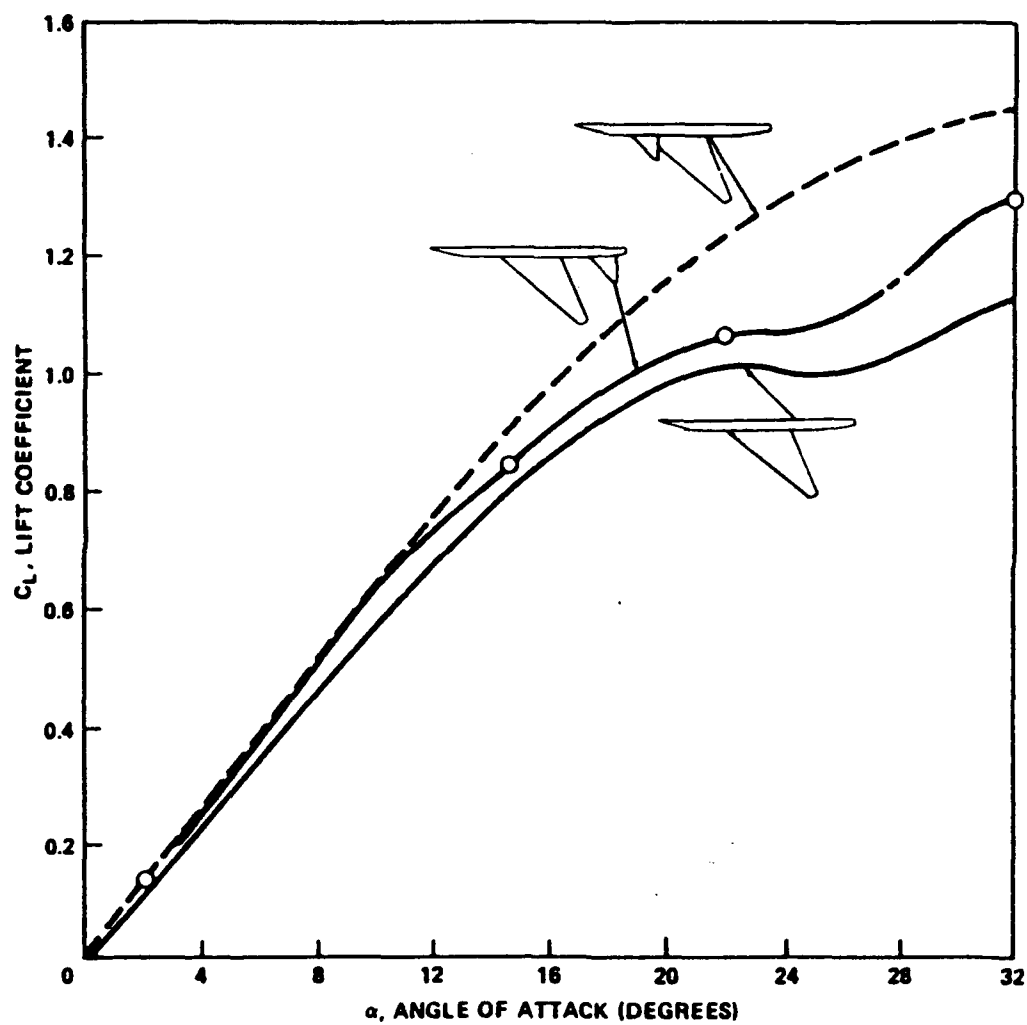


Figure 4a. Lift Coefficient due to a Canard and Horizontal Tail [Ref. 2]



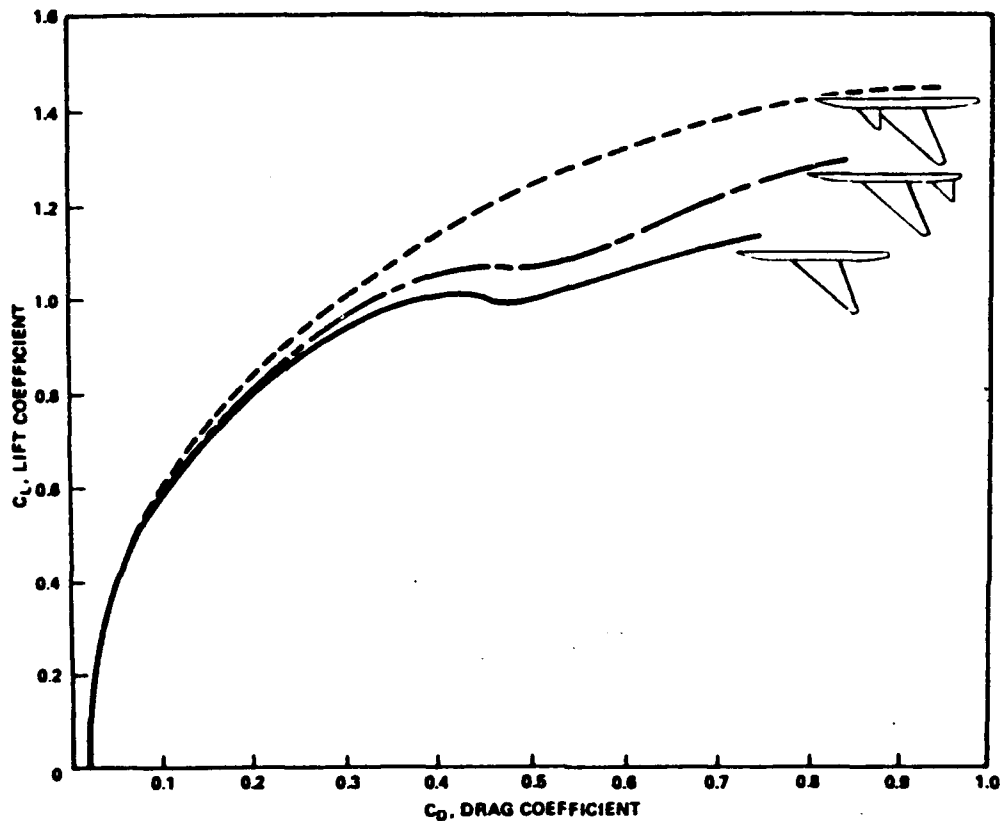


Figure 4b. Drag Polar for a Canard and Horizontal Tail [Ref. 2]

### C. VORTEX INTERACTION

Er-El [Ref. 3] conducted an investigation of vortex trajectory and breakdown using canard/wing configurations at angles of attacks between  $13^\circ$  and  $30^\circ$ . Er-El states that near the wing apex, the downwash of the canard forces the wing vortex down closer to the wing, while further downstream the vortex trajectory is more influenced by the canard leading-edge vortex than by its downwash. That is, near the trailing edge, the wing vortex

is displaced upward and outward, away from the adverse pressure gradient. Er-El also states that a close-coupled canard causes a delay in the onset of the breakdown of the wing leading-edge vortex, which originates at the wing apex. This delay is possibly a result of the wing vortex movement away from the adverse pressure gradient, thereby making it more stable.

#### **D. PREVIOUS TESTING**

At the Naval Postgraduate School, Kersh performed force measurements on a model designed in accordance with Lacey's guidelines. [Ref. 6] Kersh investigated the effects of canard-enhanced lift at five angles of attack between  $10^\circ$  and  $48^\circ$ . Figure 5 [Ref. 6] is the lift curve that resulted from that study. Note that as mentioned earlier the point of maximum lift enhancement occurred at  $22^\circ$ , the point of first stall for the wing/body configuration. At  $22^\circ$  there was a 34% increase in lift for the canard/wing configuration over that for the wing/body configuration. In addition, surface flow visualization indicated the dramatic effect the canard vortex had on the main wing flowfield. However, while the flow visualization gave outstanding insight into the nature of the flow on the surface of the wing, it did not say much about what occurred off the wing surface. That flowfield study was the major objective of this study.

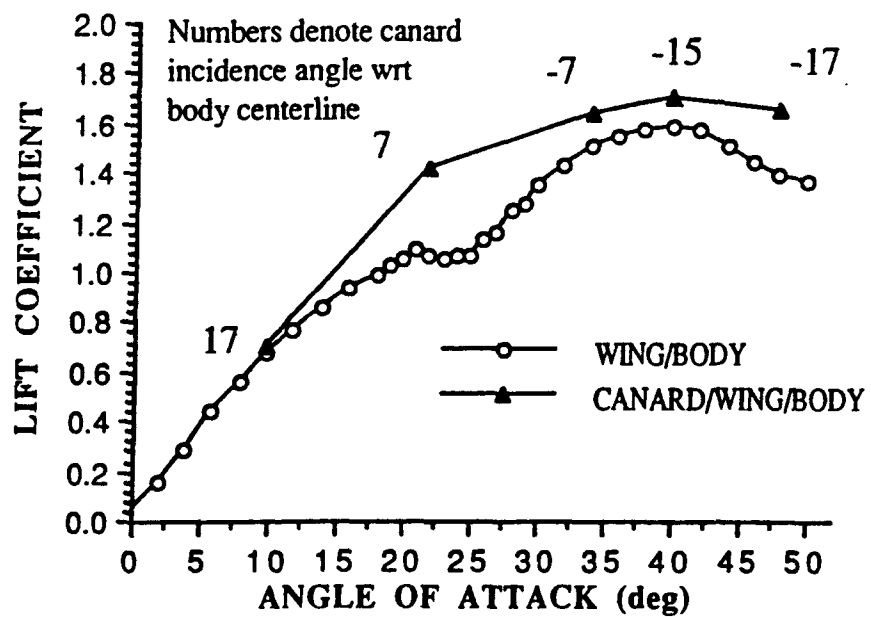


Figure 5. Lift Coefficient of Wing/body and Maximum Lift of Canard/Wing  
[Ref. 6]

### III. EXPERIMENT AND PROCEDURES

#### A. PURPOSE

This study was conducted to investigate the effects of vortex interference on the flowfield around the main wing of a close-coupled canard and wing combination. A nulling five-hole pressure probe was used to make flowfield pressure measurements in the three crossplanar grid locations shown in Figure 6. These pressure measurements were then used to determine local flow velocities, pressures, and pitch and yaw angles for use in mapping the position and interaction of canard and wing vortices.

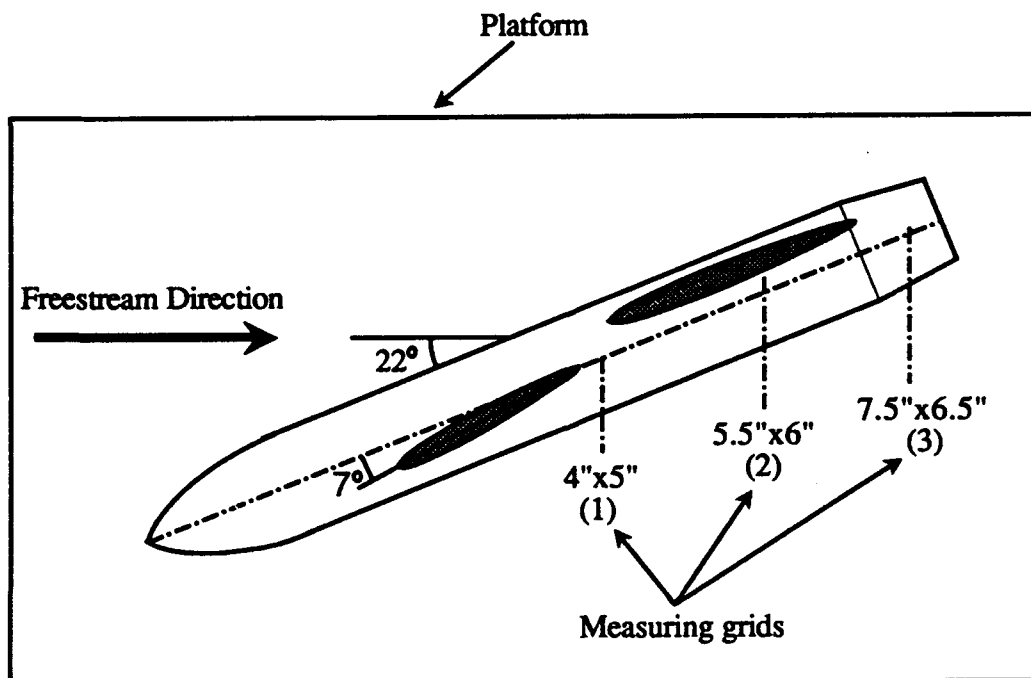


Figure 6. Model Overview

## B. APPARATUS

The primary equipment used in this study were a wind tunnel, a close-coupled canard model, a three-dimensional traversing mechanism, a rotary pressure transducer, a data acquisition system, and a nulling five-hole pressure probe.

### 1. Wind Tunnel

The tunnel was of the close-circuit, single-return type. It measured 64 feet in length and between 21.5 and 25.5 feet in width with a test section cross-sectional area of 8.75 square feet. The tunnel was powered by a 100hp electric motor coupled to a three-bladed variable pitch fan via a four-speed transmission. Figure 7 is a schematic of the tunnel.

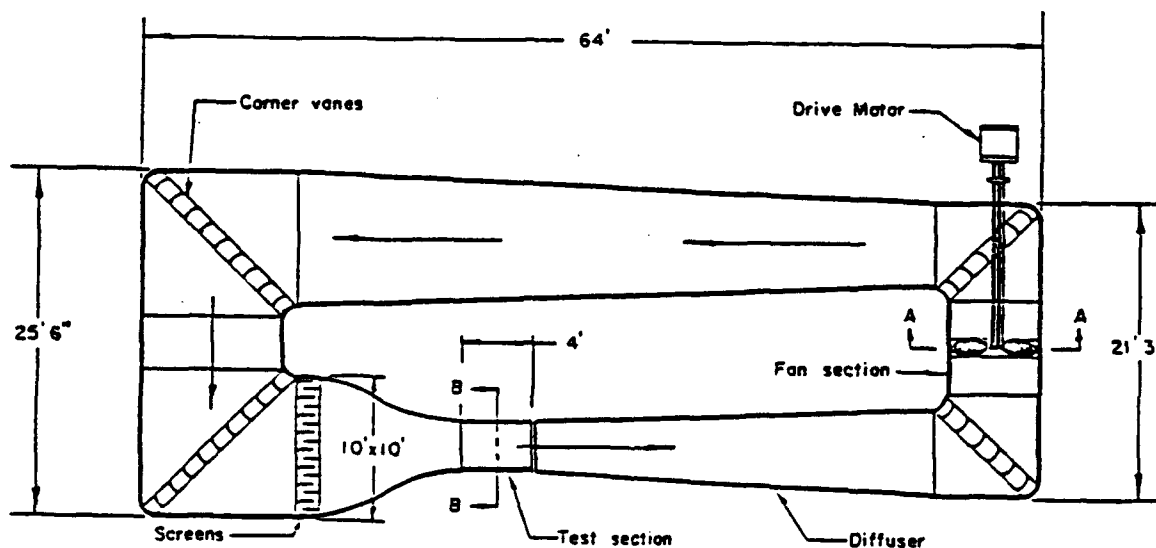


Figure 7. Naval Postgraduate School Wind Tunnel [Ref. 8]

Tunnel turbulence was minimized by the use of stator blades, turning vanes and turbulence screens. Eight stator blades were used to remove swirl imparted to the flow by the fan blades. Turning vanes were located at each corner to turn the flow while maintaining its kinetic energy and turbulence screens were placed in the settling chamber.

The test section measured 45 inches by 28.5 inches with a cross-sectional area about one tenth that of the settling chamber. The test section was rectangular with slightly divergent walls to account for boundary layer growth. Breather slots at the far end of the test section were used to keep the test section at approximately atmospheric pressure. Due to the configuration of the pressure measuring equipment, ambient atmospheric pressure was used as the reference static pressure rather than test section static pressure. [Ref. 8]

Tunnel velocity was set by reference to a water manometer that measured the difference in static pressure between the settling chamber and the test section. The static pressures in the settling chamber and at the test section entrance were determined by reference to four pressure ports, one on each wall. The pressures from these ports were averaged by a common manifold prior to the manometer. The manometer measured the pressure difference in centimeters of water and the test section velocity was then determined by equation (1).

$$V = \{(2 \cdot 2.0475 \cdot P_{\text{cmH}_2\text{O}}) / (\rho \cdot K)\}^{1/2} \quad (1)$$

where:

V	Test Section Velocity (ft/sec)
2.0475	Converts From Centimeters of Water to Lbf / ft <sup>2</sup>
P <sub>cmH<sub>2</sub>O</sub>	Manometer Reading (cm of water)
ρ	Density of Air (slugs/ft <sup>3</sup> )
K	Tunnel Calibration Factor (P <sub>cmH<sub>2</sub>O</sub> /q)

The tunnel calibration factor, the ratio of the static-pressure ratio to the test section dynamic pressure, was determined to be 0.925.

## **2. Model Design**

The model used in this study was originally used by Kersh [Ref. 6] and was designed in accordance with the earlier work of Lacey [Ref. 2]. During Lacey's studies, a canard-area-to-wing-area ratio of 0.20 as referenced to the model centerline of the fuselage was used. Because it was desired to accommodate an internal mechanism for a movable canard, the fuselage of this model was larger than that of Lacey's model. Therefore, this model was designed with an exposed canard-area-to-wing-area (wing referenced to the centerline of the fuselage) ratio of 0.20. If the area ratio had not been determined this way, a canard exposed area much smaller than Lacey's would have resulted. If the area ratio of Lacey's model had been determined by this same method, a ratio of 0.13 would have resulted. Consequently, an exposed canard-area-to-wing-area ratio of 0.20 compared favorably with that of Lacey's model.

Lacey's work also showed that the relative position of the canard to the wing was crucial for constructive canard/wing interference. According to Reference 2, the longitudinal position of the canard ( $X$ ), non-dimensionalized by the mean aerodynamic chord (MAC) of the wing referenced to the fuselage centerline ( $X/C_{mac}$ ), should not be greater than  $X/C_{mac}=1.5$ . The longitudinal distance was measured from the 40% chord location of the exposed canard root to the quarter chord of the wing MAC. Also, there should be no overlap of the main wing and canard. As a result, the canard was positioned at  $X/C_{mac}=1.2$ . The canard vertical position was  $Z/C_{mac}=0.2$ ; which was chosen such that it would match Lacey's model.

The wing and canard were both an NACA 64A008 airfoil section, which was the same section used by Lacey. The canard had a leading-edge sweep of  $60^\circ$ , a straight-taper of 0.1 and an aspect ratio of 2.0. The wing had a leading-edge sweep of  $50^\circ$ , a straight-

taper of 0.15 and an aspect ratio of 3.0. These planforms were chosen to ensure that strong leading-edge vortices would be generated. Unlike the sharp leading-edge model used in Er-El's studies [Ref. 3], both the canard and wing had rounded leading edges. No attempt was made to trip the boundary layer. Planform geometry was derived from equations (2), (3) and (4). [Ref. 6]

$$AR = 2\{b/C_R(1+\lambda)\} \quad (2)$$

$$AR = b^2/S \quad (3)$$

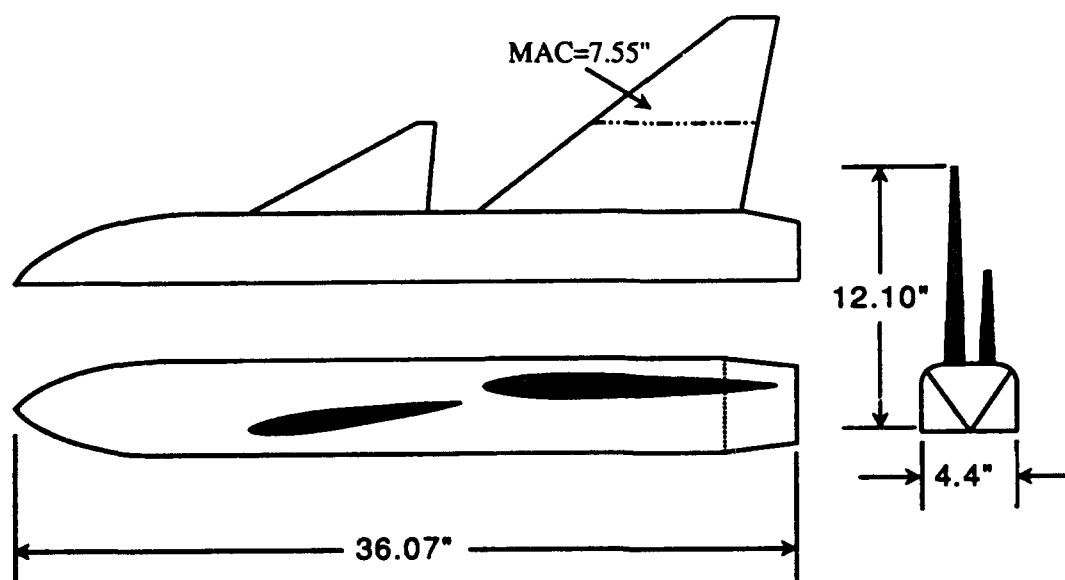
$$MAC = 2/3\{C_R + C_t - [C_R C_t / (C_R + C_t)]\} \quad (4)$$

Where:

AR	Aspect Ratio
b	Span
C <sub>R</sub>	Length of Root Chord
C <sub>t</sub>	Length of Tip Chord
λ	Taper Ratio (C <sub>t</sub> /C <sub>R</sub> )
S	Area of Wing or Canard
MAC	Wing Mean Aerodynamic Chord

Figure 8 is a schematic of the model and contains a listing of its geometric data. Reference 6 contains a thorough description of the model's design. Because the five-hole pressure probe was not long enough to reach the model mounted on the tunnel floor, a platform was constructed to elevate the model (see Figure 9). The effect on the flowfield should be minimal for the half-model, as the raised platform acted in a similar manner to the reflection plane.





	<u>WING</u>	<u>CANARD</u>
Airfoil Section (NACA)	64A008	64A008
Area (semi-span), in <sup>2</sup>		
Projected Area	97.9	50.7
Exposed Area	59.6	19.3
Exposed Semi-Span, inches	9.1	4.4
Centerline Semi-Span, inches	12.1	7.4
Chord, inches		
Exposed Root	11.0	8.0
Centerline Root	14.0	13.3
Tip	2.1	0.8
Aspect Ratio	3	2
Taper Ratio	0.15	0.1
Sweep Angle in Degrees		
Leading Edge	50	60
Trailing Edge	10.6	5.5
Incidence Angle in Degrees	0	-
Dihedral	0	0
Twist	0	0

**Figure 8. Model Geometric Data**

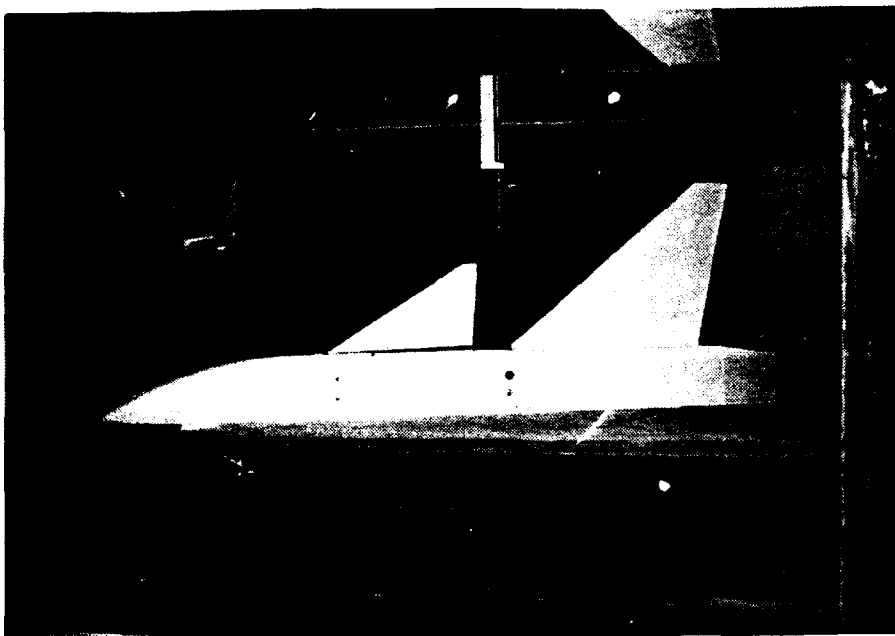


**Figure 9(a). Side View of the Model Mounted in the Tunnel**

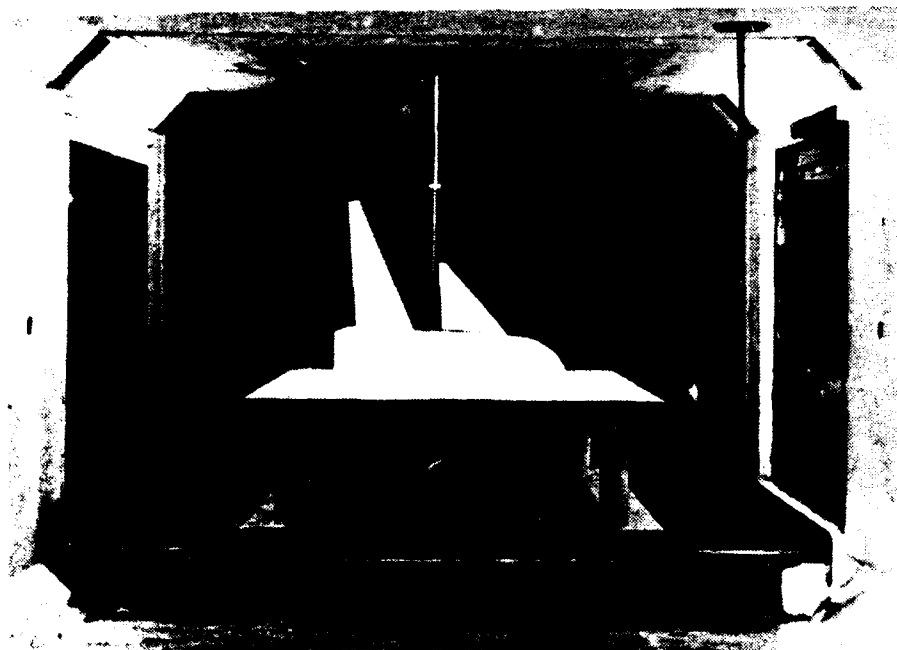


**Figure 9(b). Front View of the Model Mounted in the Tunnel**

### **3. Velmex 8300 Three-Dimensional Traverser System**

The Velmex system, shown in Figure 10, was used to accurately position the five-hole pressure probe in the test section. The system consisted of the traverser mechanism, Figure 10(b), and the motor controller, Figure 10(a). The traverser mechanism was composed of leadscrews, slides and motor/jackscrew assemblies. Each motor was a 200-step-per-revolution, 10-amp stepping motor with a maximum velocity of 3000 steps per second. The motor step size was 1/200 of a revolution which equated to 0.000125 inch. The three motor assemblies received their commands from the controller which was capable of interpreting signals from either a parent computer or manual inputs at the controller. During this study the controller received its commands from a parent PC/AT.[Ref. 9]

### **4. Rotary Pressure Transducer and Data Acquisition System**

A 48-port rotary pressure transducer (commonly referred to as a Scanivalve®) read each port of the pressure probe twice per measurement point. The data acquisition system, shown in Figure 11, consisted of the required hardware and software to allow a PC/AT to acquire the pressure data. The Scanivalve® put out a 7-bit binary coded decimal signal that corresponded to the port currently being monitored. This arrangement allowed remote, electronic monitoring and control of the Scanivalve® assembly. [Ref. 10] After the pressure signal, in the form of an analog voltage, left the Scanivalve® it was passed to the Relay Multiplexer, then to the Digital Multimeter (DMM). The DMM converted the analog voltage signals to a digital form which were then sent to the computer for further processing.

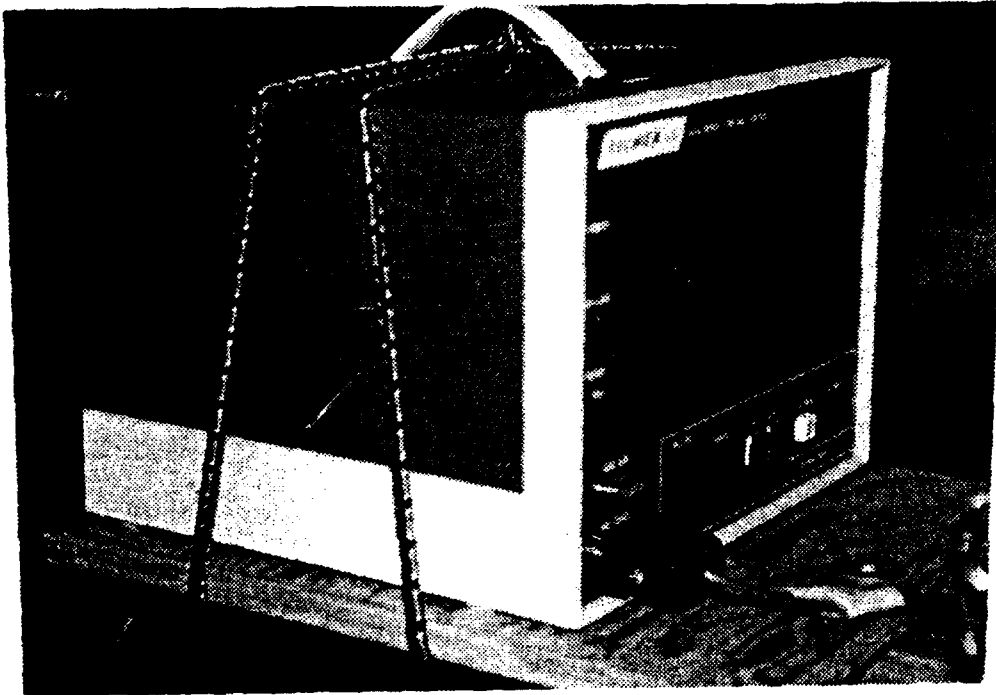


**Figure 10(a). Velmex 8300 Traverser - Motor Controller**

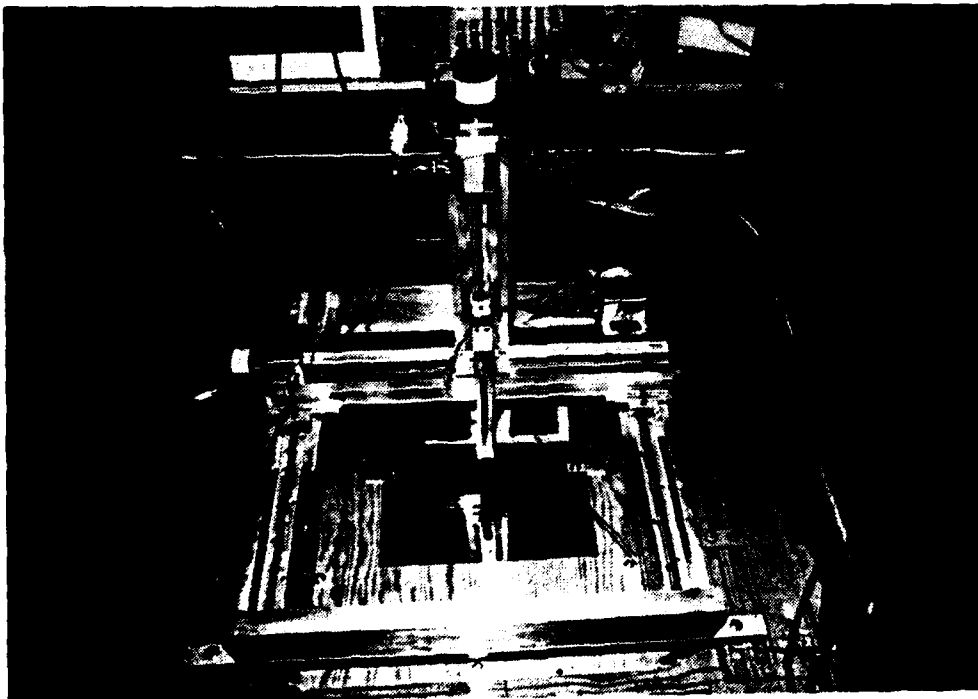


**Figure 10(b). Velmex 8300 Traverser Assembly**

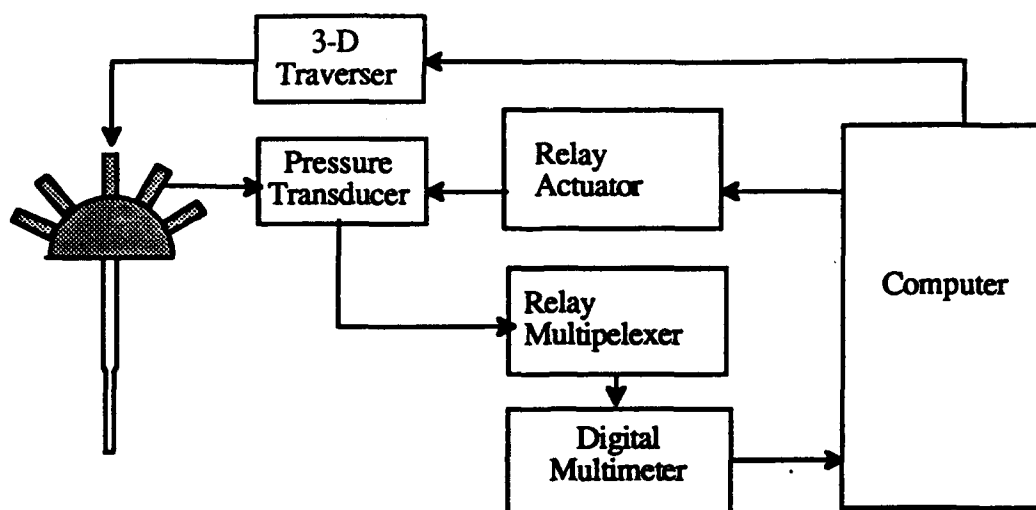


**Figure 11. Data Acquisition Hardware [Ref 10]**

### 5. Five-Hole Pressure Probe

The three-dimensional five-hole pressure probe, shown in Figure 12, was made of corrosion-resistant, non-magnetic, stainless steel. It was 0.125 inches in diameter and 24 inches in total length. At the tip of the probe were five measuring holes. The center hole of the probe ( $P_1$ ) measured total pressure, the two lateral holes ( $P_2, P_3$ ) were used to measure yaw angle and static pressure, and the top and bottom holes ( $P_4, P_5$ ) were used for pitch information. [Ref. 11]

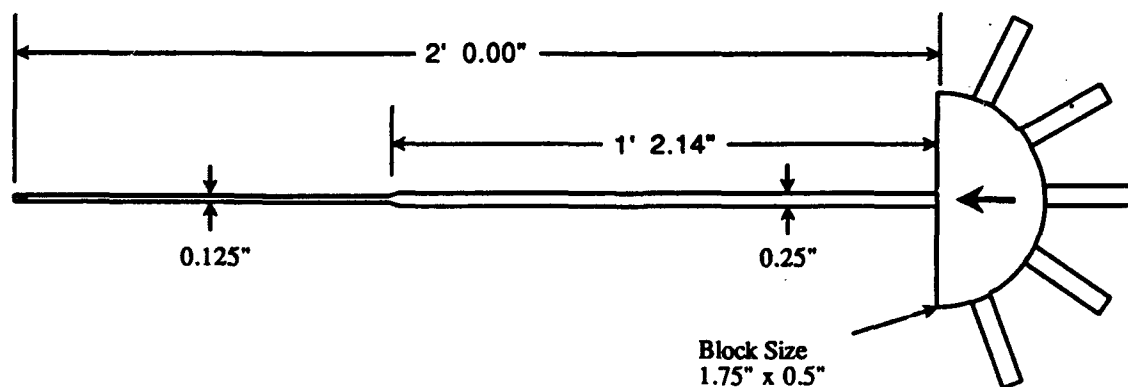


**Figure 12. The Five-Hole Pressure Probe [Ref. 11]**

## **C. EXPERIMENT SOFTWARE**

The software used in this study was developed by Lung during his work with the five-hole pressure probe [Ref. 10]. Some modifications were made to accommodate this work, but the flow of data remained essentially the same. Figure 13 is a schematic flowchart of the various programs and data files. The following sections discuss the individual programs.

### **1. PPROBE**

PPROBE (Appendix A), written in BASICA by Kindelspire [Ref. 12], and modified by Lung [Ref. 10], was used to control the data acquisition process. Figure 14 is the program flow chart for PPROBE. The two primary responsibilities of PPROBE were the control of the traverser and the recording of the data.

First, PPROBE was used to manually position the probe to the proper starting point in the tunnel, then the dimensions of the grid to be measured and the desired step size were entered. PPROBE calculated the total number of points to be measured, created the required number of data files and initialized the data acquisition equipment. The operator then physically nulled the probe and entered the observed yaw angle into PPROBE. PPROBE rotated the pressure transducer to the appropriate port and began measuring the analog voltage which corresponded to the pressure at that port. Finally, the data were displayed to the operator and he was given a chance to remeasure the data point. If the data were acceptable PPROBE moved the traverser to the next measuring point. At the completion of each column in the grid, the data were placed into a file to be used in the program PVA.

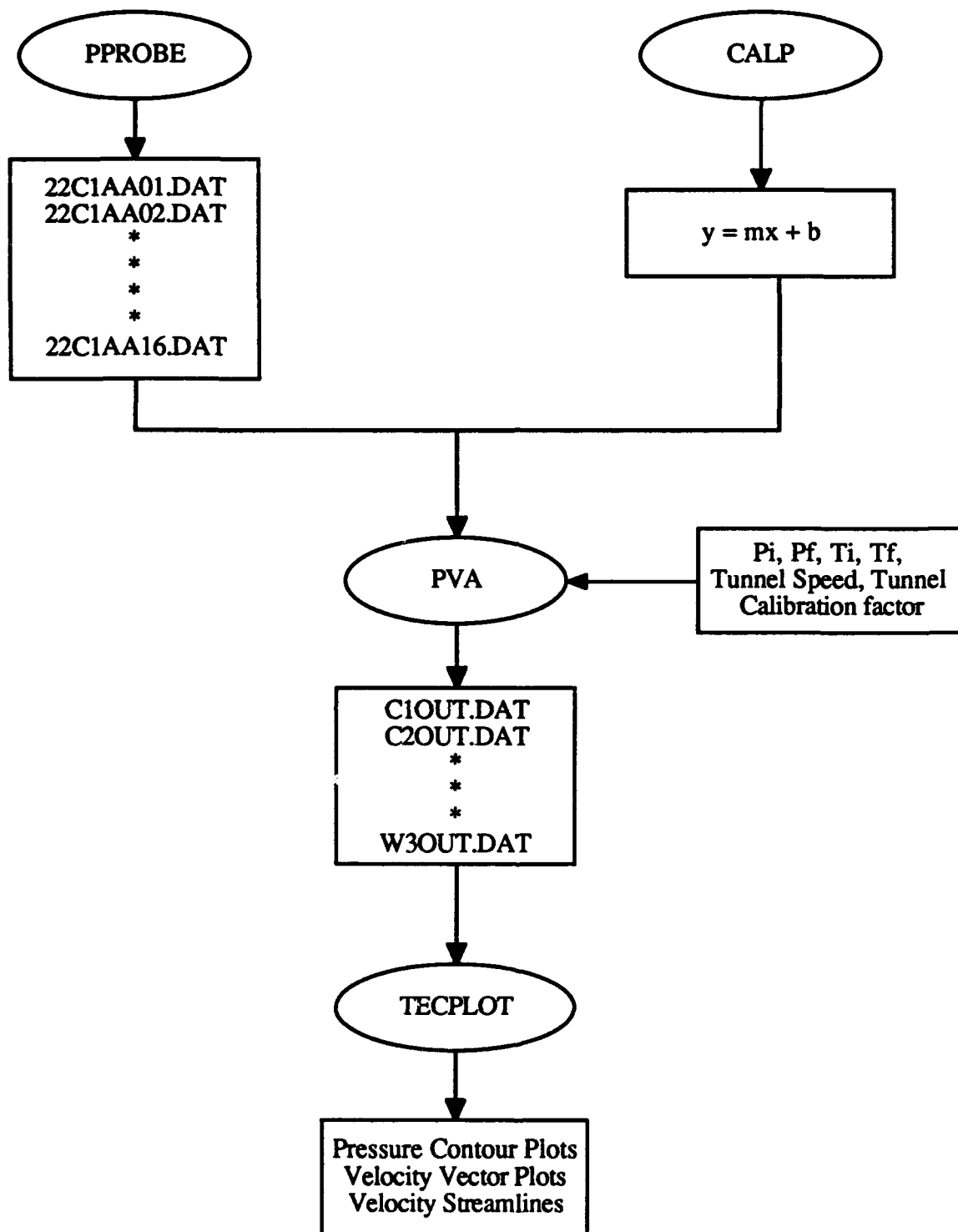


**Figure 13. Data Flow Path**

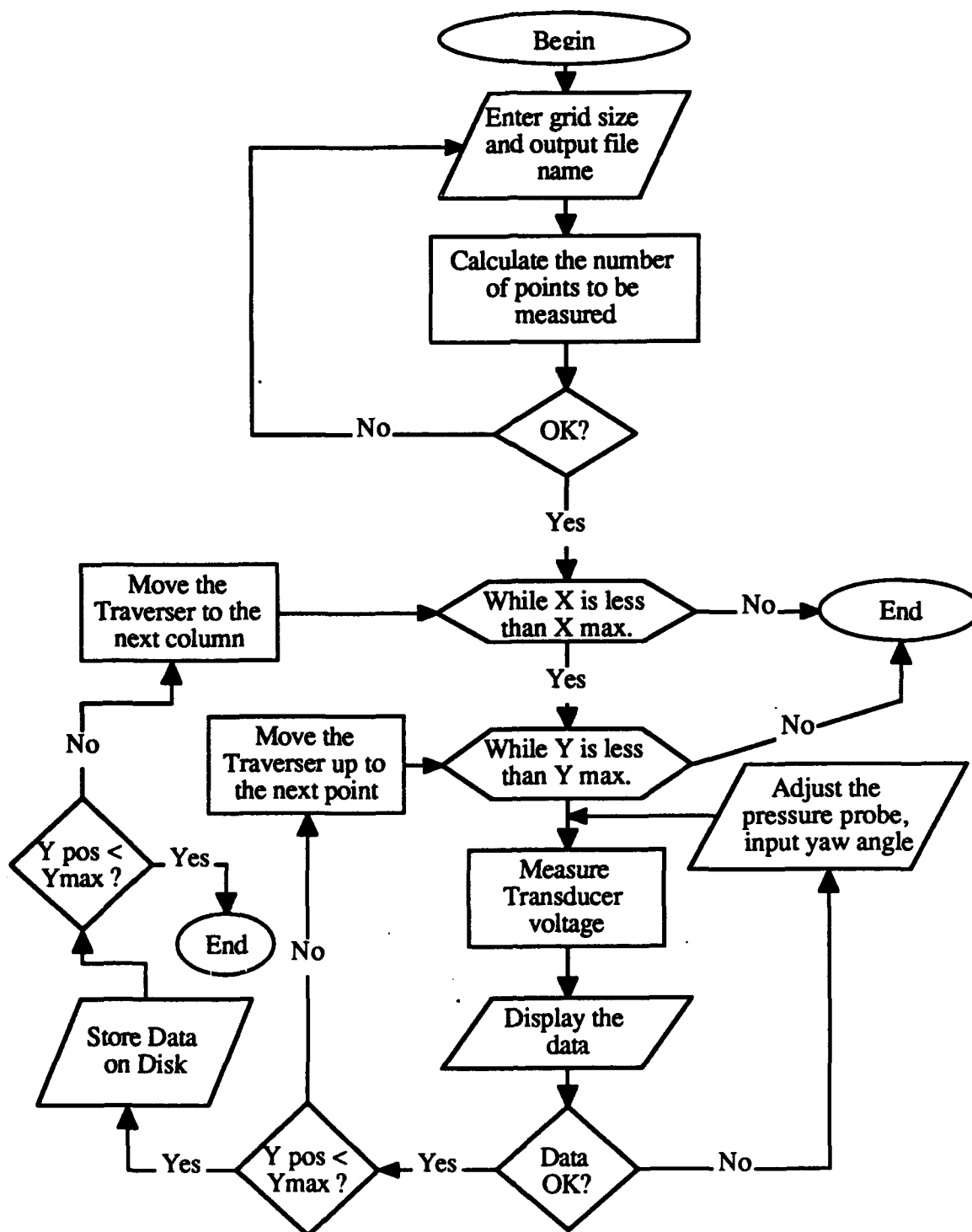


Figure 14. PPROBE Flow Chart



## 2. CALP

CALP (Appendix B), was written in BASICA and used to calibrate the pressure transducer prior to each data collection period. The calibration manometer is shown in Figure 15. Six pressures were recorded using the calibration manometer and the pressure transducer in the Scanivalve<sup>®</sup> to provide a known calibration curve for the experiment. A straight line was fit to the data, whose slope and intercept were input to the PVA program.

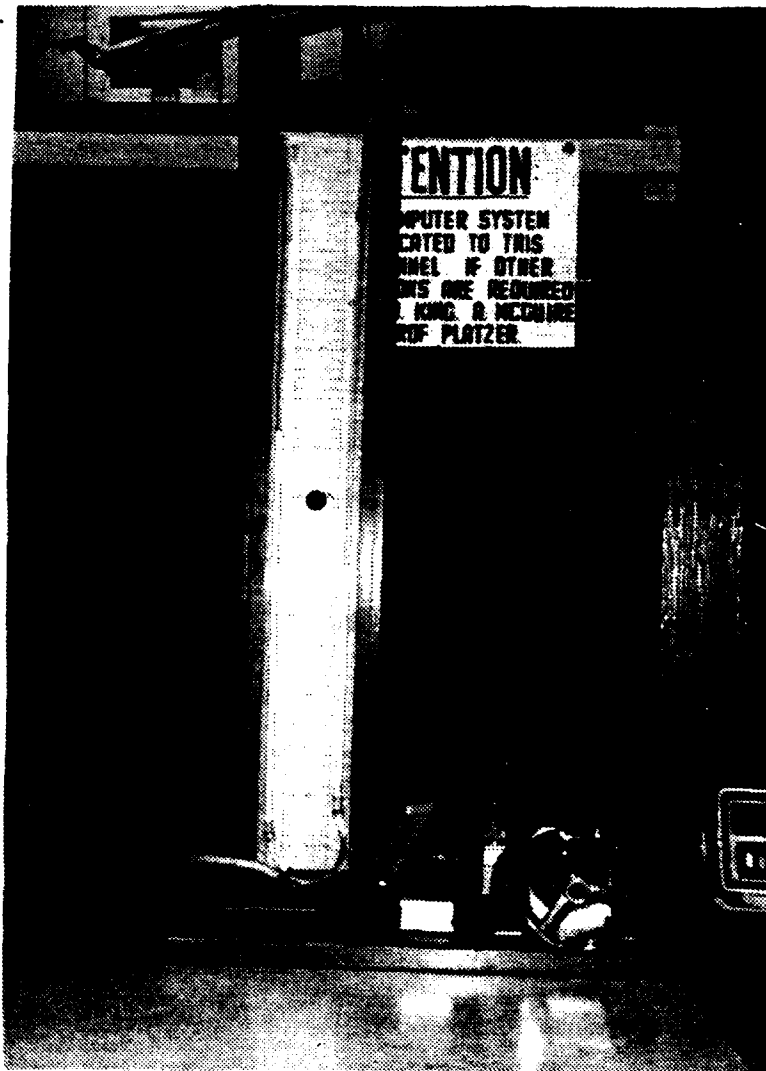


Figure 15. Calibration Manometer

### 3. PVA (Pressure Velocity Angle)

PVA (Appendix C) was a modified version of CONVERT, a Fortran program which combined the output of PPROBE and CALP to calculate the flowfield properties [Ref 10]. PVA used the pressure data, in the form of analog voltages, and yaw data from PPROBE, and combined them with the curve fit derived from the CALP output to determine the desired flowfield characteristics. See Figure 16 for the PVA flow chart.

Specifically, PVA determined:

- freestream velocity (V)
- crossflow components of freestream velocity ( $V_x$  and  $V_y$ )
- total pressure and total pressure coefficients
- static pressure and static pressure coefficients
- flow yaw and pitch angles

The pressure coefficients were determined as follows:

$$C_{PT} = (P_{T1} - P_{amb} - Q_1) / Q_1 \quad (5)$$

$$C_{ps} = (P_{s1} - P_{amb}) / Q_1 \quad (6)$$

Where:

$P_{T1}$  = Local Dynamic Pressure

$P_{s1}$  = Local Static Pressure

$P_{amb}$  = Room Ambient Pressure

$Q_1$  = Freestream (Tunnel) Dynamic Pressure

Due to the configuration of the pressure-measuring equipment, room ambient pressure was used as the reference static pressure in the pressure coefficient calculations. The output of PVA was put in an ASCII file for use by commercially available graphic software for plotting the desired output.

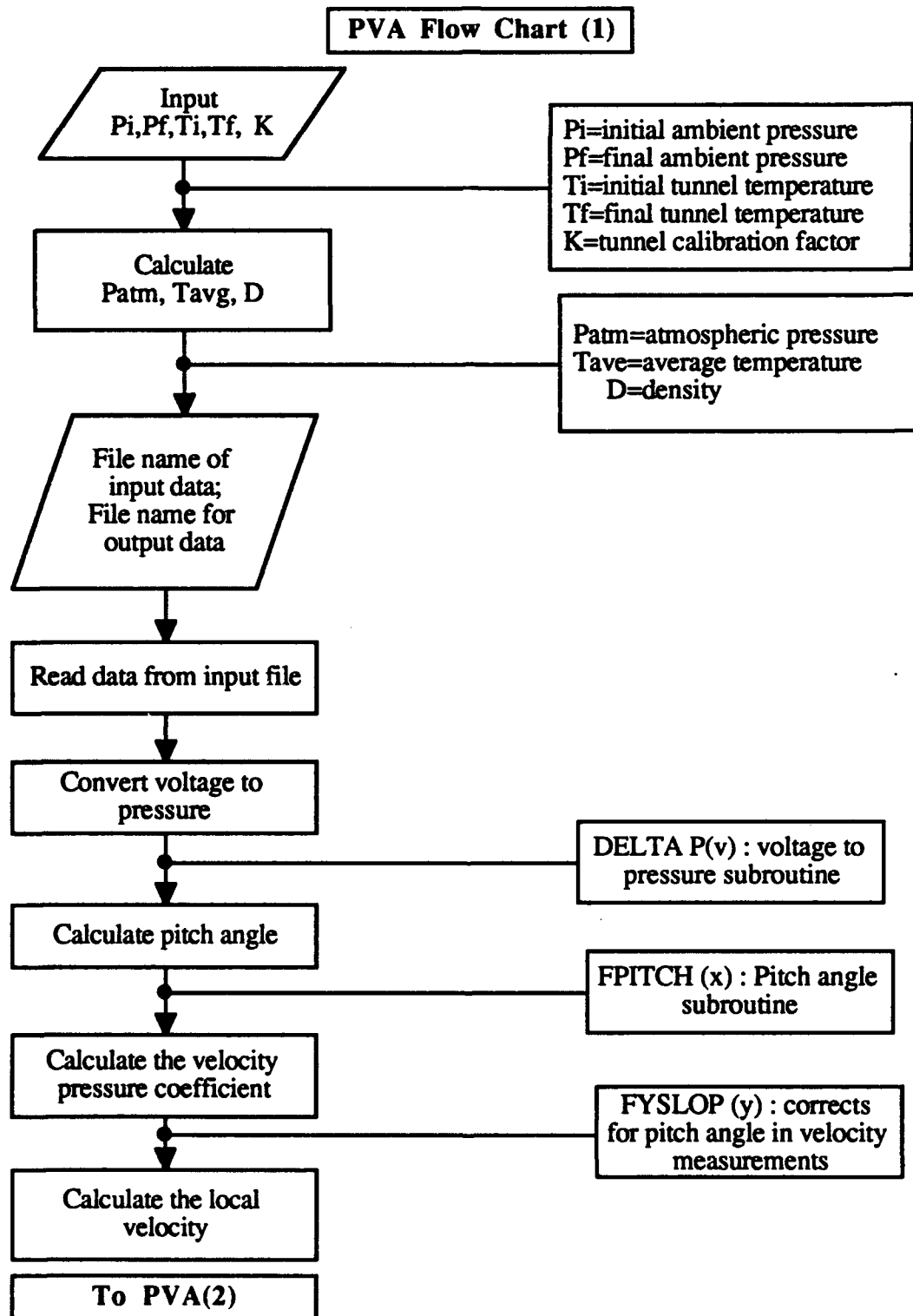


Figure 16(a). PVA Program Flow Chart

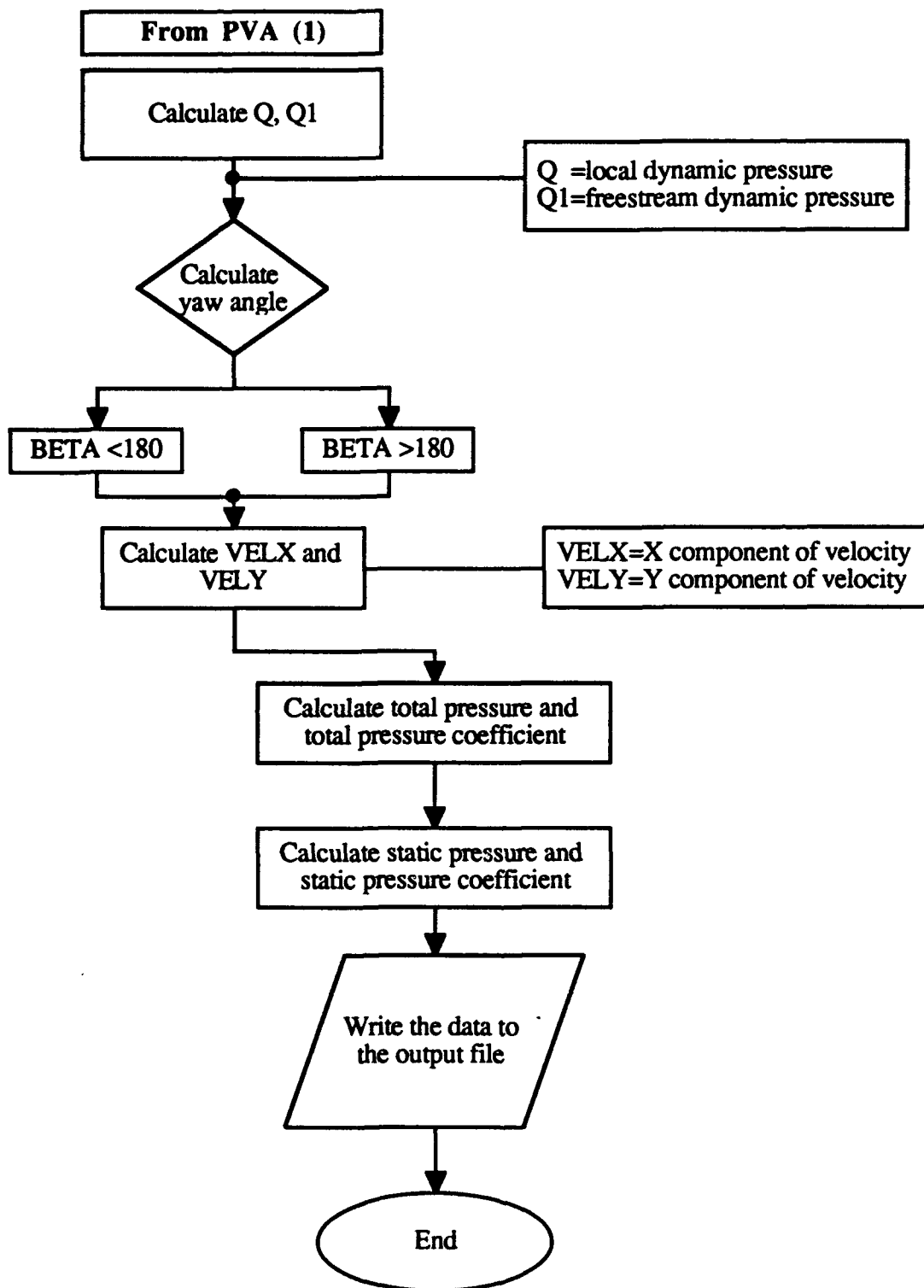


Figure 16(b). PVA Program Flow Chart

#### **D. EXPERIMENTAL CONDITIONS AND PROCEDURES**

To correlate these results with the results of Kersh, the experimental conditions were kept as constant as possible. A reference measured pressure difference of 17 cm of H<sub>2</sub>O was set, resulting in a test-section dynamic pressure of 37.63 lbf/ft<sup>2</sup> and an average velocity of 177 ft/s. The Reynolds number was  $Re=9.5 \times 10^5$  based on the main wing mean aerodynamic chord.

To account for possible tunnel crossflow, probe installation effects and flowfield disturbances caused by the model platform, an initial run was made without the model installed, to establish baseline yaw and pitch values. This measurement was again run at the end of testing to ensure the baseline values had not changed appreciably.

Measurements were made at three locations, numbered as shown in Figure 6. Grids 1 and 2 were mapped at 1/4" intervals, while grid 3 was mapped at 1/2" intervals. Note that the measuring plane of the grids were perpendicular to the freestream direction, rather than to the wing chord.

Grid 1 was 4" by 5" and was set just behind the canard trailing edge in order to capture the canard leading-edge vortex. Grid number 2 was 5.5" by 6" and was placed at the mid-point of the wing to capture the effect of the canard leading-edge vortex on the flowfield at that point. Finally, since flow visualization, completed earlier, had shown the flowfield beginning to lose its coherency near the trailing edge of the wing, grid number 3 was placed just behind the trailing edge of the wing. Grid 3 measured 7.5" by 6"; because its size would have necessitated an excessive amount of tunnel time to complete at 1/4" intervals, it was mapped at 1/2" intervals.

#### IV. RESULTS

The following sections discuss the results of this study. In each section there will be three plots. The first will be a plot of flowfield velocity vectors, then a plot of the velocity streamlines, followed finally by a plot of total-pressure-coefficient contours. Flow visualization results are also included to correlate with the measured data. All the plots are scaled in inches, with "X" plotted horizontally, transversely to the tunnel and "Y" plotted vertically to the tunnel. Locations on the plots will be identified by listing the coordinates in the standard (X,Y) convention. Also, the plotted data are shown with cutaway views of the model geometry to establish the relative position of the measuring plane to the model. At grid 1 the actual measuring plane was just beyond the canard trailing edge, but the canard cross-section at the trailing edge will be shown for reference. Likewise, at station three the grid was located after the main wing trailing edge, but the wing cross section 3 is shown to indicate the relative position of the vortices and main wing (see Figure 17).

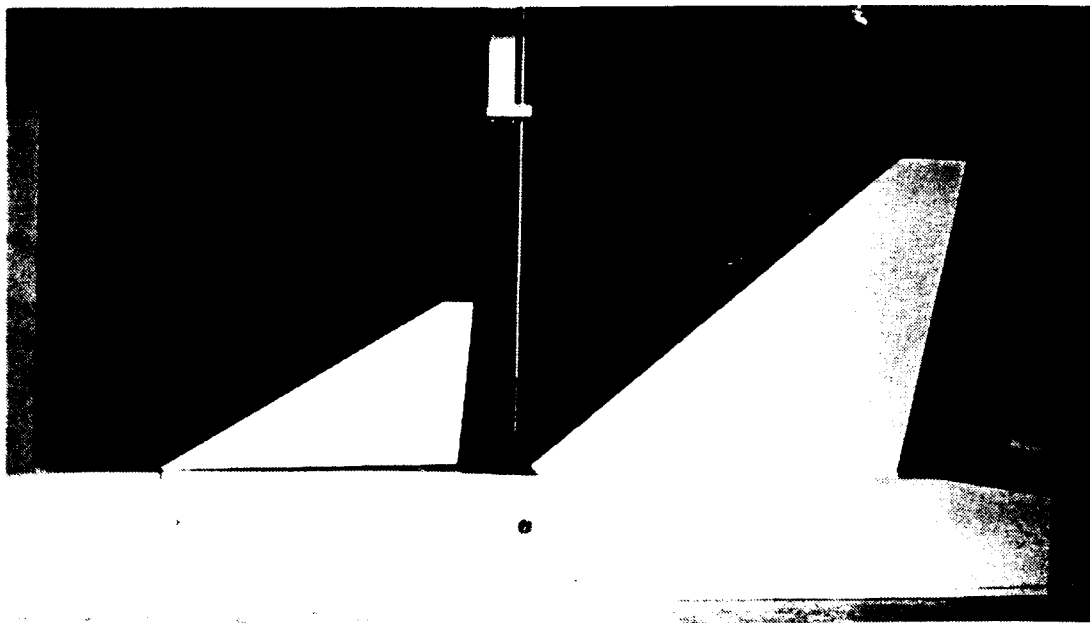


Figure 17. Model Side view

Because of the dynamic nature of flowfields surrounding aerodynamic surfaces at high angles of attack, there were regions in which the capabilities of the probe were exceeded. In particular, the probe was unable to make accurate measurements downstream of stalled aerodynamic surfaces or near the core of a vortex. Precisely, in these regions the probe could not be nulled - that is,  $P_2$  and  $P_3$  could not be made equal. The main effect of this probe limitation was that the exact positions of the vortex cores could not be determined. During data reduction, to account for the regions of the flowfield where the probe could not be nulled, a value of zero velocity was assigned and a limiting value of total pressure drop was established based on observed trends in the area of the flowfield where accurate data were available. Therefore, the velocity vector plots and velocity streamline plots have areas where there are no data present; these areas are the sections of the flowfield where the probe capabilities were exceeded. Likewise, on the pressure contour plots an area of uniform total pressure loss indicates the section in which the data are inaccurate. The isobar along which the pressure data become unreliable will be delineated in the section which refers to that plot.

An additional problem of the probe's lack of capabilities arises from the fact that both vortical flow and the reversed flow from a stalled aerodynamic surface appear as blank areas in the data or as areas of total pressure loss. Since there is insufficient data to indicate a difference between the two flow states, flow visualization results have been included to discern between regions of separated/reversed flow and those of separated coherent vortex flow.

#### **A. WING-ALONE**

With the canard off, the flow over the main wing was characterized by large regions of reversed flow, indicative of a stalled wing. In general, as can be seen from Figure 18, there was a large amount of oil over the majority of the wing indicating wing stall. Particularly,

the oil on the inboard portion of the wing was mostly stagnate or flowing spanwise; this response indicated that this section of the wing had stalled and thereby created an area of large total pressure loss. Along the leading edge of the wing there appeared to be a weak, poorly organized, separated vortex, which apparently lost its coherency over the outboard section. This separated vortex was indicated in Figure 18 by the heavy line of oil which started at the wing apex and then seemingly burst at the wing mid-point. Therefore, it would be expected that at each measuring grid there would be evident a general tendency for the flow to move spanwise, in a root-to-tip fashion, with a large area of total pressure loss. In this case, the loss in total pressure would be due to chaotic, disorganized, separated reversed flow rather than coherent, vortical flow.

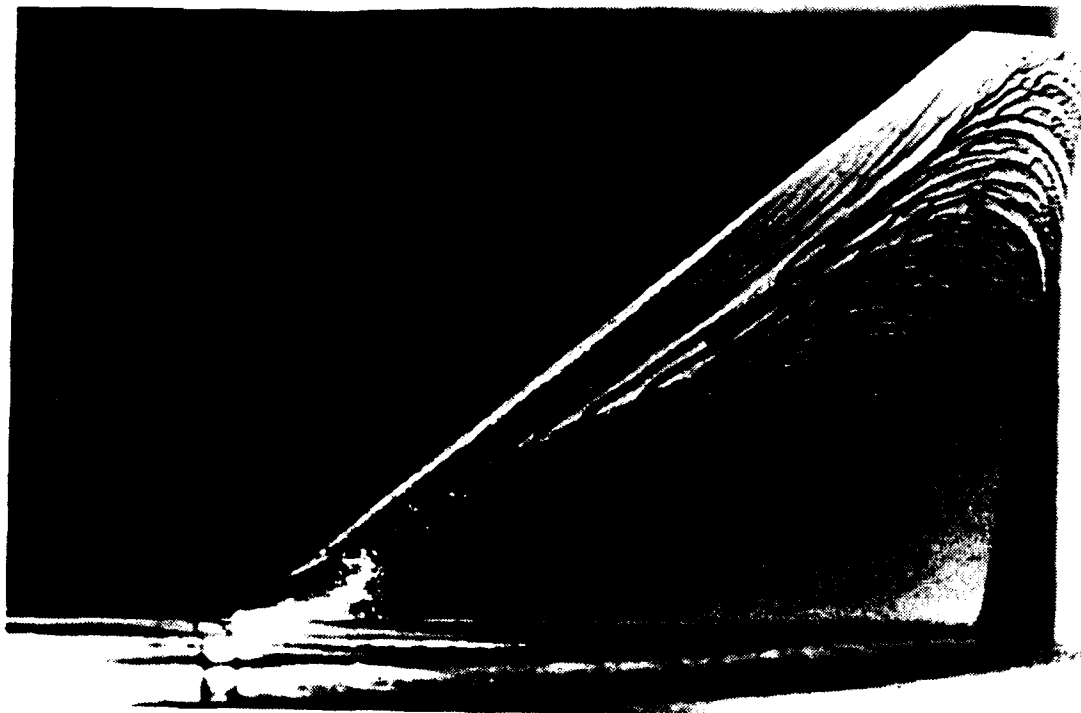


Figure 18. Wing Alone Set at 22°



### **1. Mid-Point of the Main Wing (Grid 2)**

Figure 19(a) is a plot of the "X" and "Y" components of the local velocities at grid 2. The blank area inside the heavy line indicates the area where the data were unreliable due to flow separation. The crossflow component of freestream velocity increased as the probe was traversed from the wing tip to the root. The crossplane velocity streamline plot of Figure 19(b) shows a vortical pattern which compares favorably with the flow visualization of Figure 18. Crossplane velocities are vertical (in the model reference sense) near the leading edge or tip, but horizontal at 26% mean aerodynamic chord (MAC) above the wing. Figure 20 is a contour plot of total-pressure-coefficient loss. This plot also shows an area of total pressure loss increasing in size as the probe was moved inboard toward the wing root. At the outboard section of the wing it is possible that the cause of this loss was the disintegrating vortex that appeared to form there; however, at the inboard section, the loss was certainly caused by reversed flow. Pressures inside the -1.24 isobar are unreliable. The separated region extends up to 29% MAC.

### **2. Trailing Edge of the Main Wing (Grid 3)**

At grid 3, which was located just past the trailing edge of the wing, Figures 21(a) and (b) clearly indicated a strong spanwise flow pattern from the wing root to the tip near the fuselage. This flow pattern is believed to be caused by entrainment due to the separated reversed flow commonly associated with wing stall, rather than by a coherent vortex. The separation now extends about 57% of the MAC above the wing plane at the trailing edge. The total-pressure-coefficient gradients in Figure 22 show that the region of total pressure loss, due to the stalled reversed flow, had grown substantially as the flow moved downstream from grid 2. Pressures inside the -1.20 isobar are considered to be unreliable. Though the region of uncertain data is large, the results seem to indicate the extent to which the flow separation affects the wing flowfield, just as the oil flow visualization seemed to indicate the same on the wing surface.

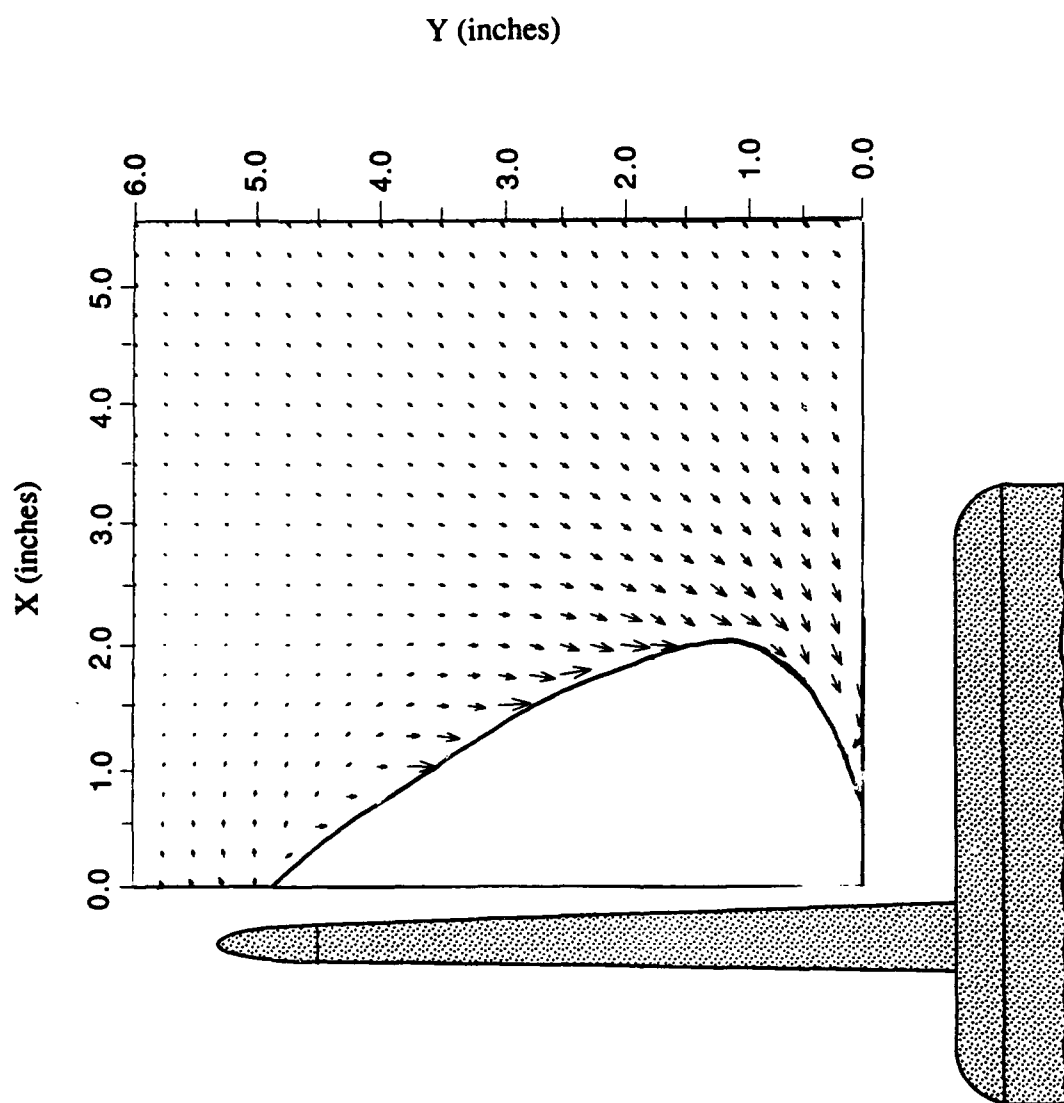


Figure 19(a). Velocity Vectors, Mid-point of the Wing, No Canard

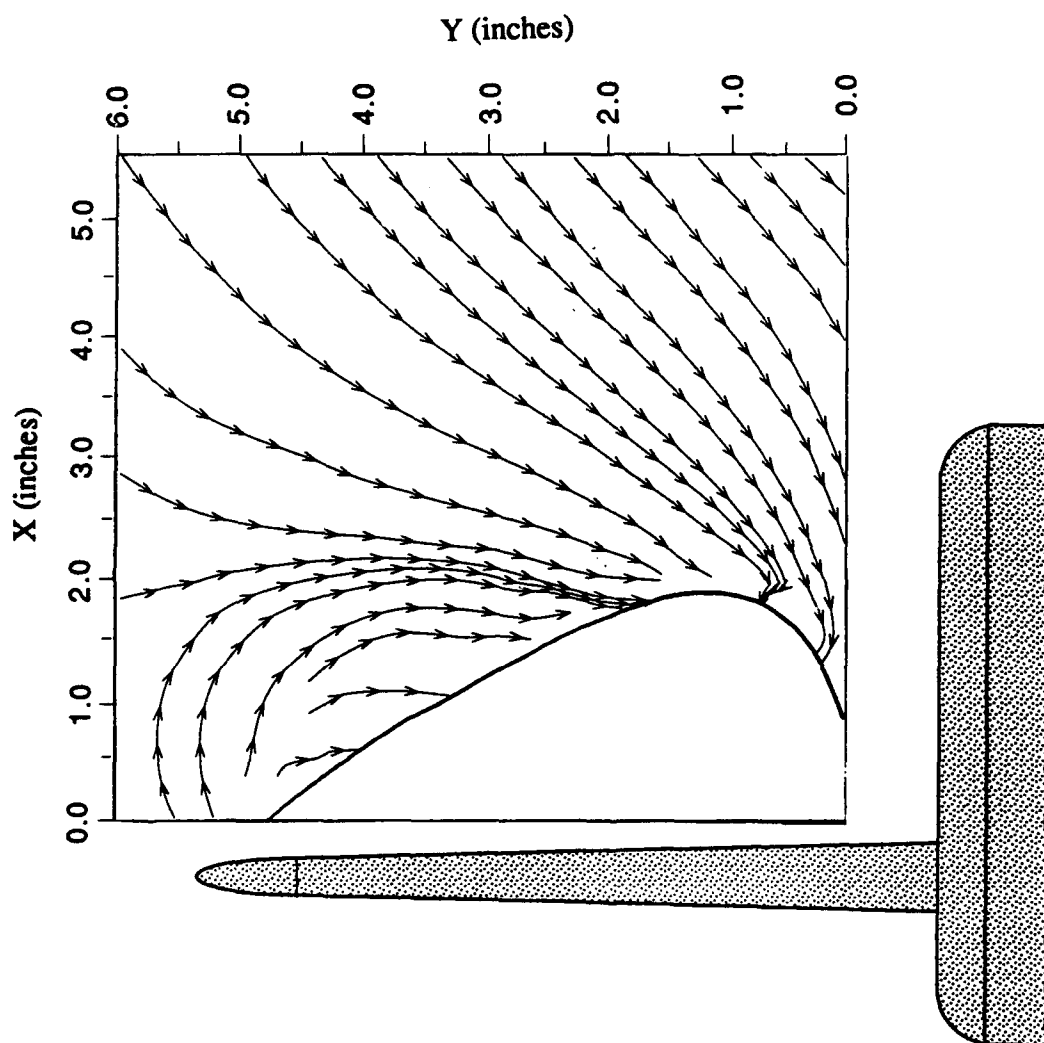


Figure 19(b). Streamlines, Mid-point of the Wing, No Canard

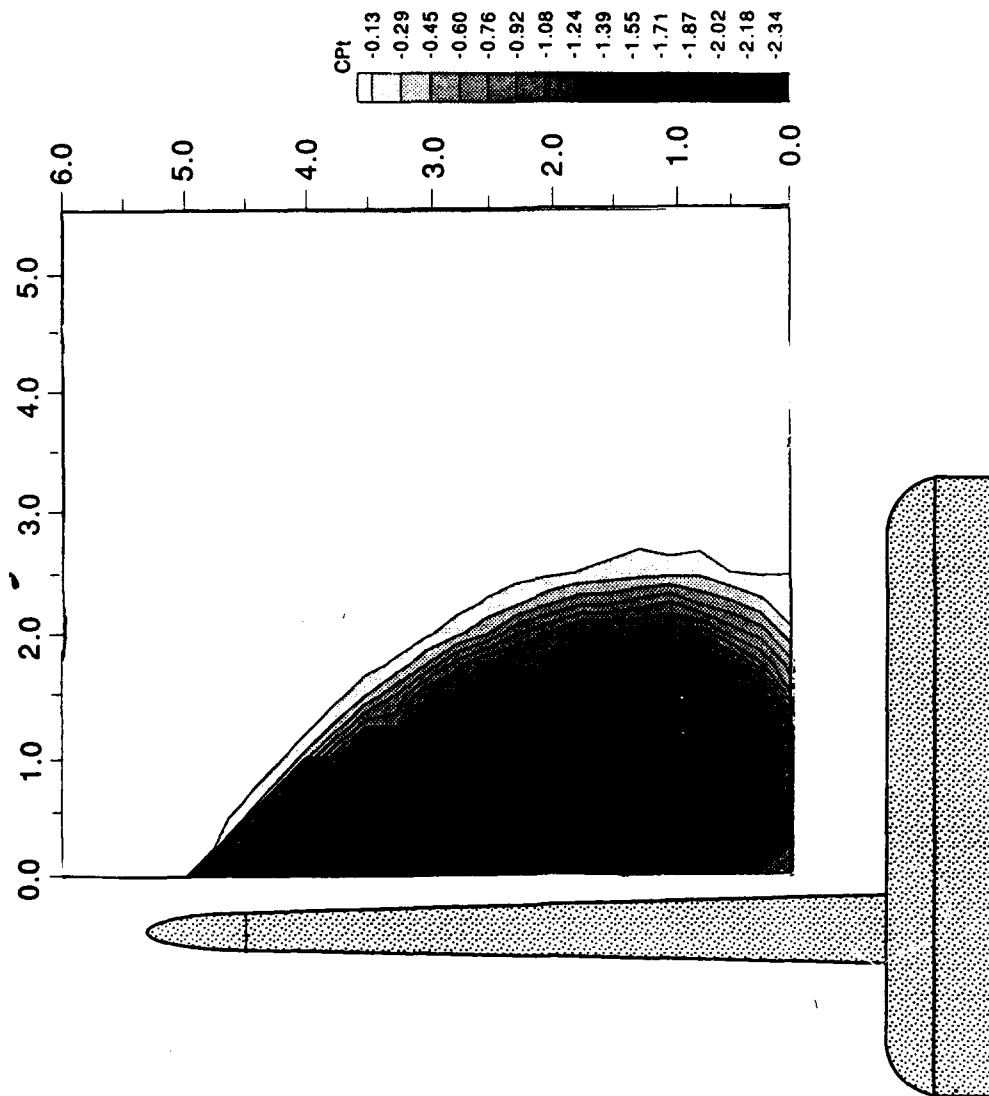
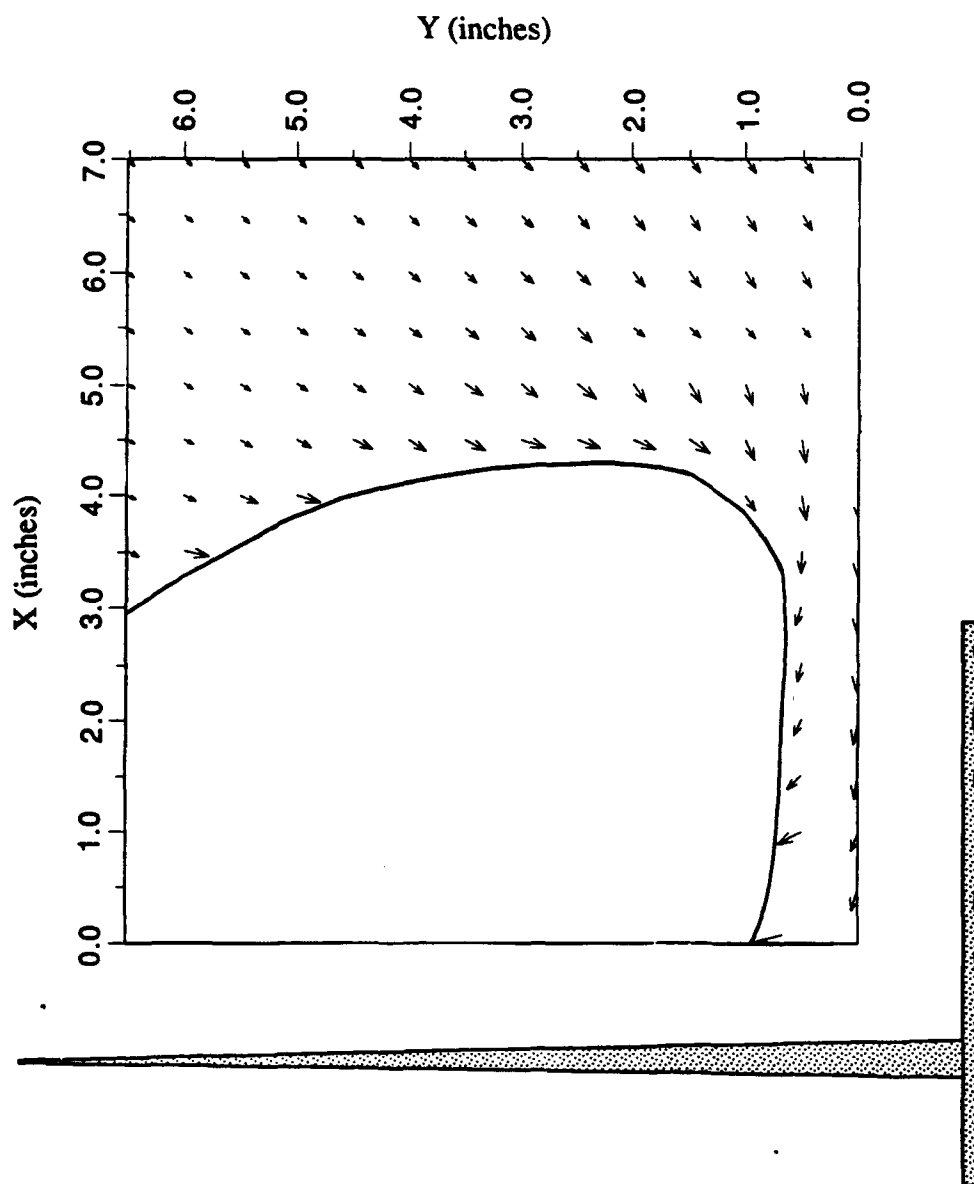


Figure 20. Total Pressure Coefficient Contours, Mid-point of the Wing, No Canard



**Figure 21(a). Velocity Vectors, Trailing-Edge of the Wing, No Canard**

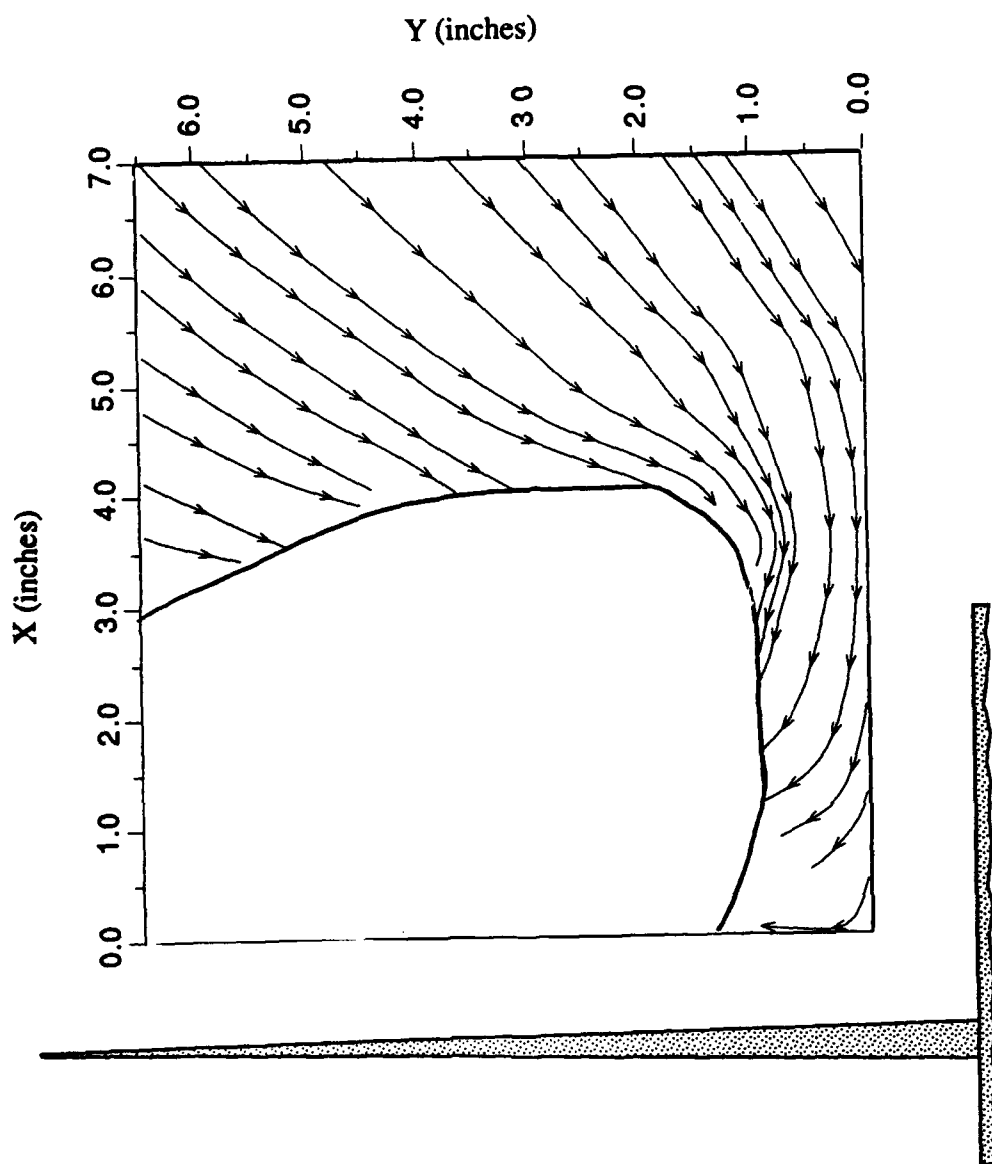


Figure 21(b). Streamlines, Trailing-Edge of the Wing, No Canard

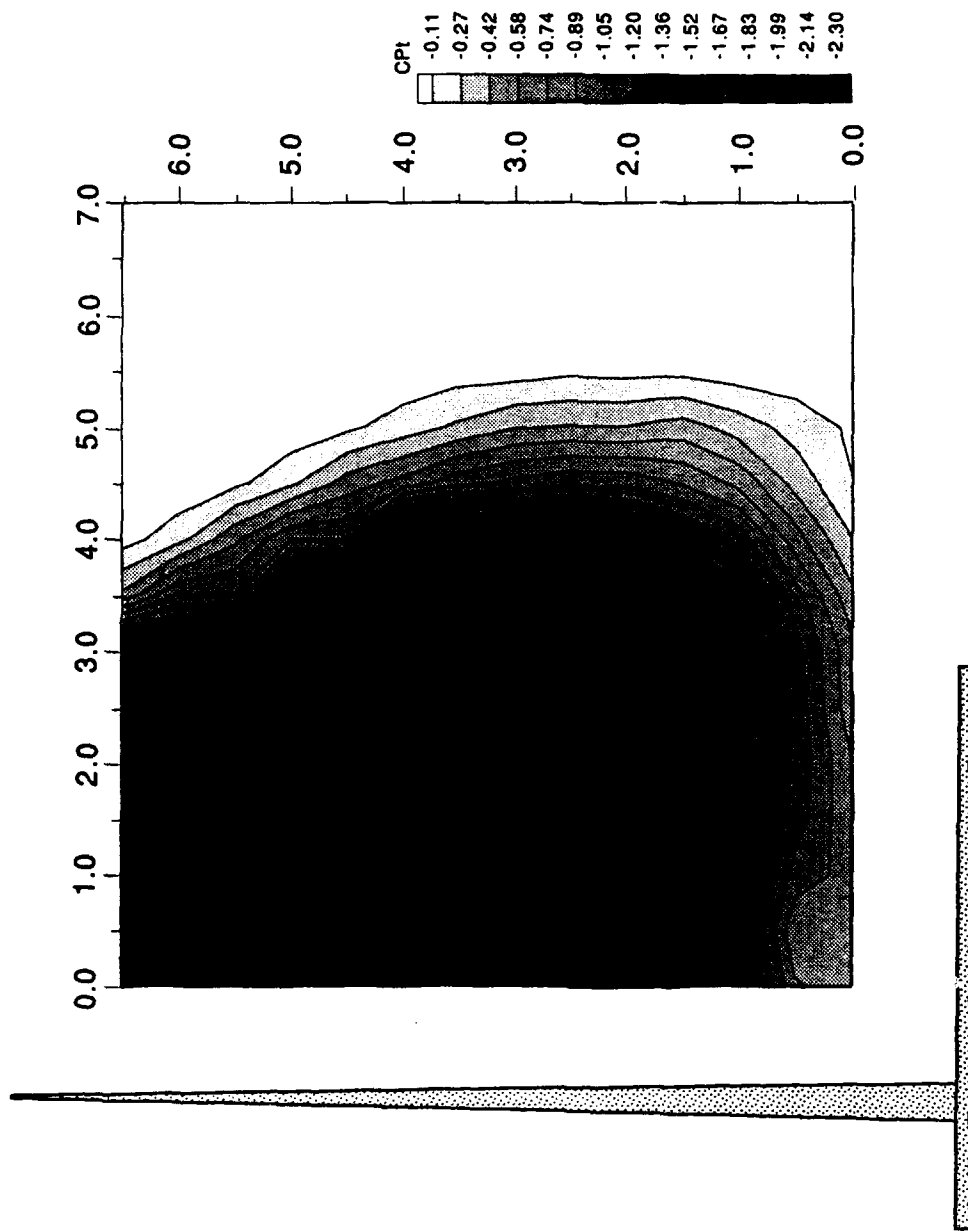


Figure 22. Total Pressure Coefficient Contours, Trailing-Edge of the Wing, No Canard

## B. WING/CANARD COMBINATION

The addition of the canard to the model caused large-scale reattachment of the flow over the wing. Figure 23 shows a well-defined secondary separation line along the leading edges of both the canard and wing. These separation lines are characteristic of strong, highly coherent leading-edge vortices. Note in Figure 23 that despite the high angle of attack of the canard ( $29^\circ$ ), the flow appeared to remain completely attached (not separated and reversed) and that the large leading-edge sweep ( $60^\circ$ ) produced a strong vortex even though the leading edge was rounded. In reference to Figure 23, the wing can be seen to be fairly clean of oil with the exception of a wedge which started just aft of the apex and grew as it proceeded downstream parallel to the fuselage. Also, there is a line of oil along the trailing edge of the wing which indicated that the flow had begun to separate there, particularly at the point where the trailing-edge line joined the line which had started near the apex and moved parallel to the fuselage. Additionally, looking at the top surface of the fuselage where the canard and wing join the body, one can see there is a section of the fuselage free of oil. It is thought that this result was due to a secondary vortex forming near the surface of the fuselage. The exact origin of this secondary fuselage vortex, however, is not clear. It could have been the result of either the forebody or of the leading-edge vortices formed on the canard and wing, or possibly some combination of the two effects.

The discussions that follow will be in the same format used in the preceding wing-alone discussion. The path of the canard and wing vortices will be analyzed and the effects of the one on the other noted.



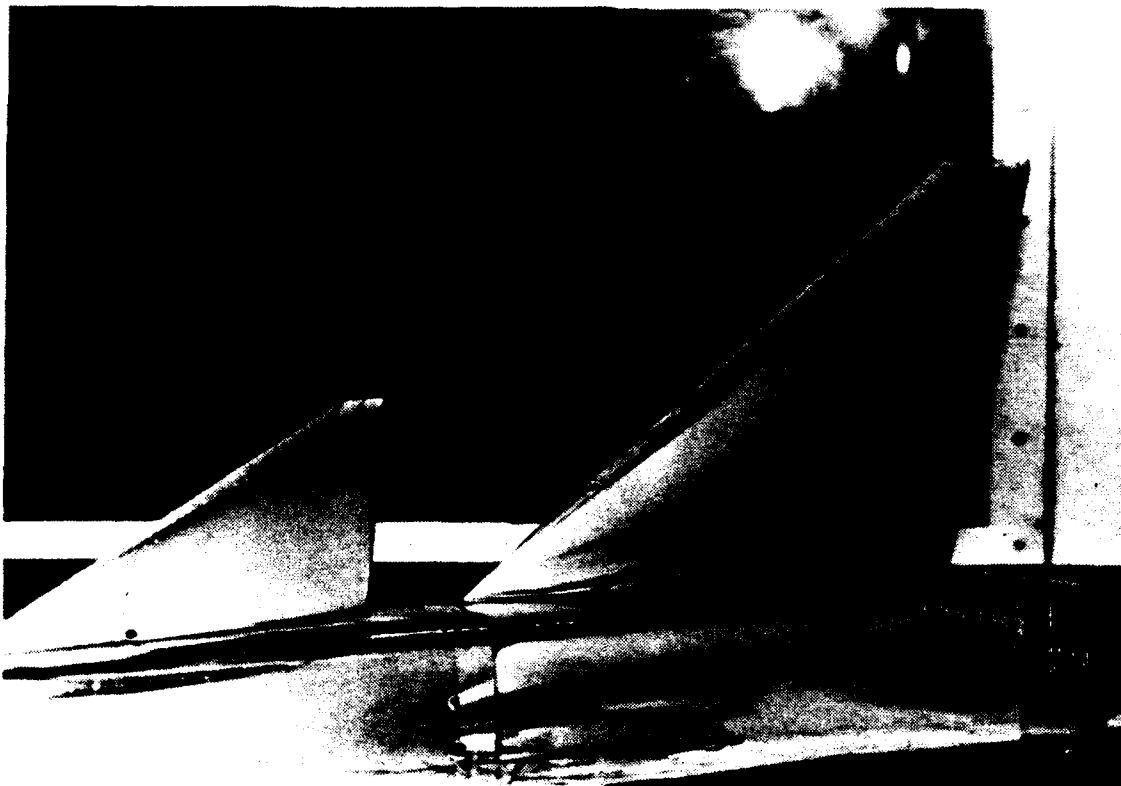


**Figure 23. Model set at  $22^\circ$ , Canard set at  $7^\circ$  Incidence**

### **1. Trailing Edge of the Canard (Grid 1)**

The flow at this grid, which was located just aft of the canard trailing edge, was dominated by a strong vortex generated at the canard leading edge. Figure 24(a) shows that for a large portion of the measuring grid, the probe was unable to accurately record flow field pressures. However, Figures 24(a) and (b) do indicate the presence of very strong vortical flow in a clockwise direction. Also, Figures 24(a) and (b) indicate the presence of a secondary vortex forming toward the fuselage surface near the canard/body juncture. The secondary vortex was rotating in a counter-clockwise direction, which indicated that it had probably formed as a result of the canard leading-edge vortex in much the same manner as

a secondary vortex forms near a wing leading-edge vortex. The mechanism for such a vortex would be the same as that depicted in Figure 1, but would be a result of an interaction of the wing and fuselage rather than the wing and itself. Such a phenomenon had not been noted in previous testing because the models used did not have a substantial fuselage. If this secondary vortex had resulted from the model forebody, it would have been expected to be rotating clockwise.

Figure 25 shows the steep pressure gradients which resulted from this vortex. The data inside the -1.26 isobar are unreliable, but clearly, the trend was for a tight, coherent core vortex standing approximately 1.5 to 2.5 inches off the canard surface at the trailing edge. The presence of the secondary vortex near the canard root is better indicated in the plot of total-pressure-coefficient-loss contours. Notice that a freestream value of total pressure extends all the way to the canard surface, which agrees with the flow visualization of Figure 23.

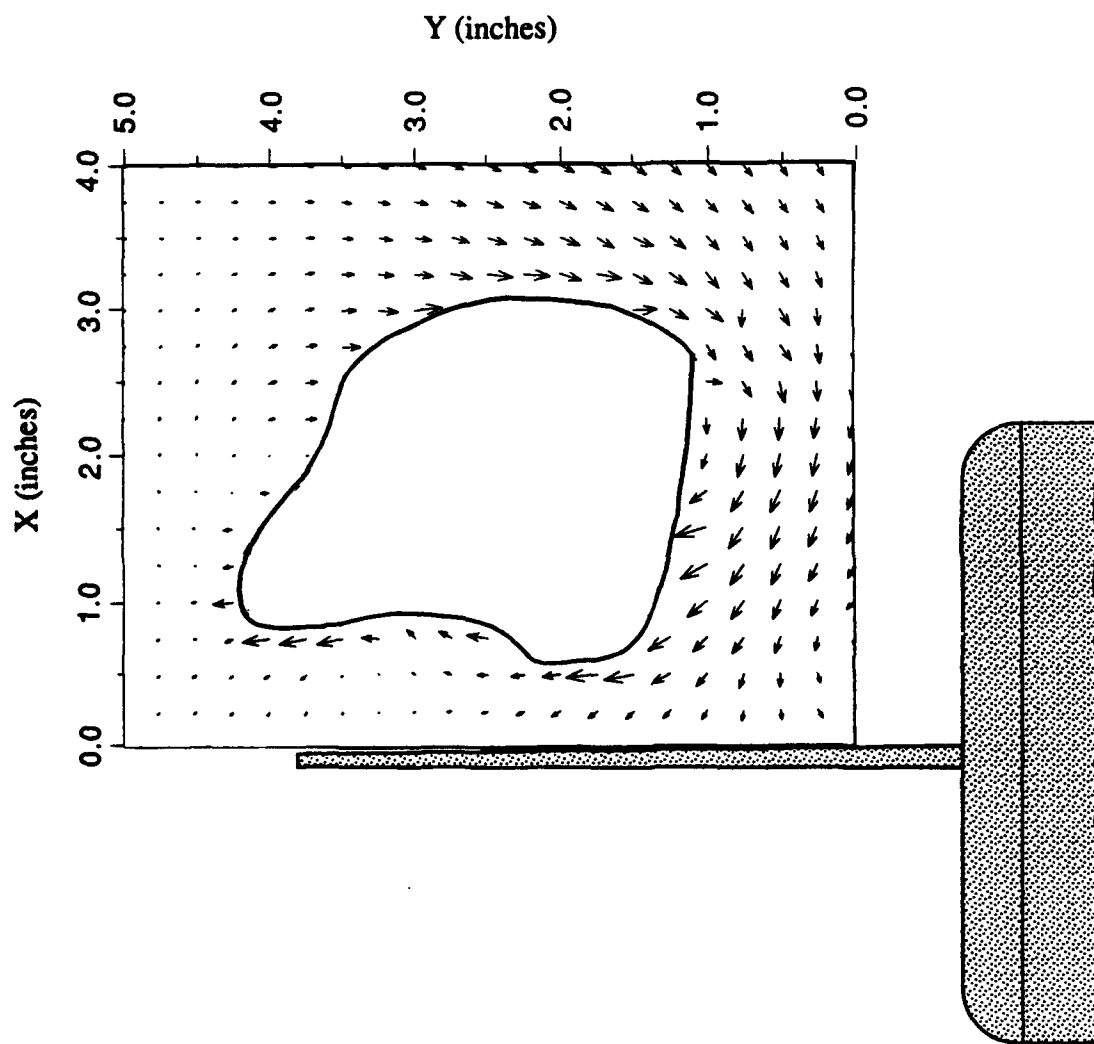


Figure 24(a). Velocity Vectors, Trailing-Edge of the Canard

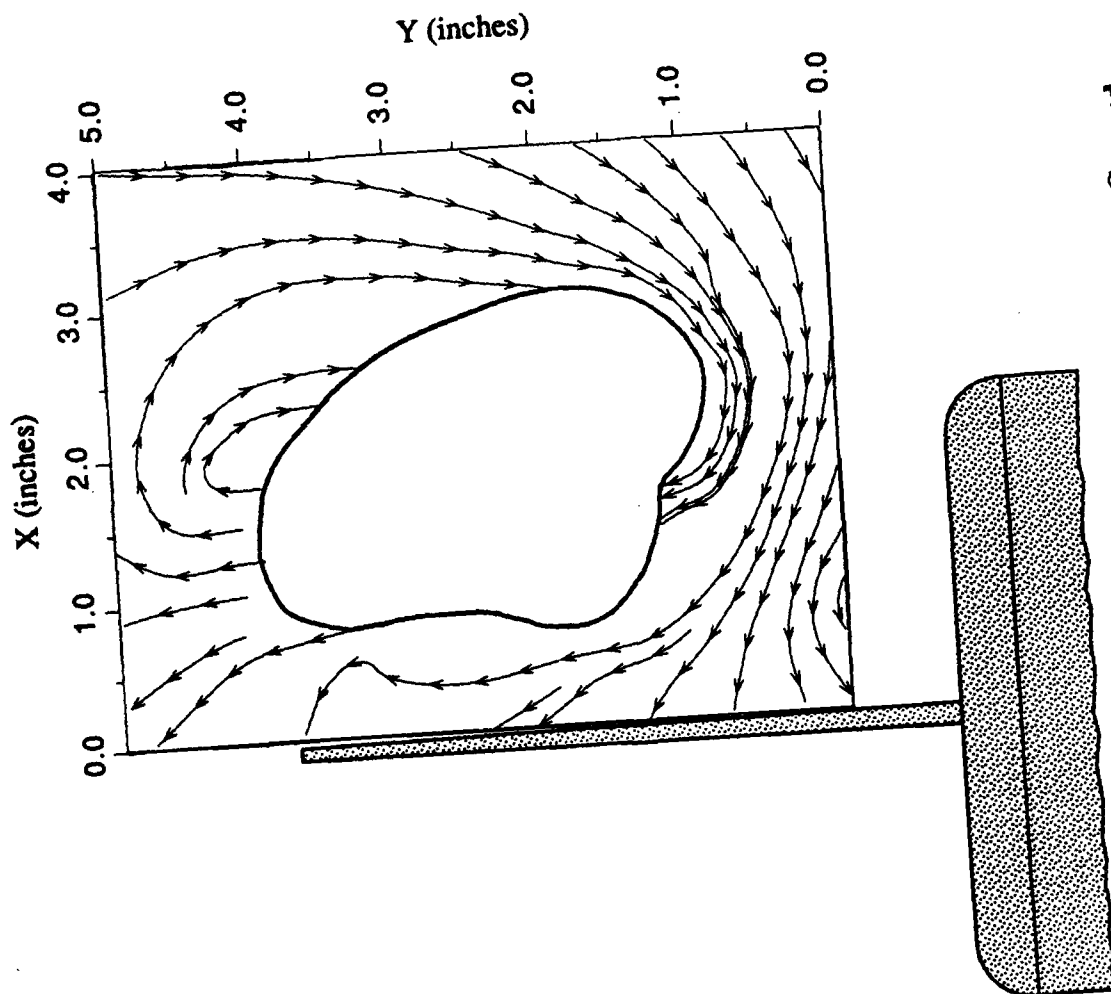


Figure 24(b). Streamlines, Trailing-Edge of the Canard

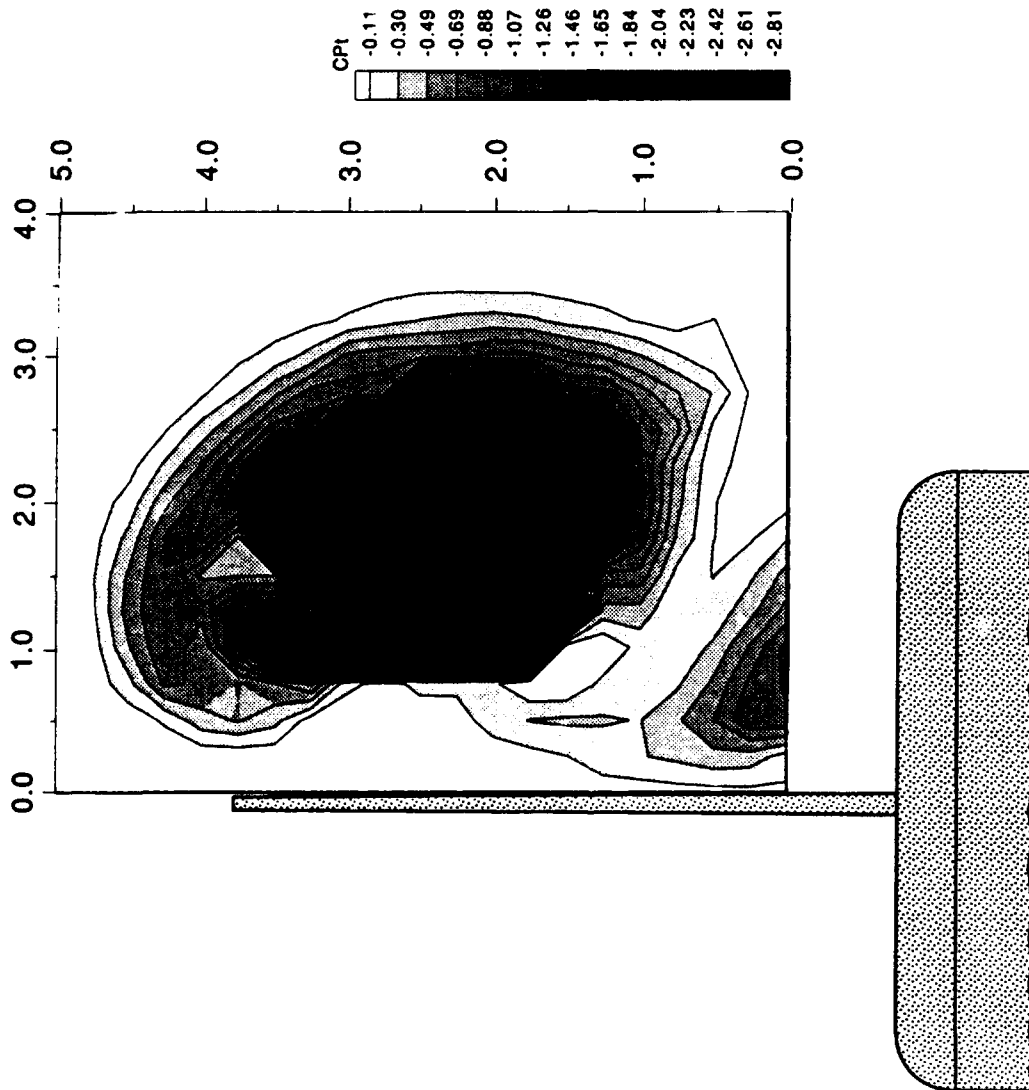


Figure 25. Total Pressure Coefficient Contours, Trailing-Edge of the Canard

## **2. Mid-Point of the Main Wing (Grid 2)**

A comparison of Figures 26 and 19 shows a dramatic difference in the flowfield due to the addition of the canard to the model. Figure 26(a) shows two regions of unobtainable data, one at approximately (5,2) and the other very near the wing leading edge at about (0.5,3.5). The area located near (5,2) was the canard leading-edge vortex which had moved downstream from grid 1. The area near (0.5,3.5) could have been the result of two possible phenomena. One is that the large region of chaotic flow seen in Figure 19 had been forced into a small "pocket" of separated reversed flow. The second is that the wing leading-edge vortex had reformed due to the presence of the canard vortex. The flow visualization in Figure 27 indicates the presence of a wing leading-edge vortex. Furthermore, the pattern formed by the streamlines in Figure 26(b) indicates that rather than the flow having merely been forced into a "separation-pocket", the leading-edge vortex was actually energized by the canard vortex and had reformed. The flow visualization suggests that a strong vortex has formed along the wing surface.

The energizing of the wing leading-edge vortex in this manner and the reattached flow over the inboard wing section would lead to a level of enhanced lift which would be greater than that obtained by simply adding the lifting surface of the canard. In fact, as was mentioned earlier, this was found to be exactly the case in previous studies [Ref. 2,3]. The mechanism is clearly demonstrated here. Also in Figure 26 can be seen a significant crossflow component between the canard vortex and the wing leading-edge vortex. In the vicinity of (2,1) the crossflow is as much as 65% of the total freestream velocity and approaches the wing perpendicular to its surface. The formation of oil parallel to the fuselage in Figure 27 could have been due, at least in part, to the stagnation of this large crossflow component on the wing surface.

The total-pressure-coefficient contours of Figure 28 show the presence of a third vortex not completely captured by the velocity-vector or velocity-streamline plots. Centered

at (2.1,0.6), this vortex is believed to be the secondary vortex that had formed on the fuselage surface at grid 1. Most importantly, the contours of Figure 28 show that freestream total pressure extended to the wing surface over the inboard section. Clear evidence is provided that the flow had reattached over the inboard portion of the wing, enhancing significantly the lifting ability of the previously stalled wing.

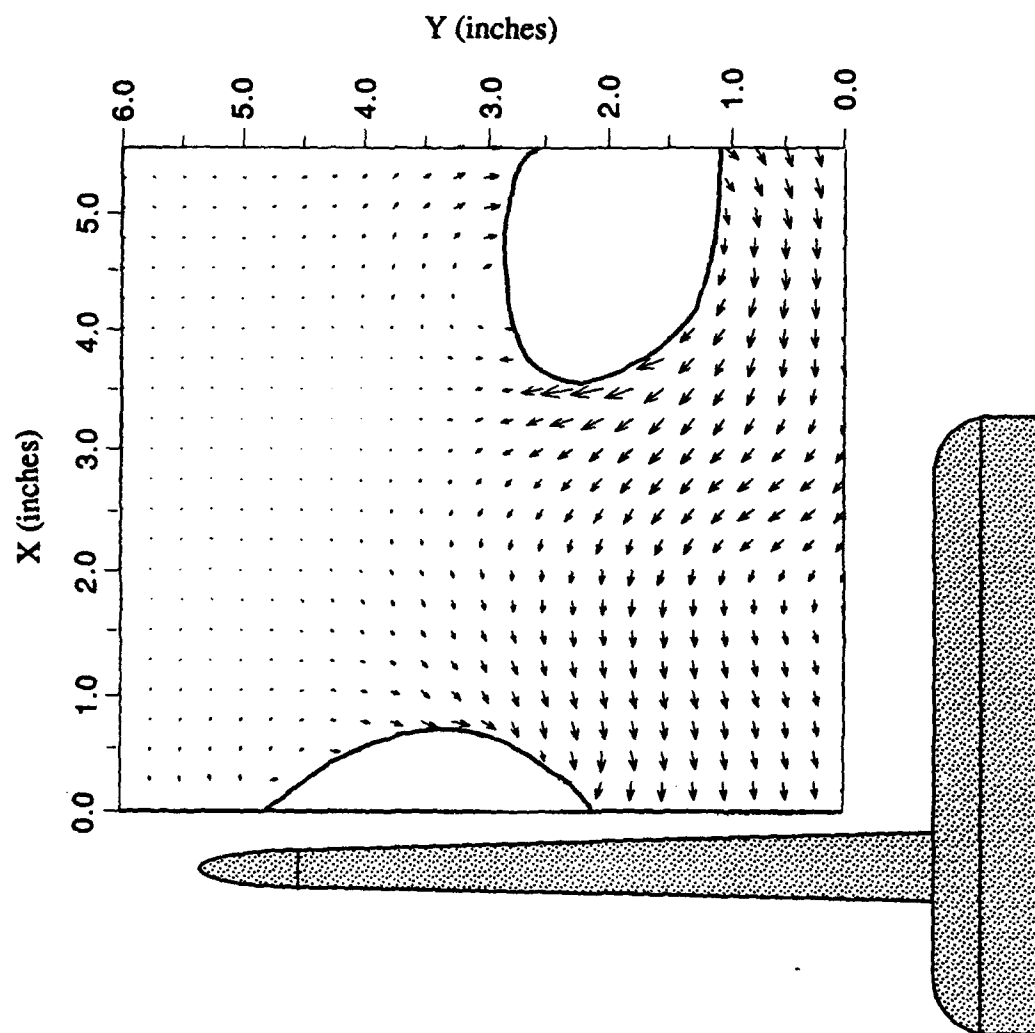
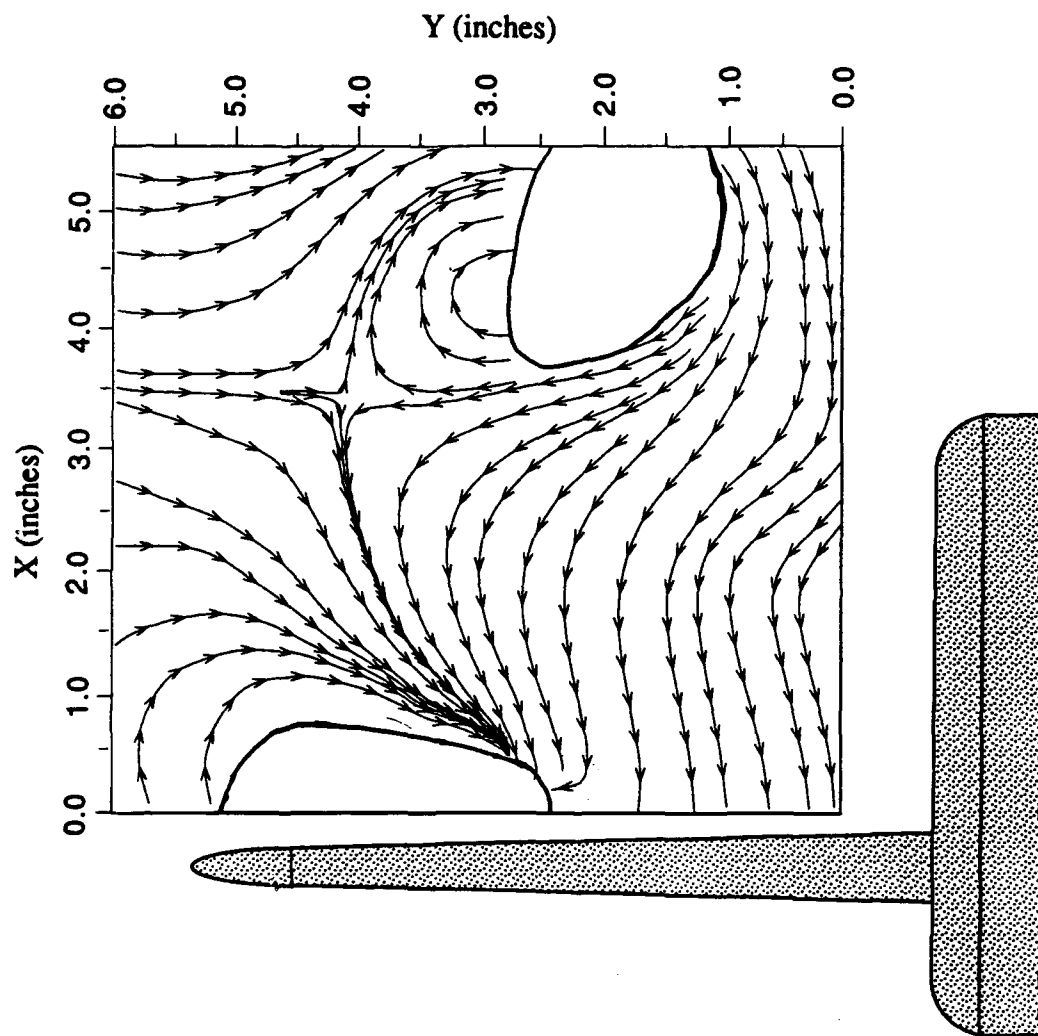


Figure 26(a). Velocity Vectors Mid-point of the Wing, With Canard





**Figure 26(b). Streamlines, Mid-point of the Wing, With Canard**

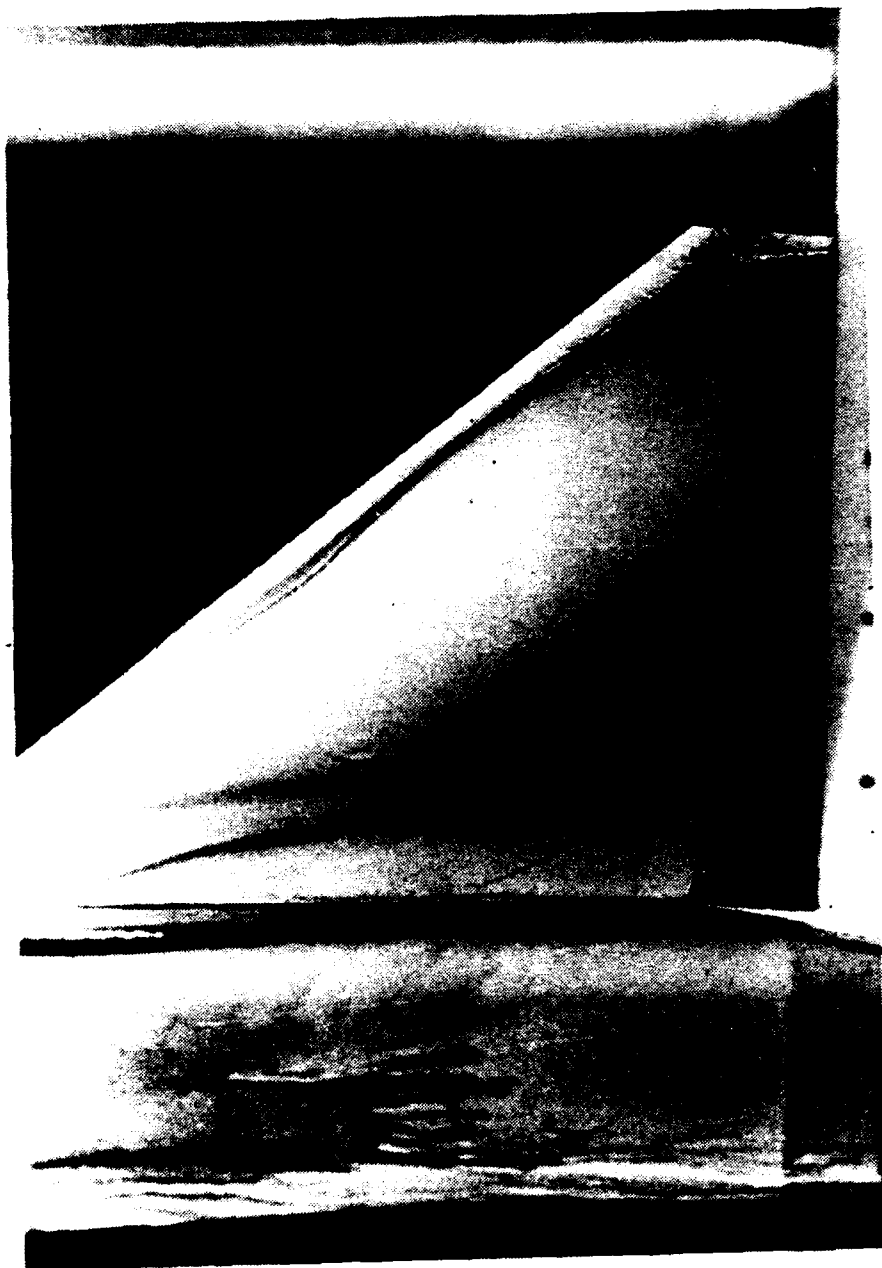


Figure 27. Wing at  $22^\circ$  with Canard Deflected  $7^\circ$

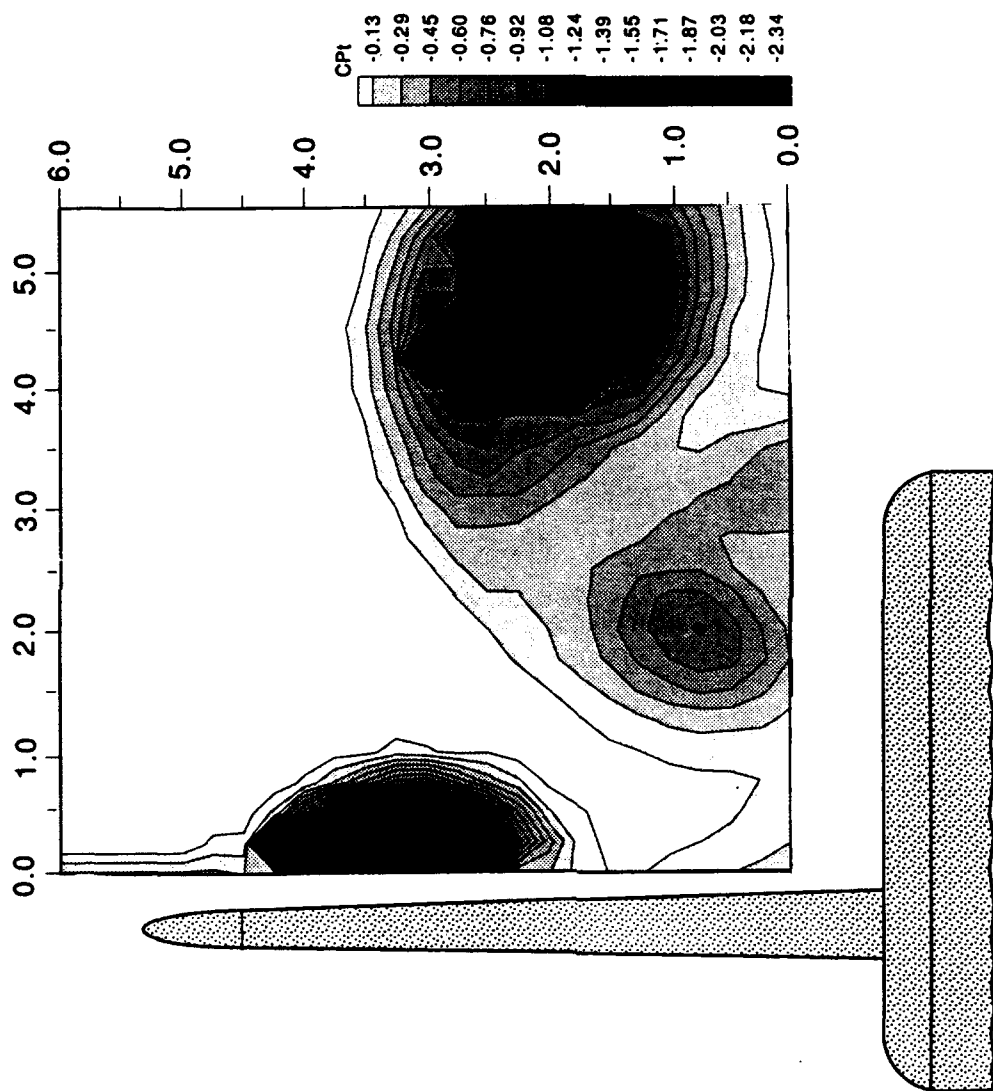


Figure 28. Total Pressure Coefficient Contours, Mid-point of Wing, With Canard

### 3. Trailing Edge of the Main Wing (Grid 3)

While the velocity vectors and streamlines of Figure 29 indicate a similar pattern to that of grid 2, the flow, in general, was less coherent and slightly more diffuse than at grid 2.

Figure 29(a) shows that there were two areas devoid of obtainable data. One of these areas was the result of the canard vortex which had moved downstream to a point near the (5.5,1.5) position and the other was caused by the wing leading-edge vortex which had reformed as a result of the presence of the canard. The streamlines in Figure 29(b) show that the flow at these locations was strongly vortical. In addition, the flow visualization of Figure 27 shows the presence of a secondary separation line consistent with the formation of a leading-edge vortex. Figure 29 also indicated that there still existed a strong crossflow component moving from the canard vortex to the wing vortex. The magnitude of this crossflow reached 66% of the freestream as at grid 2; however, the freestream velocity on the wing surface of grid 3, near (0,2.5), had slowed to 74% of that at the same position on grid 2. This was substantiated by the growth in the width of the oil line parallel to the fuselage. A comparison of Figures 18 and 21 with 29 shows that the energy introduced to the flow by the canard vortex moved the burst point of the wing leading-edge vortex past the trailing edge of the wing.

The pressure contours in Figure 30 show the presence of the two vortices already mentioned and a third area of pressure loss. This third area was most likely a combination of the remnants of the secondary fuselage vortex and the stagnation of the spanwise crossflow component on the wing. Note also that even though the canard vortex had traveled the length of the model, the pressure gradient around it was approximately equal to that around the wing leading-edge vortex. This further indicates that it was the energy in the canard vortex which allowed or entrained the wing vortex to reform. The -1.21 isobar marks the limit of the probe capabilities.

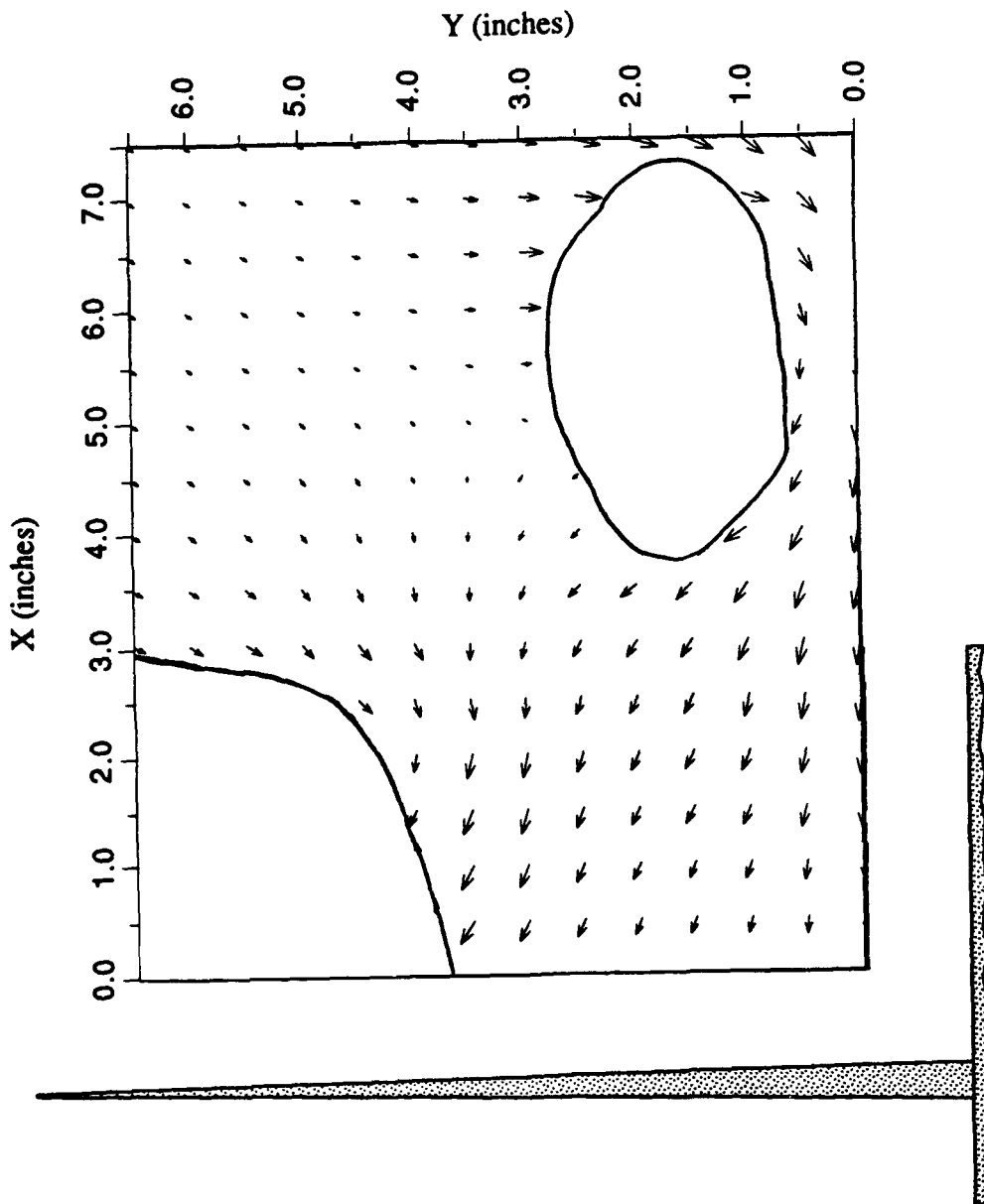


Figure 29(a). Velocity Vectors, Trailing-Edge of the Wing, With Canard

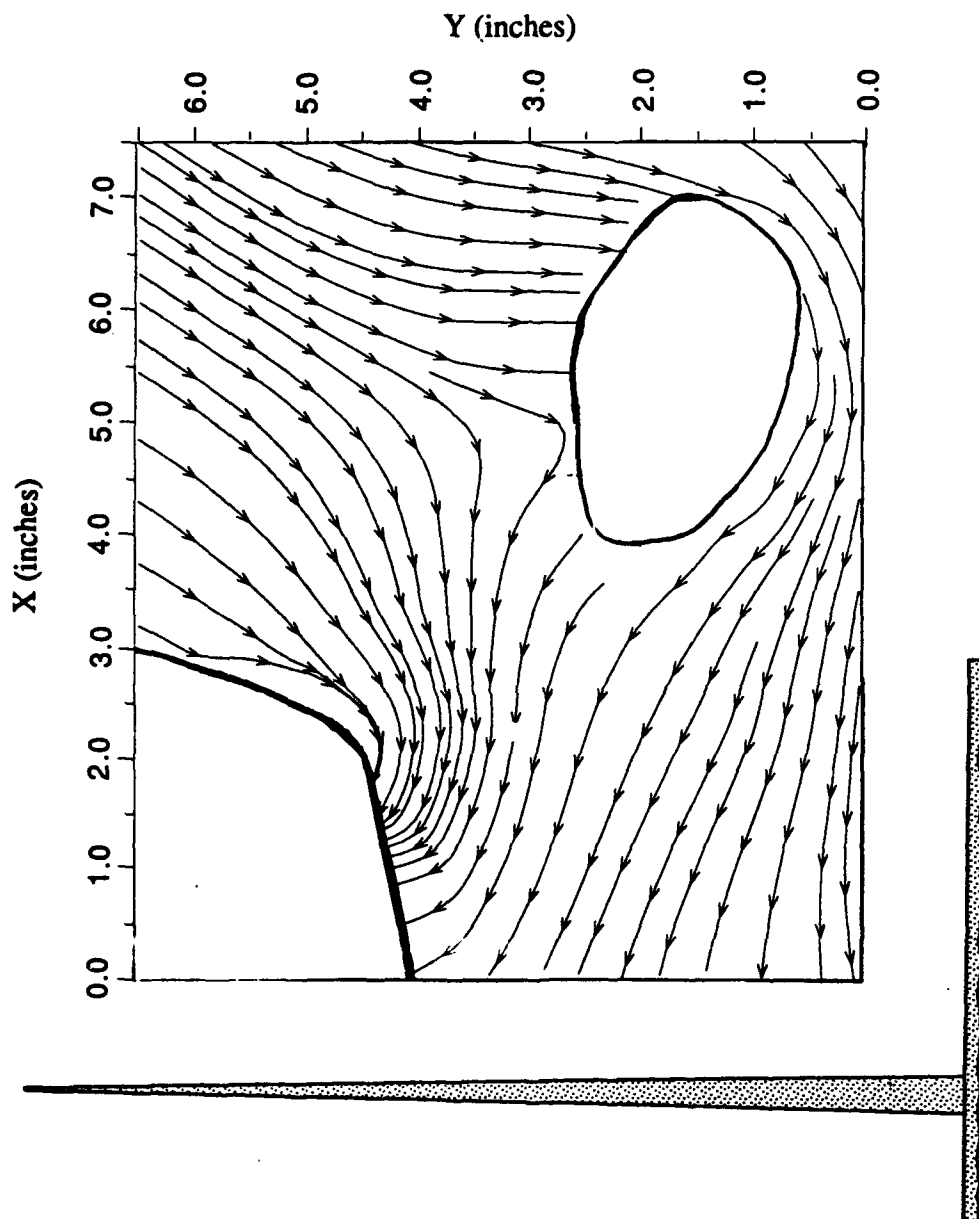


Figure 29(b). Streamlines, Trailing-Edge of the Wing, With Canard

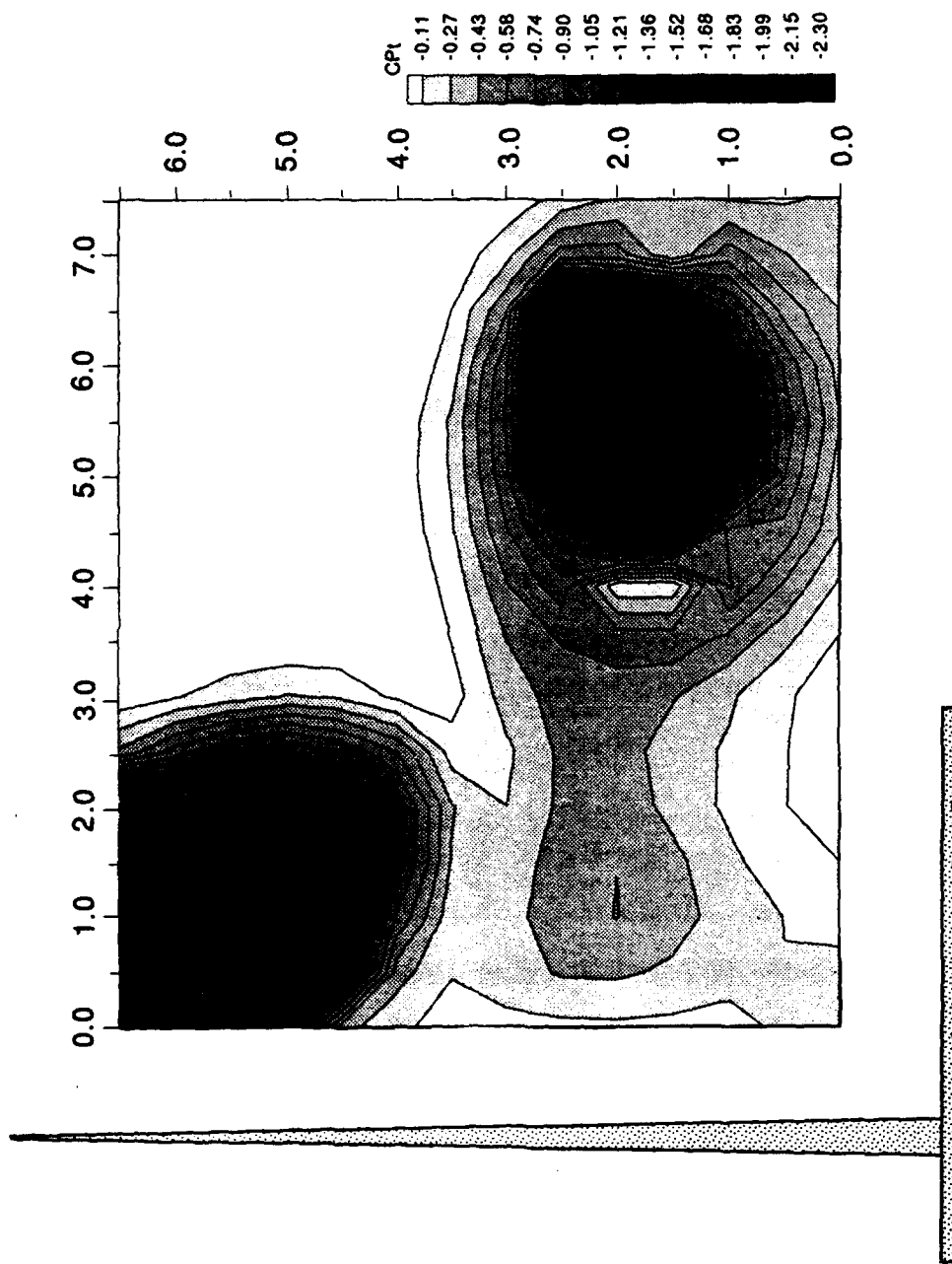


Figure 30. Total Pressure Coefficient Contours, Trailing-Edge of the Wing, With Canard

### C. CONCLUSION

The addition of the canard had a dramatic effect on the wing flowfield at an angle of attack of  $22^\circ$ . Without the canard, the flow across the wing was characterized by large areas of chaotic, incoherent flow with a resultant loss in lift. The addition of the canard vortex established a large crossflow component moving toward the wing surface which caused the flow over the inboard section of the wing to reattach.

In addition to reattachment, the crossflow provided energy to the wing vortex which delayed its breakdown. Therefore, with the canard in this position relative to the wing, the wing leading-edge vortex was enhanced and stabilized. This crossflow-induced breakdown delay substantiates the conclusions made by Lacey, in Reference 2.

The energy contained in the canard vortex is not lost. Consider the drag force as a measure of the energy required to propel two models with the same wing planform. The first model employs a canard/wing configuration and the second model a wing/conventional-tail configuration. If the flow over the wing of the second model remains attached (this study shows it would not), both models would have approximately the same drag. The difference is that the energy (in the form of drag) placed in the tail vortex of the second model would be lost to the freestream. In the canard/wing configuration, some of the energy placed in the canard vortex was used to benefit the flow over the wing thereby, making the canard configuration more efficient.

Figure 31 is provided as a schematic of the approximate path of the vortices as they moved downstream through the grids.



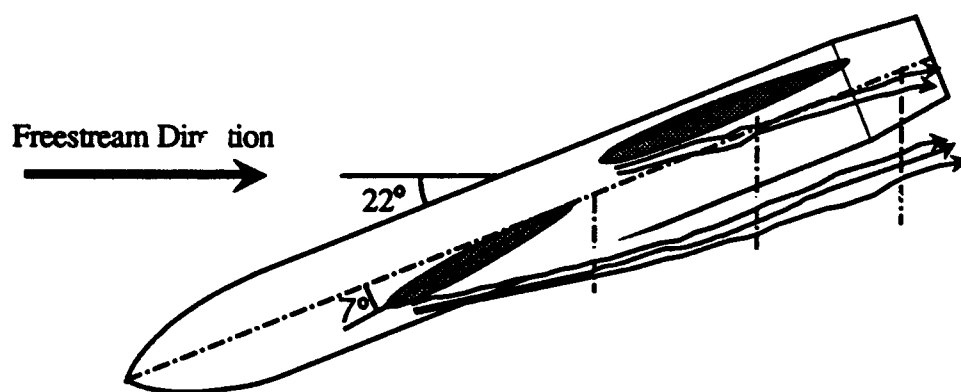


**Figure 31. Vortex Path**

## LIST OF REFERENCES

1. SAAB TN 60, *Basic Low Speed Aerodynamics of the Short-Coupled Canard Configuration of Small Aspect Ratio*, Behrdohm, H., July 1965.
2. David W. Taylor Naval Ship Research and Development Center, Bethesda, MD, Report DTNSRDC-79/001, *Aerodynamic Characteristics of the Close-Coupled Canard as Applied to Low-to-Moderate Swept Wings, Volume I: General Trends*, Lacey, D.W., January 1979.
3. Er-EL, J., and Seginer, A., "Vortex Trajectories and Breakdown on Wing-Canard Configurations," *Journal of Aircraft*, Vol. 22, No. 8, pp. 641-648, August 1985.
4. Stoll, F., and Koenig, D.G., "Large-Scale Wind-Tunnel Investigation of a Close-Coupled Canard-Delta-Wing Fighter Model Through High Angles of Attack," paper presented at the AIAA Aircraft Design, Systems and Technology Meeting, Fort Worth, TX, 17-19 October 1983.
5. Calarese, W., "Vortex Interaction Effects on the Lift/Drag Ratio of Close-Coupled Canard Configurations," paper presented at the AIAA 19th Fluid Dynamics, Plasma Dynamics and Lasers Conference, Honolulu, HI, 8-10 June 1987.
6. Kersh, J.M. Jr., *Lift Enhancement Using Close-Coupled Canard/Wing Vortex Interaction*, Master's Thesis, Naval Postgraduate School, Monterey, CA, December 1990.
7. Oelker, H.,-C., and Hummel, D., "Investigations on the Vorticity Sheets of a Close-Coupled Delta-Canard Configuration," *Journal of Aircraft*, Vol. 26, No. 7, pp. 657-666, July 1989.
8. *Laboratory Manual for Slow-Speed Wind Tunnel Testing*, Department of Aeronautics, Naval Postgraduate School, Monterey, CA., 1989.
9. Velmex, Inc., *User's Guide to 8300 Series Stepping Motor Controller/Drivers*, East Bloomfield, NY, January 1988.
10. Lung, M.H., *Flowfield Measurements in the Vortex Wake of a Missile at High Angle of Attack in Turbulence*, Master's Thesis, Naval Postgraduate School, Monterey, CA, December 1988.
11. United Sensors, Inc., *Five-hole Probes Calibration Manual*, Watertown, MA, June 1988.
12. Kindelspire, D.W., *The Effects of Freestream Turbulence on Airfoil Boundary Layer Behavior at Low Reynolds Numbers*, Master's Thesis, Naval Postgraduate School, Monterey, CA, September 1988.

## APPENDIX A

```

1 DEF SEG : CLEAR , &HFE00: GOTO 4'Begin PCIB Program Shell
2 GOTO 1000 ' User program
3 GOTO 900 ' Error handling
4 I = &HFE00' Copyright Hewlett-Packard 1984,1985
5 PCIB.DIR$ = ENVIRON$("PCIB")
6 I$ = PCIB.DIR$ + "\PCIBILC.BLD"
7 BLOAD I$, I
8 CALL I(PCIB.DIR$, I%, J%): PCIB.SEG = I%
9 IF J% = 0 THEN GOTO 13
10 PRINT "Unable to load.";
11 PRINT "      (Error #"; J%; ")"
12 END
13 '
14 DEF SEG = PCIB.SEG: O.S = 5: C.S = 10: I.V = 15
15 I.C = 20: L.P = 25: LD.FILE = 30
16 GET.MEM = 35: L.S = 40: PANELS = 45: DEF.ERR = 50
17 PCIB.ERR$ = STRING$(64, 32): PCIB.NAME$ = STRING$(16, 32)
18 CALL DEF.ERR(PCIB.ERR, PCIB.ERR$, PCIB.NAME$, PCIB.GLBERR):
PCIB.BASERR = 255
19 ON ERROR GOTO 3
20 J = -1
21 I$ = PCIB.DIR$ + "\PCIB.SYN"
22 CALL O.S(I$)
23 IF PCIB.ERR <> 0 THEN ERROR PCIB.BASERR
24 I = 0
25 CALL I.V(I, READ.REGISTER, READ.SELFID, DEFINE,
INITIALIZE.SYSTEM)
26 IF PCIB.ERR <> 0 THEN ERROR PCIB.BASERR
27 CALL I.V(I, ENABLE.SYSTEM, DISABLE.SYSTEM, INITIALIZE,
POWER.ON)
28 IF PCIB.ERR <> 0 THEN ERROR PCIB.BASERR
29 CALL I.V(I, MEASURE, OUTPUT, START, HALT)
30 IF PCIB.ERR <> 0 THEN ERROR PCIB.BASERR
31 CALL I.V(I, ENABLE.INT.TRIGGER, DISABLE.INT.TRIGGER,
ENABLE.OUTPUT, DISABLE.OUTPUT)
32 IF PCIB.ERR <> 0 THEN ERROR PCIB.BASERR
33 CALL I.V(I, CHECK.DONE, GET.STATUS, SET.FUNCTION,
SET.RANGE)
34 IF PCIB.ERR <> 0 THEN ERROR PCIB.BASERR
35 CALL I.V(I, SET.MODE, WRITE.CAL, READ.CAL, STORE.CAL)
36 IF PCIB.ERR <> 0 THEN ERROR PCIB.BASERR
37 CALL I.V(I, DELAY, SAVE.SYSTEM, J, J)
38 IF PCIB.ERR <> 0 THEN ERROR PCIB.BASERR
39 I = 1
40 CALL I.V(I, SET.GATETIME, SET.SAMPLES, SET.SLOPE,
SET.SOURCE)

```

```

41 IF PCIB.ERR <> 0 THEN ERROR PCIB.BASERR
42 CALL I.C(I, FREQUENCY, AUTO.FREQ, PERIOD, AUTO.PER)
43 IF PCIB.ERR <> 0 THEN ERROR PCIB.BASERR
44 CALL I.C(I, INTERVAL, RATIO, TOTALIZE, R100MILLI)
45 IF PCIB.ERR <> 0 THEN ERROR PCIB.BASERR
46 CALL I.C(I, R1, R10, R100, R1KILO)
47 IF PCIB.ERR <> 0 THEN ERROR PCIB.BASERR
48 CALL I.C(I, R10MEGA, R100MEGA, CHAN.A, CHAN.B)
49 IF PCIB.ERR <> 0 THEN ERROR PCIB.BASERR
50 CALL I.C(I, POSITIVE, NEGATIVE, COMN, SEPARATE)
51 IF PCIB.ERR <> 0 THEN ERROR PCIB.BASERR
52 I = 2
53 I = 3
54 CALL I.V(I, ZERO.OHMS, SET.SPEED, J, J)
55 IF PCIB.ERR <> 0 THEN ERROR PCIB.BASERR
56 CALL I.C(I, DCVOLTS, ACVOLTS, OHMS, R200MILLI)
57 IF PCIB.ERR <> 0 THEN ERROR PCIB.BASERR
58 CALL I.C(I, R2, R20, R200, R2KILO)
59 IF PCIB.ERR <> 0 THEN ERROR PCIB.BASERR
60 CALL I.C(I, R20KILO, R200KILO, R2MEGA, R20MEGA)
61 IF PCIB.ERR <> 0 THEN ERROR PCIB.BASERR
62 CALL I.C(I, AUTOM, R2.5, R12.5, J)
63 IF PCIB.ERR <> 0 THEN ERROR PCIB.BASERR
64 I = 4
65 CALL I.V(I, SET.COMPLEMENT, SET.DRIVER, OUTPUT.NO.WAIT,
ENABLE.HANDSHAKE)
66 IF PCIB.ERR <> 0 THEN ERROR PCIB.BASERR
67 CALL I.V(I, DISABLE.HANDSHAKE, SET.THRESHOLD,
SET.START.BIT, SET.NUM.BITS)
68 IF PCIB.ERR <> 0 THEN ERROR PCIB.BASERR
69 CALL I.V(I, SET.LOGIC.SENSE, J, J, J)
70 IF PCIB.ERR <> 0 THEN ERROR PCIB.BASERR
71 CALL I.C(I, POSITIVE, NEGATIVE, TWOS, UNSIGNED)
72 IF PCIB.ERR <> 0 THEN ERROR PCIB.BASERR
73 CALL I.C(I, OC, TTL, R0, R1)
74 IF PCIB.ERR <> 0 THEN ERROR PCIB.BASERR
75 CALL I.C(I, R2, R3, R4, R5)
76 IF PCIB.ERR <> 0 THEN ERROR PCIB.BASERR
77 CALL I.C(I, R6, R7, R8, R9)
78 IF PCIB.ERR <> 0 THEN ERROR PCIB.BASERR
79 CALL I.C(I, R10, R11, R12, R13)
80 IF PCIB.ERR <> 0 THEN ERROR PCIB.BASERR
81 CALL I.C(I, R14, R15, R16, J)
82 IF PCIB.ERR <> 0 THEN ERROR PCIB.BASERR
83 I = 6
84 CALL I.V(I, SET.FREQUENCY, SET.AMPLITUDE, SET.OFFSET,
SET.SYMMETRY)
85 IF PCIB.ERR <> 0 THEN ERROR PCIB.BASERR
86 CALL I.V(I, SET.BURST.COUNT, J, J, J)

```

```

87 IF PCIB.ERR <> 0 THEN ERROR PCIB.BASERR
88 CALL I.C(I, SINE, SQUARE, TRIANGLE, CONTINUOUS)
89 IF PCIB.ERR <> 0 THEN ERROR PCIB.BASERR
90 CALL I.C(I, GATED, BURST, J, J)
91 IF PCIB.ERR <> 0 THEN ERROR PCIB.BASERR
92 I = 7
93 CALL I.V(I, AUTOSCALE, CALIBRATE, SET.SENSITIVITY,
SET.VERT.OFFSET)
94 IF PCIB.ERR <> 0 THEN ERROR PCIB.BASERR
95 CALL I.V(I, SET.COUPLING, SET.POLARITY, SET.SWEEPSPEED,
SET.DELAY)
96 IF PCIB.ERR <> 0 THEN ERROR PCIB.BASERR
97 CALL I.V(I, SET.TRIG.SOURCE, SET.TRIG.SLOPE,
SET.TRIG.LEVEL, SET.TRIG.MODE)
98 IF PCIB.ERR <> 0 THEN ERROR PCIB.BASERR
99 CALL I.V(I, GET.SINGLE.WF, GET.TWO.WF, GET.VERT.INFO,
GET.TIMEBASE.INFO)
100 IF PCIB.ERR <> 0 THEN ERROR PCIB.BASERR
101 CALL I.V(I, GET.TRIG.INFO, CALC.WFVOLT, CALC.WFTIME,
CALC.WF.STATS)
102 IF PCIB.ERR <> 0 THEN ERROR PCIB.BASERR
103 CALL I.V(I, CALC.RISETIME, CALC.FALLTIME, CALC.PERIOD,
CALC.FREQUENCY)
104 IF PCIB.ERR <> 0 THEN ERROR PCIB.BASERR
105 CALL I.V(I, CALC.PLUSWIDTH, CALC.MINUSWIDTH,
CALC.OVERSHOOT, CALC.PRESHOOT)
106 IF PCIB.ERR <> 0 THEN ERROR PCIB.BASERR
107 CALL I.V(I, CALC.PK.TO.PK, SET.TIMEOUT, SCOPE.START,
MEASURE.SINGLE.WF)
108 IF PCIB.ERR <> 0 THEN ERROR PCIB.BASERR
109 CALL I.V(I, MEASURE.TWO.WF, J, J, J)
110 IF PCIB.ERR <> 0 THEN ERROR PCIB.BASERR
111 CALL I.C(I, R10NANO, R100NANO, R1MICRO, R10MICRO)
112 IF PCIB.ERR <> 0 THEN ERROR PCIB.BASERR
113 CALL I.C(I, R100MICRO, R1MILLI, R10MILLI, R100MILLI)
114 IF PCIB.ERR <> 0 THEN ERROR PCIB.BASERR
115 CALL I.C(I, R1, R10, R20NANO, R200NANO)
116 IF PCIB.ERR <> 0 THEN ERROR PCIB.BASERR
117 CALL I.C(I, R2MICRO, R20MICRO, R200MICRO, R2MILLI)
118 IF PCIB.ERR <> 0 THEN ERROR PCIB.BASERR
119 CALL I.C(I, R20MILLI, R200MILLI, R2, R20)
120 IF PCIB.ERR <> 0 THEN ERROR PCIB.BASERR
121 CALL I.C(I, R50NANO, R500NANO, R5MICRO, R50MICRO)
122 IF PCIB.ERR <> 0 THEN ERROR PCIB.BASERR
123 CALL I.C(I, R500MICRO, R5MILLI, R50MILLI, R500MILLI)
124 IF PCIB.ERR <> 0 THEN ERROR PCIB.BASERR
125 CALL I.C(I, R5, R50, CHAN.A, CHAN.B)
126 IF PCIB.ERR <> 0 THEN ERROR PCIB.BASERR
127 CALL I.C(I, EXTERNAL, POSITIVE, NEGATIVE, AC)

```

```

128 IF PCIB.ERR <> 0 THEN ERROR PCIB.BASERR
129 CALL I.C(I, DC, TRIGGERED, AUTO.TRIG, AUTO.LEVEL)
130 IF PCIB.ERR <> 0 THEN ERROR PCIB.BASERR
131 CALL I.C(I, X1, X10, STANDARD, AVERAGE)
132 IF PCIB.ERR <> 0 THEN ERROR PCIB.BASERR
133 I = 8
134 CALL I.V(I OPEN.CHANNEL, CLOSE.CHANNEL, J, J)
135 IF PCIB.ERR <> 0 THEN ERROR PCIB.BASERR
136 CALL C.S
137 IF PCIB.ERR <> 0 THEN ERROR PCIB.BASERR
138 I$ = PCIB.DIR$ + "\PCIB.PLD"
139 CALL L.P(I$)
140 IF PCIB.ERR <> 0 THEN ERROR PCIB.BASERR
141 I$ = "DMM.01": I = 3: J = 0: K = 0: L = 1
142 CALL DEFINE(DMM.01, I$, I, J, K, L)
143 IF PCIB.ERR <> 0 THEN ERROR PCIB.BASERR
144 I$ = "Func.Gen.01": I = 6: J = 0: K = 1: L = 1
145 CALL DEFINE(Func.Gen.01, I$, I, J, K, L)
146 IF PCIB.ERR <> 0 THEN ERROR PCIB.BASERR
147 I$ = "Scope.01": I = 7: J = 0: K = 2: L = 1
148 CALL DEFINE(Scope.01, I$, I, J, K, L)
149 IF PCIB.ERR <> 0 THEN ERROR PCIB.BASERR
150 I$ = "Counter.01": I = 1: J = 0: K = 3: L = 1
151 CALL DEFINE(Counter.01, I$, I, J, K, L)
152 IF PCIB.ERR <> 0 THEN ERROR PCIB.BASERR
153 I$ = "Dig.In.01": I = 4: J = 0: K = 4: L = 1
154 CALL DEFINE(Dig.In.01, I$, I, J, K, L)
155 IF PCIB.ERR <> 0 THEN ERROR PCIB.BASERR
156 I$ = "Dig.Out.01": I = 4: J = 1: K = 4: L = 1
157 CALL DEFINE(Dig.Out.01, I$, I, J, K, L)
158 IF PCIB.ERR <> 0 THEN ERROR PCIB.BASERR
159 I$ = "Relay.Act.01": I = 8: J = 0: K = 5: L = 1
160 CALL DEFINE(RELAY.ACT.01, I$, I, J, K, L)
161 IF PCIB.ERR <> 0 THEN ERROR PCIB.BASERR
162 I$ = "Relay.Mux.01": I = 2: J = 0: K = 6: L = 1
163 CALL DEFINE(RELAY.MUX.01, I$, I, J, K, L)
164 IF PCIB.ERR <> 0 THEN ERROR PCIB.BASERR
800 I$ = ENVIRON$("PANELS") + "\PANELS.EXE"
801 CALL L.S(I$)
899 GOTO 2
900 IF ERR = PCIB.BASERR THEN GOTO 903
901 PRINT "BASIC error #"; ERR; " occurred in line "; ERL
902 STOP
903 TMPERR = PCIB.ERR: IF TMPERR = 0 THEN TMPERR = PCIB.GLBERR
904 PRINT "PC Instrument error #"; TMPERR; " detected at line
"; ERL
905 PRINT "Error: "; PCIB.ERR$
906 IF LEFT$(PCIB.NAME$, 1) <> CHR$(32) THEN PRINT
"Instrument: "; PCIB.NAME$

```

```

907 STOP
908 COMMON PCIB.DIR$, PCIB.SEG
909 COMMON LD.FILE, GET.MEM, PANELS, DEF.ERR
910 COMMON PCIB.BASERR, PCIB.ERR, PCIB.ERR$, PCIB.NAME$,
PCIB.GLBERR
9 1 1 C O M M O N
READ.REGISTER, READ.SELFID, DEFINE, INITIALIZE.SYSTEM, ENABLE.SY
STEM, DISABLE.SYSTEM, INITIALIZE, POWER.ON, MEASURE, OUTPUT, START
, HALT, ENABLE.INT.TRIGGER, DISABLE.INT.TRIGGER, ENABLE.OUTPUT, D
ISABLE.OUTPUT, CHECK.DONE, GET.STATUS
912 COMMON SET.FUNCTION, SET.RANGE, SET.MODE, WRITE.CAL,
READ.CAL, STORE.CAL, DELAY, SAVE.SYSTEM, SET.GATETIME,
SET.SAMPLES, SET.SLOPE, SET.SOURCE, ZERO.OHMS, SET.SPEED,
SET.COMPLEMENT, SET.DRIVER, OUTPUT.NO.WAIT, ENABLE.HANDSHAKE,
DISABLE.HANDSHAKE
913 COMMON SET.THRESHOLD, SET.START.BIT, SET.NUM.BITS,
SET.LOGIC.SENSE, SET.FREQUENCY, SET.AMPLITUDE, SET.OFFSET,
SET.SYMMETRY, SET.BURST.COUNT, AUTOSCALE, CALIBRATE,
SET.SENSITIVITY, SET.VERT.OFFSET, SET.COUPLING, SET.POLARITY,
SET.SWEEPSPEED
914 COMMON SET.DELAY, SET.TRIG.SOURCE, SET.TRIG.SLOPE,
SET.TRIG.LEVEL, SET.TRIG.MODE, GET.SINGLE.WF, GET.TWO.WF,
GET.VERT.INFO, GET.TIMEBASE.INFO, GET.TRIG.INFO, CALC.WFVOLT,
CALC.WFTIME, CALC.WF.STATS, CALC.RISETIME, CALC.FALLTIME,
CALC.PERIOD
915 COMMON CALC.FREQUENCY, CALC.PLUSWIDTH, CALC.MINUSWIDTH,
CALC.OVERSHOOT, CALC.PRESHOOT, CALC.PK.TO.PK, SET.TIMEOUT,
SCOPE.START, MEASURE.SINGLE.WF, MEASURE.TWO.WF, OPEN.CHANNEL,
CLOSE.CHANNEL
916 COMMON FREQUENCY, AUTO.FREQ, PERIOD, AUTO.PER, INTERVAL,
RATIO, TOTALIZE, R100MILLI, R1, R10, R100, R1KILO, R10MEGA,
R100MEGA, CHAN.A, CHAN.B, POSITIVE, NEGATIVE, COMN, SEPARATE,
DCVOLTS, ACVOLTS, OHMS, R200MILLI, R2, R20, R200, R2KILO,
R20KILO
, R200KILO
917 COMMON R2MEGA, R20MEGA, AUTOM, R2.5, R12.5, POSITIVE,
NEGATIVE, TWOS, UNSIGNED, OC, TTL, R0, R1, R2, R3, R4, R5, R6,
R7, R8, R9, R10, R11, R12, R13, R14, R15, R16, SINE, SQUARE,
TRIANGLE, CONTINUOUS, GATED, BURST, R10NANO, R100NANO,
R1MICRO,
R10MICRO, R100MICRO
918 COMMON R1MILLI, R10MILLI, R100MILLI, R1, R10, R20NANO,
R200NANO, R2MICRO, R20MICRO, R200MICRO, R2MILLI, R20MILLI,
R200MILLI, R2, R20, R50NANO, R500NANO, R5MICRO, R50MICRO,
R500MICRO, R5MILLI, R50MILLI, R500MILLI, R5, R50, CHAN.A,
CHAN.B,
EXTERNAL, POSITIVE
919 COMMON NEGATIVE, AC, DC, TRIGGERED, AUTO.TRIG, AUTO.LEVEL,
X1, X10, STANDARD, AVERAGE

```

```

920  COMMON  DMM.01,  Func.Gen.01,  Scope.01,  Counter.01,
Dig.In.01, Dig.Out.01, RELAY.ACT.01, RELAY.MUX.01
999  'End PCIB Program Shell
1000 REM This step initializes the HP system
1010 CLS
1020 OPTION BASE 1
1030 DIM P(5), PA(50, 5), PP(50, 5), XPT(50), YPT(50), X(50),
Y(50), YAW(50)
1040 REM
1050 CALL INITIALIZE.SYSTEM(PGMSHEL.HPC)
1060 REM
1070 REM SET FUNCTIONON THE 'DMM' , 'RELAY MUX , 'RELAY
ACTUATOR'
1080 REM
1090 CALL SET.FUNCTION(DMM.01, DCVOLTS)
1100 CALL SET.RANGE(DMM.01, AUTOM)
1110 CALL DISABLE.INT.TRIGGER(DMM.01)
1120 CALL ENABLE.OUTPUT(RELAY.MUX.01)
1130 CALL ENABLE.OUTPUT(RELAY.ACT.01)
1140 REM ***** PROGRAM TRAVERSE *****
1150 REM
1160 REM          OPEN THE COM PORT AND INITIALIZE THE MOTOR
SETTINGS
1170 OPEN "com1:1200,n,8,1,rs,cs,ds,cd" FOR RANDOM AS #1
1180 REM SET MOTOR DEFAULT VALUES
1190 DATA 2000,2000,2000,2,2,2,0.000125,0.000125,0.000125
1200 READ V1, V2, V3, R1, R2, R3, C1, C2, C3
1210 REM DEFINE CHARACTERS FOR DATA REDUCTION ALGORITHM
1220 RN2$ = "RENAME A:RAW.DAT "
1230 HEAD1$ = " #      X      Y      P1      P2      P3
P4      P5      YAW  "
1240 FORMAT$ = "##  ##.##  ##.##  ###.###  ###.###  ###.###
###.###  ###.###  ###.##"
1250 PRINT
1260 PRINT "*****"
1270 PRINT "** USER MUST SELECT 'CAPS LOCK' FUNCTION **"
1280 PRINT "*****"
1290 REM          DISPLAY MOTOR DEFAULT SETTINGS
1300 PRINT "          *****"
1310 PRINT "          INITIALIZED VALUES FOR ALL MOTOR
SETTINGS:"
1320 PRINT "          VELOCITY = 1000 STEPS/SEC"
1330 PRINT "          RAMP(MOTOR ACCELERATION) = 2  (6000
STEPS/SEC^2)"
1340 PRINT "          DEFAULT INCREMENTAL UNITS ARE
INCHES"
1350 PRINT "          *****"
1360 PRINT
1370 PRINT "NOTE!! USE MANUAL CONTROL TO INITIALIZE PROBE

```



```

POSITION BEFORE"
1380 PRINT "                SELECTING COMPUTER CONTROLLED MOVEMENT.
"
1390 PRINT
1400 INPUT "MANUAL CONTROL OR COMPUTER CONTROL (ENTER 'MAN' or
'CP')"; CON$
1410 IF CON$ = "CP" THEN 3490
1420 REM  OPTION TO CHANGE DEFAULT SETTINGS OF VELOCITY OR
ACCELERATION RAMP
1430 PRINT
1440 PRINT
1450 PRINT " DO YOU WANT TO CHANGE THE VELOCITY OR
ACCELERATION RAMP"
1460 PRINT "                DEFAULT SETTINGS? (Y or N)"
1470 PRINT
1480 PRINT "IF 'NO', THIS PROGRAM WILL THEN LET YOU DEFINE
THE"
1490 PRINT "DISTANCE YOU WANT TO MOVE (IN INCHES). IF 'YES',"
1500 PRINT "YOU CAN CHANGE ANY OR ALL OF THE DEFAULT SETTINGS
FOR ANY MOTOR."
1510 PRINT
1520 PRINT
1530 PRINT
1540 INPUT "DO YOU WANT TO CHANGE ANY OF THE DEFAULT SETTINGS?
(Y or N)"; D$
1550 IF D$ = "Y" THEN 1590
1560 IF D$ = "N" THEN 2220
1570 REM
1580 REM  **** OPERATOR SELECTED MOTOR VARIABLES ****
1590 PRINT
1600 PRINT
1610 INPUT "WHICH DEFAULT VALUE? (ENTER '1' FOR VELOC OR '2'
FOR ACCEL RAMP)"; L
1620 ON L GOTO 1690, 1930
1630 PRINT "DO YOU WANT TO CHANGE THE DEFAULT VELOCITY? (Y OR
N)"
1640 INPUT V$
1650 IF V$ = "Y" THEN 1690
1660 PRINT "DO YOU WANT TO CHANGE THE DEFAULT ACCELERATION
RAMP? (Y or N)"
1670 IF R$ = "Y" THEN 1990
1680 IF R$ = "N" THEN 1450
1690 PRINT
1700 PRINT
1710 INPUT "WHICH MOTOR VELOCITY DO YOU WISH TO CHANGE? (1,2,
or 3)"; J
1720 ON J GOTO 1730, 1830, 1880
1730 PRINT
1740 PRINT

```

```

1750 INPUT "ENTER DESIRED VELOCITY OF MOTOR #1"; V1
1760 PRINT
1770 PRINT
1780 PRINT
1790 PRINT "DO YOU WANT TO CHANGE VELOCITY OF ANOTHER MOTOR?
(Y OR N)"
1800 INPUT V$
1810 IF V$ = "Y" THEN 1690
1820 IF V$ = "N" THEN 1430
1830 PRINT
1840 PRINT
1850 INPUT "ENTER DESIRED VELOCITY OF MOTOR 2"; V2
1860 PRINT
1870 GOTO 1780
1880 PRINT
1890 PRINT
1900 INPUT "ENTER DESIRED VELOCITY OF MOTOR #3"; V3
1910 PRINT
1920 GOTO 1780
1930 PRINT
1940 PRINT
1950 INPUT "WHICH MOTOR ACCEL RAMP DO YOU WANT TO CHANGE? (1,
2, or 3)"; K
1960 ON K GOTO 1970, 2060, 2120
1970 PRINT
1980 PRINT
1990 INPUT "ENTER DESIRED ACCELERATION RAMP OF MOTOR #1"; R1
2000 PRINT
2010 PRINT
2020 PRINT "DO YOU WANT TO CHANGE THE ACCEL RAMP OF ANOTHER
MOTOR? (Y or N)?"
2030 INPUT RM$
2040 IF RM$ = "Y" THEN 1930
2050 IF RM$ = "N" THEN 1450
2060 PRINT
2070 PRINT
2080 INPUT "ENTER DESIRED ACCELERATION RAMP OF MOTOR #2"; R2
2090 PRINT
2100 PRINT
2110 GOTO 2000
2120 PRINT
2130 PRINT
2140 INPUT "ENTER DESIRED ACCELERATION RAMP OF MOTOR #3"; R3
2150 PRINT
2160 PRINT
2170 GOTO 2000
2180 REM
2190 REM DEFINE DISTANCE TO MOVE MOTOR
2200 PRINT

```

```

2210 PRINT
2220 PRINT
2230 REM INITIALIZE MOTOR INCREMENTS TO ZERO
2240 I1 = 0
2250 I2 = 0
2260 I3 = 0
2270 PRINT
2      2      8      0      P      R      I      N      T      "
*****
2290 PRINT " **          DEFINE WHICH MOTOR YOU WANT TO MOVE
      **"
2300 PRINT " **
      **"
2310 PRINT " **          NOTE!!! A POSITIVE ('+') INCREMENT TO
A MOTOR **"
2320 PRINT " **          MOVES TRAVERSER AWAY FROM THAT PARTICULAR
MOTOR **"
2330 PRINT " **
      **"
2340 PRINT " **  -- MOTOR #1 MOVES THE PROBE UPSTREAM AGAINST
THE FLOW **"
2350 PRINT " **  -- MOTOR #2 MOVES THE PROBE TOWARD THE ACCESS
WINDOW **"
2360 PRINT " **  -- MOTOR #3 MOVES THE PROBE VERTICALLY
DOWNWARD **"
2      3      7      0      P      R      I      N      T      "
*****
2380 PRINT
2390 PRINT
2400 INPUT "WHICH MOTOR DO YOU WANT TO MOVE? (1,2, or 3)"; L
2410 ON L GOTO 2420, 2680, 2970
2420 PRINT
2430 PRINT
2440 PRINT "HOW FAR DO YOU WANT TO MOVE MOTOR #1?"
2450 PRINT " ***** (ENTER DISTANCE IN INCHES) *****"
2460 INPUT I1
2470 PRINT
2480 PRINT " *****"
2490 PRINT
2500 PRINT "SUMMARY OF OPERATOR INPUTS:"
2510 PRINT "          MOTOR #1  VELOCITY = "; V1
2520 PRINT "          ACCELERATION RAMP = "; R1
2530 PRINT "          INCREMENTAL DISTANCE = "; I1;
"INCHES"
2540 PRINT " *****"
2550 PRINT "DO YOU WANT TO CHANGE ANY OF THESE VALUES? (Y or
N) "
2560 PRINT
2570 PRINT "ENTER 'N' TO START MOTOR MOVEMENT.  ENTER 'Y' TO

```

```

RETURN"
2580 PRINT "TO VARIABLE SELECTION SUBROUTINE."
2590 INPUT V$
2600 IF V$ = "Y" THEN 1430
2610 GOSUB 3410
2620 PRINT
2630 PRINT "DO YOU WANT TO MOVE ANOTHER MOTOR ALSO? (Y or N)?"
2640 INPUT C$
2650 IF C$ = "Y" THEN 2220
2660 IF C$ = "N" THEN 3260
2670 PRINT
2680 PRINT
2690 PRINT "HOW FAR DO YOU WANT TO MOVE MOTOR #2?"
2700 PRINT " ***** (ENTER DISTANCE IN INCHES) *****"
2710 INPUT I2
2720 PRINT
2730 PRINT
2740 REM DISPLAY OPERATOR SELECTED MOTOR VARIABLES
2750 PRINT " *****"
2760 PRINT
2770 PRINT "SUMMARY OF OPERATOR INPUTS:"
2780 PRINT "          MOTOR #2    VELOCITY = "; V2
2790 PRINT "          ACCELERATION RAMP = "; R2
2800 PRINT "          INCREMENTAL DISTANCE = "; I2;
"INCHES"
2810 PRINT " *****"
2820 PRINT
2830 PRINT
2840 PRINT "DO YOU WANT TO CHANGE ANY OF THESE VALUES? (Y or
N)"
2850 PRINT
2860 PRINT "ENTER 'N' TO START MOTOR MOVEMENT.  ENTER 'Y' TO
RETURN"
2870 PRINT "TO VARIABLE SELECTION SUBROUTINE."
2880 INPUT V$
2890 IF V$ = "Y" THEN 1430
2900 GOSUB 3410
2910 PRINT
2920 PRINT "DO YOU WANT TO MOVE ANOTHER MOTOR ALSO? (Y or N)?"
2930 INPUT C$
2940 IF C$ = "Y" THEN 2220
2950 IF C$ = "N" THEN 3260
2960 PRINT
2970 PRINT
2980 PRINT "HOW FAR DO YOU WANT TO MOVE MOTOR #3?"
2990 PRINT " ***** (ENTER DISTANCE IN INCHES) *****"
3000 INPUT I3
3010 PRINT
3020 PRINT

```

```

3030 REM DISPLAY OPERATOR SELECTED MOTOR VARIABLES
3040 PRINT " *****"
3050 PRINT
3060 PRINT "SUMMARY OF OPERATOR INPUTS:"
3070 PRINT "          MOTOR #3    VELOCITY = "; V3
3080 PRINT "          ACCELERATION RAMP = "; R3
3090 PRINT "          INCREMENTAL DISTANCE = "; I3;
"INCHES"
3100 PRINT
3110 PRINT " *****"
3120 PRINT
3130 PRINT
3140 PRINT "DO YOU WANT TO CHANGE ANY OF THESE VALUES? (Y or
N)"
3150 PRINT
3160 PRINT "ENTER 'N' TO START MOTOR MOVEMENT.  ENTER 'Y' TO
RETURN"
3170 PRINT "TO VARIABLE SELECTION SUBROUTINE."
3180 INPUT V$
3190 IF V$ = "Y" THEN 1430
3200 GOSUB 3410
3210 PRINT
3220 PRINT
3230 INPUT "DO YOU WANT TO INPUT ANOTHER MANUAL MOTOR MOVEMENT
(Y or N)"; M$
3240 IF M$ = "Y" THEN 2210
3250 PRINT
3260 PRINT "DO YOU WANT TO INPUT COMPUTER CONTROLLED MOTOR
MOVEMENT?"
3270 PRINT "          ***** NOTE!!! ***** "
3280 PRINT " ALL PREVIOUS MOTOR INCREMENT INPUTS HAVE BEEN
ZEROIZED."
3290 PRINT "PROGRAM WILL LET YOU CHOOSE MANUAL OR CP-CONTROLLED
MOVEMENT."
3300 PRINT "***** (IF 'NO', THE PROGRAM WILL END). *****"
3310 PRINT
3320 INPUT "DO YOU WANT COMPUTER CONTROLLED MOTOR MOVEMENT (Y
or N)"; N$
3330 IF N$ = "Y" THEN 3500
3340 PRINT
3350 PRINT
3360 PRINT
3370 PRINT "          *****"
3380 PRINT "          THE PROGRAM HAS ENDED."
3390 PRINT "          *****"
3400 END
3410 REM ***** MOTOR MOVEMENT SUBROUTINE *****
3420 PRINT #1, "&": PRINT #1, "E"; "C1="; C1; ":C2="; C2;
":C3="; C3

```

```

3430 PRINT #1, "I1="; I1; ":V1="; V1; ":R1="; R1;
3440 PRINT #1, ":I2="; I2; ":V2="; V2; ":R2="; R2
3450 PRINT #1, "I3="; I3; ":V3="; V3; ":R3="; R3; ":@"
3460 RETURN
3470 REM *****
3480 REM *****
3490 PRINT
3500 REM ***** COMPUTER CONTROLLED MOVEMENT *****
3510 PRINT
3520 PRINT "THE PRESSURE DATA WILL BE WRITTEN TO FILES ON
DRIVE 'A' "
3530 PRINT
3540 PRINT "YOU WILL BE ASKED TO INPUT FILE NAMES FOR THESE."
3550 PRINT
3560 INPUT "IS A FORMATTED DISK IN DRIVE 'A'? PRESS 'ENTER'
TO CONTINUE"; D$
3570 PRINT
3580 PRINT
3590 PRINT
3600 PRINT " *****"
3610 PRINT " ** NOTE !!! **"
3620 PRINT " ** COMPUTER CONTROLLED MOVEMENT **"
3630 PRINT " ** IS PROGRAMMED WITH A **"
3640 PRINT " ** DEFAULTED NEGATIVE MOTOR INCREMENT **"
3650 PRINT " ** (i.e. MOTOR #3 WILL MOVE UPWARD **"
3660 PRINT " ** BY ENTERING A (+) DISTANCE). **"
3670 PRINT " *****"
3680 PRINT
3690 REM SET INITIAL MOVEMENT DISTANCE AND NUMBER OF DATA
POINTS TO ZERO
3700 HT = 0
3710 WD = 0
3720 DIST = 0
3730 XPT = 0
3740 YPT = 0
3750 N = 0
3760 PRINT
3770 PRINT
3780 INPUT "WHAT IS THE DIMENSION ( X , Y ) (IN INCHES) THAT
YOU WANT TO MEASURE."; WD, HT
3790 PRINT
3800 INPUT "WHAT IS THE STEP (IN INCHES) THAT YOU WANT TO
MOVE."; DIST
3810 YPT = INT(HT / DIST) + 1
3820 XPT = INT(WD / DIST) + 1
3830 N = XPT * YPT
3840 PRINT
3850 PRINT "THERE ARE "; XPT; " * "; YPT; " = "; N; " POINTS
TO BE MEASURED "

```

```

3860 PRINT
3870 INPUT "ARE THE NUMBER OF POINTS IS OK.(Y OR N)"; C$
3880 IF C$ = "N" THEN 3780
3890 CLS
3900 N = XPT
3910 IF (N < 1) OR (N > 99) GOTO 3780
3920 REM *** GENERATING STRING STRING SEGMENTS FOR DATA FILE
NAMES
3930 B$ = MID$(STR$(1), 2): REM ** STRING NUMBER "1"
3940 E$ = MID$(STR$(N), 2): REM ** ENDING STRING NUMBER "N"
3950 X$ = "XXXXXX"
3960 EX$ = ".DAT"
3970 CLS
3980 PRINT "DATA FILES WILL BE INCREMENTED FROM:"
3990 PRINT
4000 PRINT (X$ + B$ + EX$); " To "; (X$ + E$ + EX$)
4010 PRINT
4020 PRINT
4030 INPUT "ENTER DATA FILE NAME (6 CHARACTERS MAX -- NO
EXTENSION)"; F2$
4040 PRINT
4050 PRINT
4060 IF LEN(F2$) > 6 OR LEN(F2$) < 1 GOTO 4030
4070 CLS
4080 PRINT N; "DATA FILES WILL BE GENERATED AND INCREMENTED AS
FOLLOWS:"
4090 PRINT
4100 PRINT
4110 PRINT (F2$ + B$ + EX$); " To "; (F2$ + E$ + EX$)
4120 PRINT
4130 PRINT
4140 INPUT "ARE THE NUMBER OF POINTS AND FILE NAMES OK.(Y OR
N)"; C$
4150 IF C$ = "N" GOTO 3780
4160 IF C$ = "Y" GOTO 4180
4170 GOTO 4140
4180 CLS
4190 PRINT
4200 PRINT
4210 REM SET INITIAL POSITION DATA
4220 X(1) = -DIST
4230 Y(1) = -DIST
4240 FOR IX = 2 TO XPT + 1
4250 X(IX) = 0
4260 NEXT IX
4270 FOR JY = 2 TO YPT + 1
4280 Y(JY) = 0
4290 NEXT JY
4300 FOR I = 1 TO XPT

```

```

4302 I1 = 0
4304 I2 = 0
4306 I3 = 0
4310 FOR J = 1 TO YPT
4320 REM MOTOR CP-CONTROLLED MOTOR MOVEMENT
4330 I1 = 0
4340 I2 = 0
4350 I3 = 0
4360 REM EACH POINT TAKE 10 TIMES READINGS
4370 X(I + 1) = X(I) + DIST
4380 XPT(J) = X(I + 1)
4390 Y(J + 1) = Y(J) + DIST
4400 YPT(J) = Y(J + 1)
4405 INPUT " ADJUST THE WHEEL TO MAKE THE P2 =P3, INPUT THE YAW
ANGLE"; YAW(J)
4408 PRINT
4410 INPUT " PRESS 'ENTER' TO START THE MEASUREMENT"; MOVE$
4420 REM
4430 REM READ FIVE CHANNELS AND DISPLAY THE DATA
4440 REM
4450 STEPPER = 4
4460 SWITCH = 3
4470 HOMER = 8
4480 DELAY1 = .1
4490 DELAY2 = 1
4500 REM SET THE S.V PORT TO #4
4510 FOR IL = 1 TO 3
4520 THYME = TIMER
4530 CALL OUTPUT(RELAY.ACT.01,STEPPER)
4540 CHKTIME = TIMER
4550 IF CHKTIME < (THYME + DELAY1) GOTO 4540
4560 CALL OPEN.CHANNEL(RELAY.ACT.01, SWITCH)
4570 CLS
4580 NEXT IL
4590 PRINT
4600 PRINT " NOW IS POINT "; J
4610 REM START MEASURE FROM PORT 4 TO PORT 8
4620 FOR JJ = 1 TO 5
4630 CALL OUTPUT(RELAY.ACT.01,STEPPER)
4640 CHKTIME = TIMER
4650 IF CHKTIME < (THYME + DELAY2) GOTO 4640
4660 REM EACH PORT SAMPLE 10 TIMES
4670 FOR II = 1 TO 10
4680 ROUT = 1
4690 CALL OUTPUT(RELAY.MUX.01,ROUT)
4700 CALL MEASURE(DMM.01, VOLTS)
4710 PA(II, JJ) = VOLTS
4720 NEXT II
4730 CALL OPEN.CHANNEL(RELAY.ACT.01, SWITCH)

```



```

4740 IF JJ = 5 THEN 4760
4750 NEXT JJ
4760 REM HOME THE S.V PORT TO #48
4770 CALL OUTPUT(RELAY.ACT.01,HOMER)
4780 CALL OPEN.CHANNEL(RELAY.ACT.01, HOMER)
4790 REM
4800 REM DISPLAY THE SAMPLE DATA
4810 REM
4820 PRINT HEAD1$
4830 FOR IS= 1 TO 10
4 8 4 0 P R I N T U S I N G
FORMAT$;IS,XPT(J),YPT(J),PA(IS,1),PA(IS,2),PA(IS,3),PA(IS,4)
,PA(IS,5),YAW(J)
4850 NEXT IS
4860 REM
4870 REM AVERAGE THE DATA
4880 REM
4890 FOR JA = 1 TO 5
4900 TOTAL = 0
4910 FOR IA = 1 TO 10
4920 TOTAL = TOTAL + PA(IA, JA)
4930 NEXT IA
4940 AVERAGE = TOTAL / 10
4950 P(JA) = AVERAGE
4960 NEXT JA
4970 PRINT
4980 PRINT "THE AVERAGES ARE: "
5000 PRINT HEAD1$
5010 FOR JD = 1 TO 5
5020 PP(J, JD) = P(JD)
5030 NEXT JD
5040 PRINT USING FORMAT$; J; XPT(J); YPT(J); PP(J, 1); PP(J,
2); PP(J, 3); PP(J, 4); PP(J, 5); YAW(J)
5045 PRINT
5048 PRINT USING "THE NULLING ERROR IS +#.####"; PP(J, 3) -
PP(J, 2)
5049 PRINT
5050 PRINT "DO YOU WANT RE-MEASURE AGAIN (Y / N)"
5060 PRINT
5062 PRINT "IF 'Y' WILL RE-SAMPLE AGAIN."
5064 PRINT
5070 INPUT "IF 'N' WILL MOVE THE TRAVERSER STEP UPWARD (WAIT
7 SEC )"; C$
5075 PRINT
5080 IF C$ = "Y" THEN 4405
5082 IF C$ = "N" THEN 5090
5084 GOTO 5070
5090 IF J = YPT THEN 5160
5100 REM

```

```

5110 REM MOVE THE TRAVERSER STEP UPWARD.
5120 REM
5130 I3 = -DIST
5140 GOSUB 3410
5150 NEXT J
5160 REM*** STORE DATA BEFORE NEXT SAMPLE***
5170 OPEN "A:\RAW.DAT" FOR OUTPUT AS #2
5180 PRINT #2, HEAD1$
5190 FOR ID = 1 TO YPT
5200 PRINT #2, USING FORMAT$; ID; XPT(ID); VPT(ID); PP(ID, 1);
PP(ID, 2); PP(ID, 3); PP(ID, 4); PP(ID, 5), YAW(ID)
5210 NEXT ID
5220 CLOSE #2
5230 REM *** GENERATING INCREMENTED DATA FILE NAME
5240 IF (I > 10) OR (I = 10) THEN I$ = MID$(STR$(I), 2)
5250 IF (I < 10) THEN I$ = (MID$(STR$(0), 2) + MID$(STR$(I),
2))
5260 FI2$ = (F2$ + I$ + EX$)
5270 PRINT
5280 PRINT " WRITING DATA FILE "; FI2$
5290 DF2$ = RN2$ + FI2$
5300 REM ** RENAME DATA FILE
5310 SHELL DF2$
5320 REM
5330 REM MOVE THE TRAVERSER TO THE NEXT SAMPLE POSITION
5340 REM
5350 PRINT
5360 IF I = XPT THEN 5430
5370 INPUT "THEN PRESS 'ENTER' FOR NEXT COLUMN SAMPLE( 90 SEC)
"; MOVE$
5390 I2 = -DIST
5400 I3 = HT
5410 GOSUB 3410
5420 NEXT I
5430 CLS
5440 PRINT "ALL MOVEMENTS COMPLETE"
5450 PRINT
5460 PRINT
5470 PRINT "YOU WANT TO REPOSITION TRAVERSER FOR ANOTHER
MOVEMENT (Y OR N)?"
5480 PRINT
5490 PRINT ".IF 'Y', THE PROGRAM WILL TAKE YOU TO MANUAL
CONTROL SUBROUTINE."
5500 PRINT "IF 'N', THE PROGRAM WILL END."
5510 PRINT
5520 INPUT "ANOTHER MOVEMENT"; R$
5530 IF R$ = "Y" THEN 1370
5540 IF R$ = "N" THEN 3370

```

## APPENDIX B

```

1 DEF SEG : CLEAR , &HFE00: GOTO 4'Begin PCIB Program Shell
2 GOTO 1000 ' User program
3 GOTO 900 ' Error handling
4 I = &HFE00' Copyright Hewlett-Packard 1984,1985
5 PCIB.DIR$ = ENVIRON$("PCIB")
6 I$ = PCIB.DIR$ + "\PCIBILC.BLD"
7 BLOAD I$, I
8 CALL I(PCIB.DIR$, I%, J%): PCIB.SEG = I%
9 IF J% = 0 THEN GOTO 13
10 PRINT "Unable to load.";
11 PRINT "      (Error #"; J%; ")"
12 END
13 '
14 DEF SEG = PCIB.SEG: O.S = 5: C.S = 10: I.V = 15
15 I.C = 20: L.P = 25: LD.FILE = 30
16 GET.MEM = 35: L.S = 40: PANELS = 45: DEF.ERR = 50
17 PCIB.ERR$ = STRING$(64, 32): PCIB.NAME$ = STRING$(16, 32)
18 CALL DEF.ERR(PCIB.ERR, PCIB.ERR$, PCIB.NAME$, PCIB.GLBERR):
PCIB.BASERR = 255
19 ON ERROR GOTO 3
20 J = -1
21 I$ = PCIB.DIR$ + "\PCIB.SYN"
22 CALL O.S(I$)
23 IF PCIB.ERR <> 0 THEN ERROR PCIB.BASERR
24 I = 0
25 CALL I.V(I, READ.REGISTER, READ.SELFID, DEFINE,
INITIALIZE.SYSTEM)
26 IF PCIB.ERR <> 0 THEN ERROR PCIB.BASERR
27 CALL I.V(I, ENABLE.SYSTEM, DISABLE.SYSTEM, INITIALIZE,
POWER.ON)
28 IF PCIB.ERR <> 0 THEN ERROR PCIB.BASERR
29 CALL I.V(I, MEASURE, OUTPUT, START, HALT)
30 IF PCIB.ERR <> 0 THEN ERROR PCIB.BASERR
31 CALL I.V(I, ENABLE.INT.TRIGGER, DISABLE.INT.TRIGGER,
ENABLE.OUTPUT, DISABLE.OUTPUT)
32 IF PCIB.ERR <> 0 THEN ERROR PCIB.BASERR
33 CALL I.V(I, CHECK.DONE, GET.STATUS, SET.FUNCTION,
SET.RANGE)
34 IF PCIB.ERR <> 0 THEN ERROR PCIB.BASERR
35 CALL I.V(I, SET.MODE, WRITE.CAL, READ.CAL, STORE.CAL)
36 IF PCIB.ERR <> 0 THEN ERROR PCIB.BASERR
37 CALL I.V(I, DELAY, SAVE.SYSTEM, J, J)
38 IF PCIB.ERR <> 0 THEN ERROR PCIB.BASERR
39 I = 1
40 CALL I.V(I, SET.GATETIME, SET.SAMPLES, SET.SLOPE,
SET.SOURCE)

```

```

41 IF PCIB.ERR <> 0 THEN ERROR PCIB.BASERR
42 CALL I.C(I, FREQUENCY, AUTO.FREQ, PERIOD, AUTO.PER)
43 IF PCIB.ERR <> 0 THEN ERROR PCIB.BASERR
44 CALL I.C(I, INTERVAL, RATIO, TOTALIZE, R100MILLI)
45 IF PCIB.ERR <> 0 THEN ERROR PCIB.BASERR
46 CALL I.C(I, R1, R10, R100, R1KILO)
47 IF PCIB.ERR <> 0 THEN ERROR PCIB.BASERR
48 CALL I.C(I, R10MEGA, R100MEGA, CHAN.A, CHAN.B)
49 IF PCIB.ERR <> 0 THEN ERROR PCIB.BASERR
50 CALL I.C(I, POSITIVE, NEGATIVE, COMN, SEPARATE)
51 IF PCIB.ERR <> 0 THEN ERROR PCIB.BASERR
52 I = 2
53 I = 3
54 CALL I.V(I, ZERO.OHMS, SET.SPEED, J, J)
55 IF PCIB.ERR <> 0 THEN ERROR PCIB.BASERR
56 CALL I.C(I, DCVOLTS, ACVOLTS, OHMS, R200MILLI)
57 IF PCIB.ERR <> 0 THEN ERROR PCIB.BASERR
58 CALL I.C(I, R2, R20, R200, R2KILO)
59 IF PCIB.ERR <> 0 THEN ERROR PCIB.BASERR
60 CALL I.C(I, R20KILO, R200KILO, R2MEGA, R20MEGA)
61 IF PCIB.ERR <> 0 THEN ERROR PCIB.BASERR
62 CALL I.C(I, AUTOM, R2.5, R12.5, J)
63 IF PCIB.ERR <> 0 THEN ERROR PCIB.BASERR
64 I = 4
65 CALL I.V(I, SET.COMPLEMENT, SET.DRIVER, OUTPUT.NO.WAIT,
ENABLE.HANDSHAKE)
66 IF PCIB.ERR <> 0 THEN ERROR PCIB.BASERR
67 CALL I.V(I, DISABLE.HANDSHAKE, SET.THRESHOLD,
SET.START.BIT, SET.NUM.BITS)
68 IF PCIB.ERR <> 0 THEN ERROR PCIB.BASERR
69 CALL I.V(I, SET.LOGIC.SENSE, J, J, J)
70 IF PCIB.ERR <> 0 THEN ERROR PCIB.BASERR
71 CALL I.C(I, POSITIVE, NEGATIVE, TWOS, UNSIGNED)
72 IF PCIB.ERR <> 0 THEN ERROR PCIB.BASERR
73 CALL I.C(I, OC, TTL, R0, R1)
74 IF PCIB.ERR <> 0 THEN ERROR PCIB.BASERR
75 CALL I.C(I, R2, R3, R4, R5)
76 IF PCIB.ERR <> 0 THEN ERROR PCIB.BASERR
77 CALL I.C(I, R6, R7, R8, R9)
78 IF PCIB.ERR <> 0 THEN ERROR PCIB.BASERR
79 CALL I.C(I, R10, R11, R12, R13)
80 IF PCIB.ERR <> 0 THEN ERROR PCIB.BASERR
81 CALL I.C(I, R14, R15, R16, J)
82 IF PCIB.ERR <> 0 THEN ERROR PCIB.BASERR
83 I = 6
84 CALL I.V(I, SET.FREQUENCY, SET.AMPLITUDE, SET.OFFSET,
SET.SYMMETRY)
85 IF PCIB.ERR <> 0 THEN ERROR PCIB.BASERR
86 CALL I.V(I, SET.BURST.COUNT, J, J, J)

```

```

87 IF PCIB.ERR <> 0 THEN ERROR PCIB.BASERR
88 CALL I.C(I, SINE, SQUARE, TRIANGLE, CONTINUOUS)
89 IF PCIB.ERR <> 0 THEN ERROR PCIB.BASERR
90 CALL I.C(I, GATED, BURST, J, J)
91 IF PCIB.ERR <> 0 THEN ERROR PCIB.BASERR
92 I = 7
93 CALL I.V(I, AUTOSCALE, CALIBRATE, SET.SENSITIVITY,
SET.VERT.OFFSET)
94 IF PCIB.ERR <> 0 THEN ERROR PCIB.BASERR
95 CALL I.V(I, SET.COUPLING, SET.POLARITY, SET.SWEEPSPEED,
SET.DELAY)
96 IF PCIB.ERR <> 0 THEN ERROR PCIB.BASERR
97 CALL I.V(I, SET.TRIG.SOURCE, SET.TRIG.SLOPE,
SET.TRIG.LEVEL, SET.TRIG.MODE)
98 IF PCIB.ERR <> 0 THEN ERROR PCIB.BASERR
99 CALL I.V(I, GET.SINGLE.WF, GET.TWO.WF, GET.VERT.INFO,
GET.TIMEBASE.INFO)
100 IF PCIB.ERR <> 0 THEN ERROR PCIB.BASERR
101 CALL I.V(I, GET.TRIG.INFO, CALC.WFVOLT, CALC.WFTIME,
CALC.WF.STATS)
102 IF PCIB.ERR <> 0 THEN ERROR PCIB.BASERR
103 CALL I.V(I, CALC.RISETIME, CALC.FALLTIME, CALC.PERIOD,
CALC.FREQUENCY)
104 IF PCIB.ERR <> 0 THEN ERROR PCIB.BASERR
105 CALL I.V(I, CALC.PLUSWIDTH, CALC.MINUSWIDTH,
CALC.OVERSHOOT, CALC.PRESHOOT)
106 IF PCIB.ERR <> 0 THEN ERROR PCIB.BASERR
107 CALL I.V(I, CALC.PK.TO.PK, SET.TIMEOUT, SCOPE.START,
MEASURE.SINGLE.WF)
108 IF PCIB.ERR <> 0 THEN ERROR PCIB.BASERR
109 CALL I.V(I, MEASURE.TWO.WF, J, J, J)
110 IF PCIB.ERR <> 0 THEN ERROR PCIB.BASERR
111 CALL I.C(I, R10NANO, R100NANO, R1MICRO, R10MICRO)
112 IF PCIB.ERR <> 0 THEN ERROR PCIB.BASERR
113 CALL I.C(I, R100MICRO, R1MILLI, R10MILLI, R100MILLI)
114 IF PCIB.ERR <> 0 THEN ERROR PCIB.BASERR
115 CALL I.C(I, R1, R10, R20NANO, R200NANO)
116 IF PCIB.ERR <> 0 THEN ERROR PCIB.BASERR
117 CALL I.C(I, R2MICRO, R20MICRO, R200MICRO, R2MILLI)
118 IF PCIB.ERR <> 0 THEN ERROR PCIB.BASERR
119 CALL I.C(I, R20MILLI, R200MILLI, R2, R20)
120 IF PCIB.ERR <> 0 THEN ERROR PCIB.BASERR
121 CALL I.C(I, R50NANO, R500NANO, R5MICRO, R50MICRO)
122 IF PCIB.ERR <> 0 THEN ERROR PCIB.BASERR
123 CALL I.C(I, R500MICRO, R5MILLI, R50MILLI, R500MILLI)
124 IF PCIB.ERR <> 0 THEN ERROR PCIB.BASERR
125 CALL I.C(I, R5, R50, CHAN.A, CHAN.B)
126 IF PCIB.ERR <> 0 THEN ERROR PCIB.BASERR
127 CALL I.C(I, EXTERNAL, POSITIVE, NEGATIVE, AC)

```

```

128 IF PCIB.ERR <> 0 THEN ERROR PCIB.BASERR
129 CALL I.C(I, DC, TRIGGERED, AUTO.TRIG, AUTO.LEVEL)
130 IF PCIB.ERR <> 0 THEN ERROR PCIB.BASERR
131 CALL I.C(I, X1, X10, STANDARD, AVERAGE)
132 IF PCIB.ERR <> 0 THEN ERROR PCIB.BASERR
133 I = 8
134 CALL I.V(I, OPEN.CHANNEL, CLOSE.CHANNEL, J, J)
135 IF PCIB.ERR <> 0 THEN ERROR PCIB.BASERR
136 CALL C.S
137 IF PCIB.ERR <> 0 THEN ERROR PCIB.BASERR
138 I$ = PCIB.DIR$ + "\PCIB.PLD"
139 CALL L.P(I$)
140 IF PCIB.ERR <> 0 THEN ERROR PCIB.BASERR
141 I$ = "DMM.01": I = 3: J = 0: K = 0: L = 1
142 CALL DEFINE(DMM.01, I$, I, J, K, L)
143 IF PCIB.ERR <> 0 THEN ERROR PCIB.BASERR
144 I$ = "Func.Gen.01": I = 6: J = 0: K = 1: L = 1
145 CALL DEFINE(FUNC.GEN.01, I$, I, J, K, L)
146 IF PCIB.ERR <> 0 THEN ERROR PCIB.BASERR
147 I$ = "Scope.01": I = 7: J = 0: K = 2: L = 1
148 CALL DEFINE(SCOPE.01, I$, I, J, K, L)
149 IF PCIB.ERR <> 0 THEN ERROR PCIB.BASERR
150 I$ = "Counter.01": I = 1: J = 0: K = 3: L = 1
151 CALL DEFINE(COUNTER.01, I$, I, J, K, L)
152 IF PCIB.ERR <> 0 THEN ERROR PCIB.BASERR
153 I$ = "Dig.In.01": I = 4: J = 0: K = 4: L = 1
154 CALL DEFINE(DIG.IN.01, I$, I, J, K, L)
155 IF PCIB.ERR <> 0 THEN ERROR PCIB.BASERR
156 I$ = "Dig.Out.01": I = 4: J = 1: K = 4: L = 1
157 CALL DEFINE(DIG.OUT.01, I$, I, J, K, L)
158 IF PCIB.ERR <> 0 THEN ERROR PCIB.BASERR
159 I$ = "Relay.Act.01": I = 8: J = 0: K = 5: L = 1
160 CALL DEFINE(RELAY.ACT.01, I$, I, J, K, L)
161 IF PCIB.ERR <> 0 THEN ERROR PCIB.BASERR
162 I$ = "Relay.Mux.01": I = 2: J = 0: K = 6: L = 1
163 CALL DEFINE(RELAY.MUX.01, I$, I, J, K, L)
164 IF PCIB.ERR <> 0 THEN ERROR PCIB.BASERR
800 I$ = ENVIRON$("PANELS") + "\PANELS.EXE"
801 CALL L.S(I$)
899 GOTO 2
900 IF ERR = PCIB.BASERR THEN GOTO 903
901 PRINT "BASIC error #"; ERR; " occurred in line "; ERL
902 STOP
903 TMPERR = PCIB.ERR: IF TMPERR = 0 THEN TMPERR = PCIB.GLBERR
904 PRINT "PC Instrument error #"; TMPERR; " detected at line
"; ERL
905 PRINT "Error: "; PCIB.ERR$
906 IF LEFT$(PCIB.NAME$, 1) <> CHR$(32) THEN PRINT
"Instrument: "; PCIB.NAME$

```

```

907 STOP
908 COMMON PCIB.DIR$, PCIB.SEG
909 COMMON LD.FILE, GET.MEM, PANELS, DEF.ERR
910 COMMON PCIB.BASERR, PCIB.ERR, PCIB.ERR$, PCIB.NAME$,
PCIB.GLBERR
9 1 1 C O M M O N
READ.REGISTER, READ.SELFID, DEFINE, INITIALIZE.SYSTEM, ENABLE.SY
STEM, DISABLE.SYSTEM, INITIALIZE, POWER.ON, MEASURE, OUTPUT, START
, HALT, ENABLE.INT.TRIGGER, DISABLE.INT.TRIGGER, ENABLE.OUTPUT, D
ISABLE.OUTPUT, CHECK.DONE, GET.STATUS
912 COMMON SET.FUNCTION, SET.RANGE, SET.MODE, WRITE.CAL,
READ.CAL, STORE.CAL, DELAY, SAVE.SYSTEM, SET.GATETIME,
SET.SAMPLES, SET.SLOPE, SET.SOURCE, ZERO.OHMS, SET.SPEED,
SET.COMPLEMENT, SET.DRIVER, OUTPUT.NO.WAIT, ENABLE.HANDSHAKE,
DISABLE.HANDSHAKE
913 COMMON SET.THRESHOLD, SET.START.BIT, SET.NUM.BITS,
SET.LOGIC.SENSE, SET.FREQUENCY, SET.AMPLITUDE, SET.OFFSET,
SET.SYMMETRY, SET.BURST.COUNT, AUTOSCALE, CALIBRATE,
SET.SENSITIVITY, SET.VERT.OFFSET, SET.COUPLING, SET.POLARITY,
SET.SWEEPSPEED
914 COMMON SET.DELAY, SET.TRIG.SOURCE, SET.TRIG.SLOPE,
SET.TRIG.LEVEL, SET.TRIG.MODE, GET.SINGLE.WF, GET.TWO.WF,
GET.VERT.INFO, GET.TIMEBASE.INFO, GET.TRIG.INFO, CALC.WFVOLT,
CALC.WFTIME, CALC.WF.STATS, CALC.RISETIME, CALC.FALLTIME,
CALC.PERIOD
915 COMMON CALC.FREQUENCY, CALC.PLUSWIDTH, CALC.MINUSWIDTH,
CALC.OVERSHOOT, CALC.PRESHOOT, CALC.PK.TO.PK, SET.TIMEOUT,
SCOPE.START, MEASURE.SINGLE.WF, MEASURE.TWO.WF, OPEN.CHANNEL,
CLOSE.CHANNEL
916 COMMON FREQUENCY, AUTO.FREQ, PERIOD, AUTO.PER, INTERVAL,
RATIO, TOTALIZE, R100MILLI, R1, R10, R100, R1KILO, R10MEGA,
R100MEGA, CHAN.A, CHAN.B, POSITIVE, NEGATIVE, COMN, SEPARATE,
DCVOLTS, ACVOLTS, OHMS, R200MILLI, R2, R20, R200, R2KILO,
R20KILO
, R200KILO
917 COMMON R2MEGA, R20MEGA, AUTOM, R2.5, R12.5, POSITIVE,
NEGATIVE, TWOS, UNSIGNED, OC, TTL, R0, R1, R2, R3, R4, R5, R6,
R7, R8, R9, R10, R11, R12, R13, R14, R15, R16, SINE, SQUARE,
TRIANGLE, CONTINUOUS, GATED, BURST, R10NANO, R100NANO,
R1MICRO,
R10MICRO, R100MICRO
918 COMMON R1MILLI, R10MILLI, R100MILLI, R1, R10, R20NANO,
R200NANO, R2MICRO, R20MICRO, R200MICRO, R2MILLI, R20MILLI,
R200MILLI, R2, R20, R50NANO, R500NANO, R5MICRO, R50MICRO,
R500MICRO, R5MILLI, R50MILLI, R500MILLI, R5, R50, CHAN.A,
CHAN.B,
EXTERNAL, POSITIVE
919 COMMON NEGATIVE, AC, DC, TRIGGERED, AUTO.TRIG, AUTO.LEVEL,
X1, X10, STANDARD, AVERAGE

```

```

920  COMMON  DMM.01,  FUNC.GEN.01,  SCOPE.01,  COUNTER.01,
DIG.IN.01, DIG.OUT.01, RELAY.ACT.01, RELAY.MUX.01
999  'End PCIB Program Shell
1000 REM
1010 REM This step initializes the HP system
1020 CLS
1030 OPTION BASE 1
1040 DIM P(10), PA(50, 6), PP(50, 6), XPT(40), CAL(40)
1050 CALL INITIALIZE.SYSTEM(PGMSHEL.HPC)
1060 REM
1070 REM All PC devices now have an initial state
1080 REM Set function on the DMM and Relay MUX
1090 REM
1100 CALL SET.FUNCTION(DMM.01, DCVOLTS)
1110 CALL SET.RANGE(DMM.01, AUTOM)
1120 CALL DISABLE.INT.TRIGGER(DMM.01)
1130 CALL ENABLE.OUTPUT(RELAY.MUX.01)
1140 FORMAT$ = "##      ##.####      ##.####      ##.####      ##.####
##.####      ##.####"
1200 FOR I = 1 TO 10
1210 CAL(I) = 0!
1220 NEXT I
1510 REM
1520 REM READ THE VOLTAGE OF 48TH CHANNEL AND DISPLAY THE
DATA
1530 REM
1540 PRINT " CHOOSE 6 POINTS"
1550 PRINT
1550 PRINT "THE CALIBRATION WILL BE STORES IN 'CAL.DAT'"
1560 REM
1570 REM Begin sampling loop
1580 REM
1600 FOR J = 1 TO 1
1610 PRINT
1630 FOR JJ = 1 TO 6
1631 INPUT "INPUT THE CALIBRATION PRESSURE"; CAL(JJ)
1632 INPUT "PRESS 'ENTER' TO START MEASUREMENT"; MOVE$
1640 FOR II = 1 TO 10
1650 ROUT = 1
1660 CALL OUTPUT(RELAY.MUX.01,ROUT)
1670 CALL MEASURE(DMM.01, VOLTS)
1680 PA(II, JJ) = VOLTS
1690 NEXT II
1700 IF JJ = 6 THEN 1740
1730 NEXT JJ
1740 REM
1750 REM DISPLAY THE SAMPLE DATA
1760 REM
1780 FOR IS= 1 TO 10

```



```

1   7   9   0   P   R   I   N   T   U   S   I   N   G
FORMAT$; IS, PA( IS, 1), PA( IS, 2), PA( IS, 3), PA( IS, 4), PA( IS, 5), PA( I
S, 6)
1800 NEXT IS
1810 REM
1820 REM AVERAGE THE DATA
1830 REM
1840 FOR JA = 1 TO 6
1850 TOTAL = 0
1860 FOR IA = 1 TO 10
1870 TOTAL = TOTAL + PA(IA, JA)
1880 NEXT IA
1890 AVERAGE = TOTAL / 10
1900 P(JA) = AVERAGE
1920 NEXT JA
1930 PRINT
1940 PRINT "THE AVERAGE ARE: "
2000 FOR JD = 1 TO 6
2010 PP(J, JD) = P(JD)
2020 NEXT JD
2055 PRINT USING FORMAT$; J; PP(J, 1); PP(J, 2); PP(J, 3);
PP(J, 4); PP(J, 5); PP(J, 6)
2070 PRINT
2080 INPUT "DO YOU WANT RE-MEASURE AGAIN ? (Y / N)"; C$
2090 IF C$ = "Y" THEN 1580
2101 REM*** STORE DATA BEFORE NEXT SAMPLE***
2102 OPEN "A:\CAL.DAT" FOR OUTPUT AS #2
2106 FOR ID = 1 TO 6
2107 PRINT #2, USING FORMAT$; ID; PP(J, ID); CAL(ID)
2108 NEXT ID
2109 CLOSE #2
2210 NEXT J

```

## APPENDIX C

```

$storage:2
$debug
*****
*****
* THIS PROGRAM CONVERTS THE VOLTAGE OF TRANSDUCER INTO
* PHYSICAL *
* PRESSURE, VELOCITY, YAW ANGLE AND PITCH ANGLE. THOSE DATA ARE
*
* USED FOR PLOT PROGRAM LATER.
*
*****
*****
      CHARACTER*14 FNAME
      CHARACTER*14 NAME
      CHARACTER*14 OUTFILE
      CHARACTER*2 A(50)
      CHARACTER*80 ST
      REAL K,INTR
      INTEGER COLS,RWS,DTPTS
      DATA A/'01','02','03','04','05','06','07','08','09',
*           '10','11','12','13','14','15','16','17','18',
*           '19','20','21','22','23','24','25','26','27',
*           '28','29','30','31','32','33','34','35','36',
*           '37','38','39','40','41','42','43','44','45',
*           '46','47','48','49','50'/
      WRITE (*,'(A\)' ) ' # OF COLUMNS IN THE GRID
(LEFT/RIGHT) = '
      READ (*,*) COLS
      WRITE (*,'(a\)' ) ' # OF DATA POINTS IN A COLUMN
(UP/DOWN) = '
      READ (*,*) RWS
      WRITE (*,'(A\)' ) ' DATA FILE NAME? (A:FILEXXXX.EXT): '
      READ (*,'(A14)' ) NAME
      WRITE (*,'(A\)' ) ' Initial ambient pressure [in. Hg]:
,
      READ (*,*) PI
      WRITE (*,'(A\)' ) ' Final ambient pressure [in. Hg]: '
      READ (*,*) PF
      WRITE (*,'(A\)' ) ' Initial temperature [deg F]: '
      READ (*,*) TI
      WRITE (*,'(A\)' ) ' Final temperature [deg F]: '
      READ (*,*) TF
      WRITE (*,'(A\)' ) ' Tunnel calibration factor, K: '
      READ (*,*) K
      WRITE (*,'(A\)' ) ' Slope from pressure calibration
curve [cm/v] '

```

```

      READ (*,*) SLOPE
      WRITE (*, '(A\)' ) ' Intercept from pressure calibration:
,
      READ (*,*) INTR
      WRITE (*, '(A\)' ) ' Tunnel delta-p for test-section q:
,
      READ (*,*) QM1FAC
* COMPUTE THE AVERAGE ATMOSPHERIC PRESSURE GIVEN inHg CONVERT
TO psf
      PATM=(PI+PF)*35.3631
      R=1716.5
C ***** "E" is blockage correction *****
      E=0.0123
C ***** COMPUTE TEST SECTION AVERAGE TEMPERATURE
      T=(TI+TF)/2.+460
C ***** TEST SECTION DENSITY
      RO=PATM/(R*T)
      DTPTS=RWS*COLS
* OPEN A NEW FILE TO STORE THE REDUCED DATA
      write(*, '(A\)' ) ' Output data file? [A:FILENAME.EXT]: '
      read(*, '(a14)' ) outfile
      OPEN(2, FILE=outfile, STATUS='new')
      WRITE (2,900) DTPTS
900    FORMAT(I5)
* OPEN A SEQUENTIAL OF DATA FILE * BE SURE THE FILE IN PPROBE
HAS 6 ELEMENTS
      DO 20 I=1, COLS
          NAME(9:10)=A(I)
          FNAME=NAME
          OPEN(1, FILE=FNAME)
          READ(1,100, END=20) ST
100    FORMAT(A65)
15      READ(1,1000, END=30) NO, X, Y, V1, V2, V3, V4, V5, BETA
1000    FORMAT(I2, F7.2, F6.2, 5F9.3, F8.2)
* CONVERT THE VOLTAGE TO PRESSURE IN LBF/FT**2      **
1cm/H2O=2.0461 PSF ***
      P1=calvp(V1, SLOPE, INTR)*2.0461+PATM
      P2=calvp(V2, SLOPE, INTR)*2.0461+PATM
      P3=calvp(V3, SLOPE, INTR)*2.0461+PATM
      P4=calvp(V4, SLOPE, INTR)*2.0461+PATM
      P5=calvp(V5, SLOPE, INTR)*2.0461+PATM

      IF ((P1-(P2+P3)/2) .LT. 0.0) THEN

* AN ATTEMP TO ACCOUNT FOR THE DELTA P NOT EQUAL TO
ZERO*****
*          P1=ABS(P1)
*          P3=ABS(P3)
*          P2=ABS(P2)

```

```

*   CALCULATE THE PITCH ANGLE IN DEGREES
      P=(P4-P5)/(P1-P2)
      ALPHA=FPITCH(P)
*   CALCULATE THE VELOCITY IN FT/SEC
      YSLOP=FYSLOP(ALPHA)
      VELM=SQRT((2*YSLOP*(ABS((P1-P3))))/(RO*K))
      VEL=VELM*(1+E)
*   CALCULATE THE LOCAL DYNAMIC PRESSURE
      QM1=QM1FAC*2.0461/K
      QM=RO*VEL**2/2.
      Q1=QM1*(1+2*E)
      Q=QM*(1+2*E)
*   CALCULATE THE YAW ANGLE IN DEGREES
C ***** beta0 is tunnel cal correction *****
      beta0 = 4.
      YAW=FYAW(BETA - beta0)
C
C ***** Calculate the velocity components
      betar = yaw*0.017453
C ***** alpha0 is tunnel cal correction *****
      alpha0 = -2.
      pitch = alpha-alpha0
      alphas = pitch*0.017453
      vely = vel*sin(alphas)
      velx = vel*cos(alphas)*sin(betar)
C
*   CALCULATE THE TOTAL PRESSURE IN LBF/IN**2
      PTC=FPT(ALPHA)
      PT1=P1-Q*PTC
      PT=PT1/144.
      CPT=(PT1-PATM-Q1)/Q1

      IF (CPT .LT. -3.0) THEN
        CPT=-3.0
      ENDIF

*   CALCULATE THE STATIC PRESSURE IN LBF/IN**2
      PS1=PT1-Q
      PS=PS1/144.
      CPS=(PS1-PATM)/Q1
      GO TO 1190
    ELSE

*   CALCULATE THE PITCH ANGLE IN DEGREES
      P=(P4-P5)/(P1-P2)
      ALPHA=FPITCH(P)
*   CALCULATE THE VELOCITY IN FT/SEC
      YSLOP=FYSLOP(ALPHA)
      VELM=SQRT((2*YSLOP*((P1-P2))))/(RO*K))

```

```

      VEL=VELM*(1+E)
*   CALCULATE THE LOCAL DYNAMIC PRESSURE
      QM1=QM1FAC*2.0461/K
      QM=RO*VEL**2/2.
      Q1=QM1*(1+2*E)
      Q=QM*(1+2*E)
*   CALCULATE THE YAW ANGLE IN DEGREES
C ***** beta0 is tunnel cal correction *****
      beta0 = 4.
      YAW=FYAW(BETA - beta0)
C
C ***** Calculate the velocity components
      betar = yaw*0.017453
C ***** alpha0 is tunnel cal correction *****
      alpha0 = -2.
      pitch = alpha-alpha0
      alphas = pitch*0.017453
      vely = vel*sin(alphas)
      velx = vel*cos(alphas)*sin(betar)
C
*   CALCULATE THE TOTAL PRESSURE IN LBF/IN**2
      PTC=FPT(ALPHA)
      PT1=P1-Q*PTC
      PT=PT1/144.
      CPT=(PT1-PATM-Q1)/Q1
*   CALCULATE THE STATIC PRESSURE IN LBF/IN**2
      PS1=PT1-Q
      PS=PS1/144.
      CPS=(PS1-PATM)/Q1
      ENDIF
      1          1          9          0
WRITE(2,2000)X,Y,VEL,velx,vely,YAW,pitch,pt,cpt,ps,cps
2000      FORMAT(11F10.4)
      GO TO 15
30      CLOSE(1)
20      CONTINUE
      CLOSE(2)
      STOP
      END
*****
*   THIS FUNCTION CONVERTS THE VOLTAGE TO PHYSICAL PRESSURE
      FUNCTION calvp(X,SLOPE,INTR)
      REAL INTR
      calvp=X*SLOPE+INTR
      END
*****
*   THIS FUNCTION CALCULATES THE PITCH ANGLE
      FUNCTION FPITCH(X)
      FPITCH=3.759+53.7568*X-1.3085*X**2-1.6583*X**3

```

```

      *      -0.8061*X**4+16.5115*X**5
      END
*****
* THIS FUNCTION CALCULATES THE VELOCITY PRESSURE COEFFICIENT
  FUNCTION FYSLOP(X)
    IF(X.LT.-10) THEN
      FYSLOP=0.981-0.0102*X-3.000E-4*X**2-2.500E-6*X**3
    ELSE IF((X.GE.-10).AND.(X.LE.10)) THEN
      FYSLOP=0.98-0.006*X+2.000E-4*X**2
    ELSE
      FYSLOP=0.9801-0.0035*X-1.143E-4*X**2+5.833E-6*X**3
    END IF
  END
*****
* THIS FUNCTION CALCULATES THE YAW ANGLE
  FUNCTION FYAW(X)
c***** NOTE: 180 deg indicates zero yaw
      FYAW=180-X
  END
*****
* THIS FUNCTION CALCULATES THE TOTAL PRESSURE COEFFICIENT
  FUNCTION FPT(X)
    IF(X.LE.-30) THEN
      FPT=-0.01
    ELSE IF((X.GT.-30).AND.(X.LT.-20)) THEN
      FPT=0.02+1.00E-3*X
    ELSE IF((X.GE.-20).AND.(X.LE.30)) THEN
      FPT=0
    ELSE
      FPT=0.03-1.00E-3*X
    END IF
  END
  END

```

## INITIAL DISTRIBUTION LIST

- |     |  |   |
|-----|--|---|
| 1.  | Commandant of the Marine Corps<br>Code TE 06<br>Headquarters, U.S. Marine Corps<br>Washington, D.C. 20380-0001                       | 1 |
| 2.  | Defense Technical Information Center<br>Cameron Station<br>Alexandria, VA 22304-6145   | 2 |
| 3.  | Library, Code 52<br>Naval Postgraduate School<br>Monterey, CA 93943-5002   | 2 |
| 4.  | Chairman<br>Department of Aeronautics and Astronautics, Code AA<br>Naval Postgraduate School<br>Monterey, CA 93943-5000              | 1 |
| 5.  | Commander<br>Naval Air Systems Command<br>Washington, D.C. 20306   | 1 |
| 6.  | NASA Langley Research Center<br>MS/1285 Technical Library<br>Hampton, VA 23655   | 1 |
| 7.  | NASA Ames Research Center<br>Technical Library<br>Moffet Field, CA 94035   | 1 |
| 8.  | Prof. R. M. Howard<br>Department of Aeronautics and Astronautics, Code AA/Ho<br>Naval Postgraduate School<br>Monterey, CA 93943-5000 | 2 |
| 9.  | Commander<br>Naval Air Systems Command<br>Air 530<br>Washington, D.C. 20306  | 1 |
| 10. | Mr. David W. Lacey<br>David W. Taylor Research Center<br>Bethesda, MD 20084  | 1 |

- |     |  |   |
|-----|--|---|
| 11. | LT. John M. Kersh, USN<br>P.O. Box 144<br>Woodstock, CT 06281          | 1 |
| 12. | CAPT. John F. O'Leary, USMC<br>209 Crestwood Dr.<br>Camillus, NY 13031 | 1 |